RICE UNIVERSITY

Single-Walled Carbon Nanotubes: Induced Decomposition of Peroxides and Non-covalent Encapsulation into Water-Soluble PEG-eggs
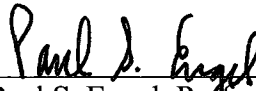
by

David William Abmayr, Jr.

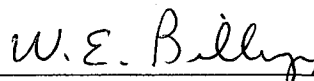A THESIS SUBMITTED
IN PARTIAL FULFILLMENT OF THE
REQUIREMENTS FOR THE DEGREE

Doctor of Philosophy

APPROVED, THESIS COMMITTEE:

Paul S. Engel, Professor, Chair
Chemistry

W. Edward Billups, Professor
Chemistry

Antonios Mikos, John W. Cox Professor
Bioengineering

HOUSTON, TEXAS

January, 2009

UMI Number: 3362121

INFORMATION TO USERS

The quality of this reproduction is dependent upon the quality of the copy
submitted.   Broken or indistinct print, colored or poor quality illustrations
and photographs, print bleed-through, substandard margins, and improper
alignment can adversely affect reproduction.
In the unlikely event that the author did not send a complete manuscript
and there are missing pages, these will be noted.   Also, if unauthorized
copyright material had to be removed, a note will indicate the deletion.

UMI®

ABSTRACT

Single-Walled Carbon Nanotubes: Induced Decomposition of Peroxides and Non-covalent Encapsulation into Water-Soluble PEG-eggs

by

David W. Abmayr, Jr.

This thesis presents two studies aimed at furthering the understanding of single-walled carbon nanotube (SWNT) chemistry for potential applications in composite and biological systems. In composite systems, SWNTs are used as structural members, and bis-acyl peroxides are frequently used as reaction initiators to cure the surrounding matrix. The behavior of the peroxide is often critical to the performance of the final composite. In this study, SWNTs are shown to induce the decomposition of a series of bis-acyl peroxides by single electron transfer. Four bis-acyl peroxides are evaluated for decomposition rate in the presence of SWNTs via iodometry. The resulting SWNTs are analyzed for functionalization by Raman microscopy and X-ray Photoelectron Spectroscopy (XPS). Benzoyl peroxide (BP), p-methoxybenzoyl peroxide (pMBP), phthaloyl peroxide (PhP), and trifluoroacetyl peroxide (TFAP) have known decomposition characteristics and known sensitivities to electron sources. This study demonstrates that all four peroxides undergo induced decomposition in the presence of SWNTs. Of the four, phthaloyl peroxide exhibits the greatest increase, followed by

TFAP, BP, and pMBP. This study also demonstrates that all but TFAP functionalize the SWNTs. The decomposition data may be used to design improved composite systems.

In aqueous solution, the ability of SWNTs to heat up upon exposure to radiofrequency energy gives them potential uses in biological systems. SWNTs are not soluble alone in aqueous solution, so one approach is to use amphiphilic triblock copolymers to capture and isolate SWNTs in water. This study addresses the difficulties encountered in synthesizing these polymers reproducibly and controllably. Presented here are modifications to the Atom Transfer Radical Polymerization (ATRP) method that not only enable the reproducible synthesis of these triblocks, but also enable them to be made in a highly controlled manner with specific block lengths. The SWNTs encapsulated by the polymers made through this new approach are shown not only to retain their fluorescence but also to demonstrate fluorescence on par with the best surfactants in current use. These structures are expected to provide a new entry into the use of non-functionalized SWNTs in biological systems such as radiofrequency heating for the destruction of cancer cells.

ACKNOWLEDGEMENTS

I would like to express my gratitude towards all those people who helped me during the course of my graduate work. First I would like to thank my advisor, Dr. Paul S. Engel, for providing excellent guidance and a marvelous work environment. I would also like to thank Dr. W. Edward Billups for providing funding for much of my graduate work as well as his time in serving on my thesis committee, and Dr. Antonios Mikos for his time in serving on my thesis committee.

I thank my wife, Dr. Beth Beason, for the time and effort she has spent supporting my work, for listening (over and over) to my presentations, and for making my studies much easier in general. I also thank my parents, Drs. David W. Abmayr, Sr. and Sandra J. Abmayr, for their support and assistance and for setting a standard of achievement that gave me the drive to succeed. I also thank my sister and brother-in-law, Janine M. Abmayr and Donald B. Hightower, for their support as well.

Finally, I would like to thank Dr. Amber Schaefer, for helpful advice, discussions, and for just being a great lab mate and friend.

TABLE OF CONTENTS

LIST OF TABLES AND FIGURES

DEFINITIONS

ATRP: Atom transfer radical polymerization

BP: Benzoyl peroxide

BSA: Bovine serum albumin

DCM: Dichloromethane

DMF: N,N-dimethylformamide

EDC: 1-[3-(dimethylamino)propyl]-3-ethylcarbodiimide methiodide

HiPCO: High-pressure carbon monoxide

MCPBA: *m*-Chloroperbenzoic acid

MPEG: Mono-methoxy-terminated poly(ethylene glycol)

MPEG-Br: Mono-methoxy-terminated poly(ethylene glycol) bromoester macroinitiator

NB: Nitrobenzene

NIR: Near-infrared

ODCB: *o*-dichlorobenzene

PAA: Poly(acrylic acid)

PEG: Poly(ethylene glycol)

PEG-egg: SWNT encapsulated inside a crosslinked MPEG-PAA-PS shell

PhP: Phthaloyl peroxide

pMBP: *p*-methoxybenzoyl peroxide

PMDETA: N,N,N',N',N''-Pentamethyldiethylenetriamine

PS: Polystyrene

RF: Radio frequency

SCK: Shell cross-linked knedel-like structure

SDBS: Sodium dodecyl benzene sulfonate

SDS: Sodium dodecyl sulfate

SET: Single electron transfer

SWNT: Single walled carbon nanotube

tBA: *t*-butyl acrylate

TEA: Triethylamine

TFA: Trifluoroacetic acid

TFAP: Trifluoroacetyl peroxide

THF: Tetrahydrofuran

UV: ultraviolet

XPS: X-ray Photoelectron Spectroscopy

INTRODUCTION

Single-Walled Carbon Nanotubes (SWNTs) have several useful properties that lend themselves to a wide variety of applications. Their high aspect ratio (long, narrow shape) and rigid nature make SWNTs an excellent structural backbone or reinforcing material in composite structures. They may need to be functionalized for improved solubility or dispersion purposes. Their near-infrared (NIR) fluorescence and radiofrequency (RF) heating make them useful as markers or as local heating elements for cell destruction in biological applications.

Peroxides are commonly used in SWNT systems. The use of nanotubes in composite systems typically requires a crosslinking agent to cure the composite matrix. Peroxides, especially benzoyl peroxide, are common crosslinking initiators. Peroxides are also used as initiators for functionalization of SWNT sidewalls, sometimes functionalizing SWNTs directly. However, in systems that contain multiple reactive materials (such as a composite with SWNTs, a matrix, and peroxides), the peroxides may react in unexpected ways. To understand these systems better, and to improve the manufacture and performance of these materials, the interaction of SWNTs and peroxides needs to be elaborated.

For SWNTs to be useful in biological applications, they must be soluble and stable in aqueous solutions. However, if the SWNTs are functionalized to produce water solubility, they lose their fluorescence and RF heating properties. Therefore, SWNTs are commonly dispersed in aqueous solutions using surfactants such as sodium dodecyl benzene sulfonate (SDBS). These SWNT suspensions are often not stable when exposed to biological materials such as proteins. Worse, surfactants such as SDBS are cytotoxic

and therefore completely unusable in biological systems. An alternative method for solubilizing SWNTs is to encapsulate them in an amphiphilic poly (ethylene glycol) block poly (acrylic acid) block polystyrene (MPEG-PAA-PS) polymer, or PEG-egg, as reported by Wang, et. al.[1] However, PEG-eggs have proven difficult to make, as the published synthesis of the triblock copolymer has been very difficult reproduce. Furthermore, the synthesis has been unable to incorporate longer PEG chains or to produce a range of PAA or PS block lengths.

The work presented in this thesis addresses these two problems. The interaction of SWNTs and bis-acyl peroxides is explored, to determine if SWNTs induce the decomposition of the peroxides, to identify the mechanism of decomposition, and to characterize the resulting SWNTs. The issues causing the difficulty in polymerizing the triblock copolymer are investigated, with the intent of identifying the problems in the methodology to reproduce previous work, optimizing the methodology to control the polymer block lengths, extending the methodology to include longer PEG starting materials, and producing a sufficient quantity of material to provide PEG-eggs for biological testing.

Chapter 1. SWNT Induced Decomposition of Peroxides: Background and Literature Review

Single walled carbon nanotubes (SWNTs) are a pure allotrope of carbon and can be thought of as essentially a rolled-up graphene sheet. This rolled up sheet can take a number of different orientations, leading to different types of tubes. Figure 1 shows different tubes resulting from different orientations of the graphene sheet.
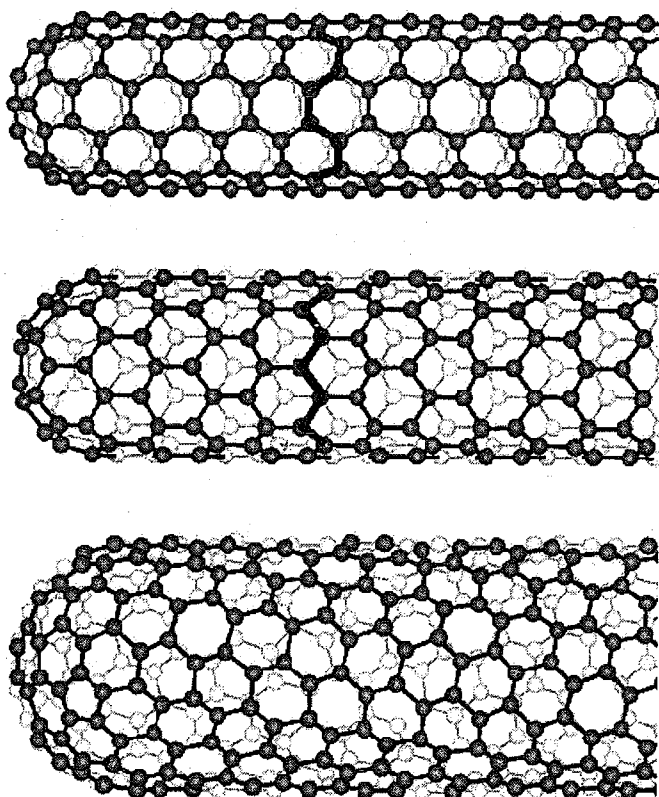
Figure 1. Single Walled Carbon Nanotube Types. The top image represents an armchair tube (black line shows "armchair" pattern), the middle image is a zig-zag tube (black line shows "zig-zag" pattern), and the bottom image is a chiral tube.[2]

Depending on the resulting appearance of the tube, they are usually referred to as "armchair", "zig-zag", or chiral tubes. These patterns arise from the roll-up angle of the graphene sheet.[3] The tubes are named according to their appearance as seen in Figure 1. Armchair tubes get their name from the "armchair" appearance of the line connecting the carbon atoms across the tube, and have a roll-up angle of 30°. Likewise, the name zig-zag originates from the zig-zag pattern of the line, and these tube have a roll-up angle of 0°. Chiral tubes are an intermediate tube with a roll-up angle between 0° and 30° and appear to have a "twist" in the hexagonal pattern.

SWNTs have a cylindrical structure with a very high aspect ratio. That is, they are very long and very narrow. SWNTs may be up to several microns in length, but they are only a few nanometers in diameter. The rigid, tubular structure gives them unique physical and mechanical properties, such as extremely high strength, high resistance to deflection, and high thermal conductivity. The extremely extended pi-aromatic system gives them unique electronic properties, such as NIR fluorescence and excellent field emission of electrons. SWNTs may be metallic or semiconductive, and some are even superconductive. These properties make SWNTs excellent building blocks for nanotechnologies. Their rigidity makes them useful in composites and other reinforced structures, and their electrical properties make them useful as potential sensors or as other electronic components.[4]

However, in order to make use of some of these properties, SWNTs must frequently be functionalized. By themselves, SWNTs form tightly grouped bundles held together by strong Van der Waals forces. In this form, they are difficult to dissolve in organic media, completely insoluble in aqueous systems, and resist interaction with other

materials in composites. Functionalization helps break up the bundles, increases the solubility of SWNTs in organic and even aqueous media, and allows direct interaction in solid systems. Furthermore, functionalization alters the chemical and physical properties of the SWNTs, allowing their properties to be "tuned" to a specific application.[4, 5]

The different methods for functionalizing SWNTs can be broken down into three general categories. The first method is a covalent modification of the tubes. Molecules are attached to the sidewall or endcap of a tube directly through a chemical bond. This method converts sp^2 carbons of SWNTs into sp^3 carbons where the attachment takes place, introducing a defect and breaking up the local pi-system. The second method is the noncovalent modification of SWNTs. This approach is typified by the wrapping of the SWNT with other molecules, usually oligomers or polymers that are held to the SWNT by pi-stacking, Van der Waals or other forces. The wrapping molecules do not alter the structure of the SWNT. The third method involves the endohedral filling of the hollow tube, introducing small molecules or atoms inside the tube itself. This approach obviously requires some alteration to the SWNT, either an opening in the sidewall or an open ended SWNT.[4,5]

Of the three methods, the one of concern here is the covalent modification of the SWNT. There are numerous ways to attach a molecule covalently to a SWNT. The method of interest in this thesis is that of free radical attack of a molecule on the sidewall or endcap of a SWNT.[4,5]

There are several precursors used to generate radicals that subsequently attack SWNTs. One common approach uses diazonium salts.[6] SWNTs are suspended in aqueous solution using sodium dodecyl sulfate (SDS) as a surfactant. A pre-formed

arenediazonium salt is added, and a single electron transfer from the SWNT to the salt generates a phenyl radical that then attacks the sidewall of the SWNT at room temperature. The reaction can be run solvent-free by generating the arenediazonium *in situ* from aniline and isoamyl nitrite at 60 °C.

Another approach involves the use of Fenton's reagent.[7] An iron (II) salt is used to decompose hydrogen peroxide in solution to a hydroxyl radical and a hydroxyl anion. The radical subsequently attacks dimethylsulfoxide, generating a methyl radical. The methyl radical then attacks the SWNTs, producing a methylated SWNT sidewall.

Other methods use the decomposition of perfluorinated compounds. When perfluoroalkyl iodides[8,9] are irradiated with ultraviolet (UV) light, the alkyl iodide decomposes to a perfluoroalkyl free radical that then attacks the SWNTs in solution. Perfluoroazo[10] compounds may be used as well. When perfluoroazooctane is irradiated at room temperature, the azo compound decomposes to nitrogen and free radicals, and the radicals functionalize the SWNT. The degree of functionalization achieved with the perfluorinated radicals is quite low, although in one case the objective was to only functionalize the nanotube end.[8]

Other azo compounds may be used, where the free radical is generated either thermally or with microwave assistance.[11,12] For example, methoxyphenylhydrazine hydrochloride will decompose slowly at 130 °C (72 h) or rapidly under microwave irradiation (10 min) to produce a methoxyphenyl radical that attacks SWNTs. Additionally, nitrogen radicals may be generated by microwave discharge of ammonia,[13] the plasma-generated radicals functionalizing the SWNTs with nitrogen directly.

Polymeric radicals may also be used to functionalize SWNTs. One approach generates polymeric radicals by the *in situ* polymerization of sodium 4-styrene sulfonate.[14] Radical polymerization of the monomer is initiated with sodium persulfate in the presence of SWNTs at 65 °C. The growing polymer chain can continue to grow by radical addition to monomer or it may attack the SWNTs in the solution, the latter producing polymer-functionalized tubes. Another method utilizes benzoyl peroxide to initiate the *in situ* radical polymerization of styrene in the presence of SWNTs.[15] As in the previous example, the growing polymer chain may continue to grow or attack the SWNTs. A slightly different approach uses a nitroxide-terminated polystyrene.[16] The nitroxide is decomposed at 125 °C to yield a polymeric benzylic radical that adds to the SWNTs.

The most common radical precursors, however, are peroxides. *bis*-Acyl peroxides such as benzoyl peroxide and lauroyl peroxide have been used to functionalize SWNTs either in solid-phase or solution phase reactions.[17,18,19] In solid phase reactions a solid mixture of the SWNTs and the peroxide is ground together and heated to 200 °C for 12 hours in a stainless-steel reactor. In solution phase functionalization, the SWNTs are dispersed in *o*-dichlorobenzene (ODCB) with the peroxide and heated to 80-100 °C for 3-120 hours[17], dispersed in toluene with the peroxide and heated to reflux for 7-9 hours (with repeated additions of peroxide)[18], or homogenized in benzene and heated to 80 °C for 2 hours (under continuous homogenization).[19] In all of the previous methods, the peroxide thermally decomposes to a radical that attacks the SWNTs present.

Other researchers have used the thermolysis of benzoyl peroxide at 75 °C to generate alkyl radicals that functionalize SWNTs in benzene.[7] The initially formed

phenyl radical reacts with an alkyl iodide, generating an alkyl radical that attacks the

SWNT. In this manner, the SWNT sidewall can be functionalized by a wide variety of

alkyl chains, which may themselves carry functional groups.

Other *bis*-acyl peroxides used for SWNT functionalization are succinic or glutaric

acid acyl peroxide.[20] SWNTs are dispersed in ODCB and heated to 80-90 °C for 10 days,

with an addition of peroxide each day. The formed radicals attack the SWNTs, yielding ~

one functional group per every 24 SWNT carbons.

Peroxyacids have been used to functionalize SWNTs as well.[21,22] Peroxytrifluoro

acetic acid (PTFAA), *m*-chloroperbenzoic acid (MCPBA), and 2-bromo-2-

methylperpropionic acid (BMPPA) were all shown to functionalize SWNTs. MCPBA is

available commercially, but PTFAA and BMPPA were synthesized *in situ* from

trifluoroacetic anhydride and hydrogen peroxide (60%, aqueous) and 2-bromo-2-

methylpropionic acid and hydrogen peroxide (60%, aqueous), respectively. In the case of

PTFAA, SWNTs were sonicated directly in the aqueous hydrogen peroxide at 0 °C

followed by the addition of trifluoroacetic anhydride. For BMPPA reactions, the SWNTs

were sonicated in a mixture of dichloromethane (DCM) and hydrogen peroxide also at 0

°C, followed by the addition of the acid. MCPBA (in DCM) was added directly to a

sonicated suspension of SWNTs in DCM at 0 °C. In all cases, sonication of the solutions

at 35 °C for 12 hours resulted in the modification of the SWNT sidewall. The

peroxyacids yield functionalized SWNTs with ester or other oxygenated functional

groups on the sidewall. The proposed mechanism is a 1,3 dipolar cycloaddition of the

peracid to a double bond on the SWNT sidewall, leaving an epoxide group. The epoxide

group is opened by a free acid, yielding a hydroxyl group and an ester.

Even hydrogen peroxide has been used to functionalize SWNTs.[23] SWNTs are dispersed in water using sodium dodecyl benzene sulfonate (SDBS) and added to a 30% hydrogen peroxide solution. The mixture is irradiated at 400-500 nm (xenon lamp using a band-pass filter). According to Zhang, et. al.,[23] the SWNTs in the suspension fluoresce upon irradiation of the solution, and the peroxide absorbs the fluorescence above 1300 nm. It is claimed that the absorption of the SWNT fluorescence induces the peroxide to dissociate into hydroxyl radicals that subsequently radicals attack and oxidize the SWNTs. However, as SWNTs fluoresce weakly and hydrogen peroxide absorbs weakly, the proposed process is unlikely.

There are situations, however, where peroxides are used in conjunction with SWNTs when the peroxide is not intended to functionalize the SWNTs. Rather, the peroxide generates a free radical that is intended to react with another component in the system. For example, the generation of polymeric radicals noted above use peroxides to initiate the polymerization, not to attack the SWNTs directly.[14,15] Another example is the benzoyl peroxide initiated polymerization of styrene to a SWNT with one styrene monomer already attached to the tube.[24] In this system, styrene monomer is grafted via Friedel-Crafts acylation to a SWNT. The SWNT is first treated with nitric acid to introduce carboxylic acid groups on the sidewall. The acid is converted to the acid chloride with thionyl chloride, and the styrene is grafted onto the SWNT via Friedel-Crafts using zinc oxide as the catalyst. The styrene on the SWNT was then free radical polymerized with styrene in solution using benzoyl peroxide as the initiator at 60 °C.

In other systems, such as composites, the free radicals generated by the peroxide are used to crosslink the composite matrix. In bone tissue engineering, for example,

SWNTs are used as structural reinforcement for biodegradeable polymeric scaffolds used to promote bone growth.[25,26,27] SWNTs are blended into the polymer matrix, and the matrix is then crosslinked by the thermolysis of the benzoyl peroxide initiator at 100 °C.

When peroxides are used as initiators in systems where the intent is not to modify the SWNTs but to initiate a reaction in some other component, it is important that the peroxide does not attack the SWNT instead. In some of the composite systems for bone tissue engineering, benzoyl peroxide seemed to decompose faster when SWNTs were present in the matrix than when they were not.[28] This observation suggested that the SWNTs were accelerating the decomposition of the benzoyl peroxide.

One of the objectives of this thesis was to determine whether this observation was in fact true. Furthermore, if SWNTs do induce the decomposition of benzoyl peroxide, the mechanism of decomposition needed to be identified. It was necessary to determine whether rate acceleration could be found in other peroxides. If so, the differing behavior of other peroxides could be used to help identify the mechanism. Finally, the reacted SWNTs needed to be characterized to determine if the radicals produced by induced decomposition would functionalize the SWNTs.

Benzoyl peroxide (BP, structure shown in Figure 2) was chosen as the first compound to study induced decomposition.
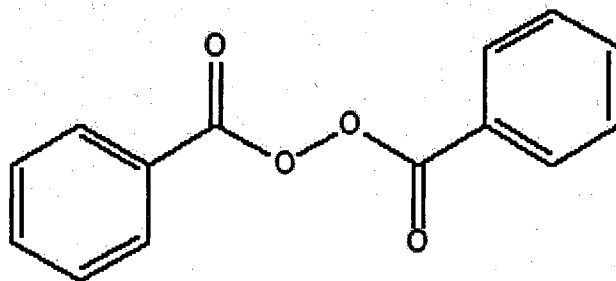
Figure 2. Benzoyl Peroxide (BP)

BP was the peroxide used in the original cases where acceleration was noticed, and it is widely used as a free radical initiator, as noted in previous paragraphs. Furthermore, the thermal decomposition behavior of BP is well known.[29,30,31] The thermolysis of BP has been studied in a wide range of solvents, and it is known to be subject to induced decomposition. For example, BP decomposition is induced by free radicals,[30] and as a result the thermolysis of BP is concentration-dependent because it is capable of autoinduction. BP has also been used for studying the effects of substituents on the decomposition,[30] and so provides an excellent baseline for the study of induced decomposition in SWNTs.

The proposed mechanism[32] for induced decomposition is shown in Figure 3.
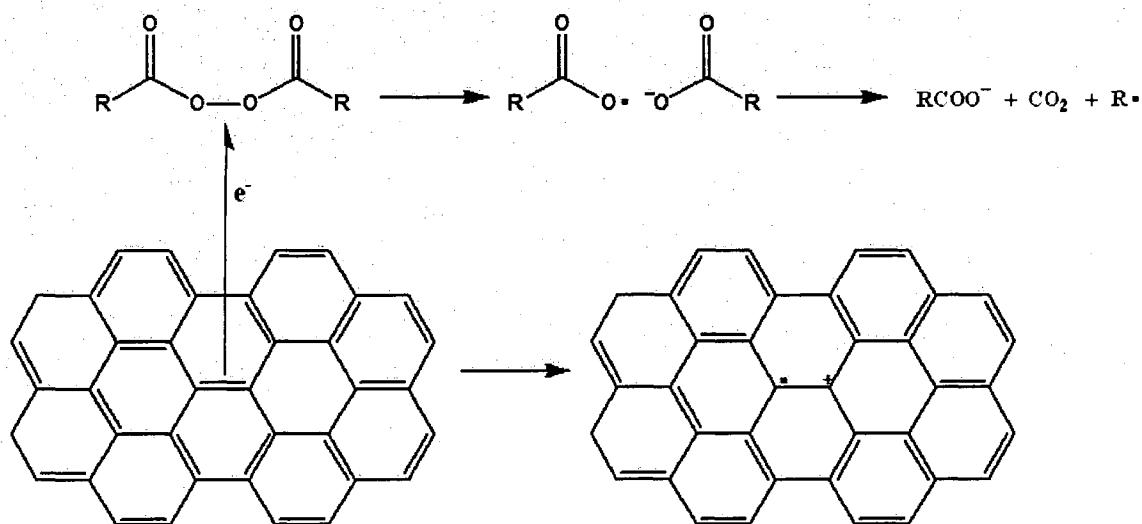
Figure 3. Mechanism of induced decomposition of a generic bis-acyl peroxide by single electron transfer from a SWNT to the peroxide

In the proposed mechanism, the SWNT injects an electron via single electron transfer (SET) from the sidewall (or endcap) into the O-O bond, leaving a radical cation on the SWNT. The O-O bond immediately undergoes bond scission, producing a carboxyl radical and a carboxylate anion. The carboxyl radical subsequently decarboxylates and produces a carbon-centered radical. This radical then may attack the sidewall of the SWNT directly, or it may combine with the SWNT radical cation.

If the SET mechanism is correct, then the rate of induced decomposition should be affected by the electronic and steric properties of the recipient peroxide. Three additional peroxides were chosen based on their substitution and structure: *p*-methoxybenzoyl peroxide (pMBP), trifluoroacetyl peroxide (TFAP), and phthaloyl peroxide (PhP). The peroxide structures are shown in Figure 4.

p-Methoxybenzoyl peroxide

Trifluoroacetyl Peroxide   Phthaloyl peroxide
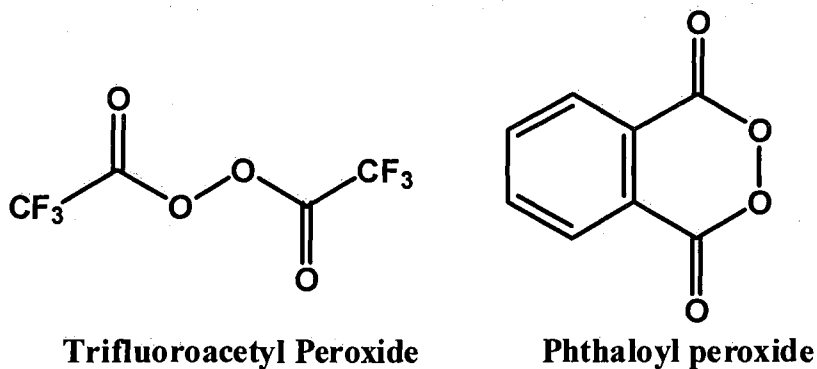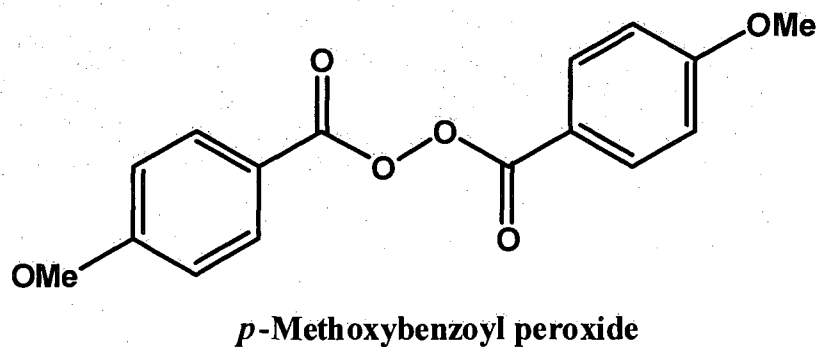
Figure 4. Structures of pMBP (top), TFAP (bottom right), and PhP (bottom left)

These peroxides represent, respectively, an electron rich peroxide, an electron poor

peroxide, and a strained peroxide. As such, they provide a series for comparison with BP.

The first peroxide, pMBP, is electron-rich at the O-O bond compared to BP as a

result of the electron donating methoxy groups on the ring. pMBP is less susceptible to

bimolecular induced decomposition, although it is more susceptible to unimolecular

homolysis.[30] TFAP, on the other hand, is an extremely electron deficient peroxide, owing

to the strongly electron withdrawing fluorine atoms. The presence of the fluorines causes

a marked reduction of the energy level of the antibonding molecular orbitals of the

oxygen-oxygen bond, making TFAP an excellent electron acceptor from even weak

electron donors.[33] TFAP is also known to undergo SET with electron rich donors,[33,34] and the thermolysis of TFAP is known to be greatly accelerated even by benzene.[35]

Phthaloyl peroxide, on the other hand, is electronically similar to BP, but exhibits a greatly different behavior.[36] The O-O bond of the peroxide is confined to be roughly planar in a six membered ring, introducing substantial strain into the bond.[37,38] This strain is believed to increase the susceptibility of PhP to SET.[38] PhP has been shown to be highly sensitive to induced decomposition in the presence of electron-rich donors such as styrene,[37] and has been demonstrated to decompose via an SET mechanism.[38]

The decomposition of the peroxides was measured in two ways. First, as the decomposition of acyl peroxides produces CO_2 gas, the pressure of the reaction vessel was monitored to determine the relative degree of decomposition of different reactions. Second, the residual amount of peroxide in a reaction was measured directly using iodometric titration.[39] Titration gives an exact measurement of remaining peroxide, thus allowing direct measurement of peroxide consumption rates.

In order to determine if these peroxides functionalize SWNTs upon induced decomposition, the recovered SWNTs used in the reactions were characterized by Raman Microscopy and X-Ray Photoelectron Spectroscopy (XPS). Raman spectroscopy has been used to determine the degree of sidewall functionalization through the ratio of the intensity of the D band (or diamond band, resulting from sp^3 hybridized carbons) to the G band (or graphite band, resulting from sp^2 hybridized carbons).[6,11,40,41] Raman D/G ratios were used to compare the SWNTs resulting from different decomposition reactions, identifying those with more or less SWNT functionalization. In addition, the radial breathing modes (RBM) observed in Raman spectroscopy have been used to determine

the distribution of nanotube diameters in a given SWNT sample.[42] However, due to the inherent complexity of the RBM spectra and the relatively low degree of functionalization seen, the RBM data were not used for SWNT characterization.

XPS has been used to determine the elemental composition of SWNTs, especially to identify functional groups.[6,14,40] The specific oxygen types present in pMBP (ether linkage) and PhP (ester group) can be identified by peaks (or shoulders) in the carbon 1s spectrum of a functionalized SWNT. The specific signals can be used to identify and quantify the functionality present. TFAP functionalization may be determined through the fluorine signal, an element unique to TFAP-functionalized tubes. XPS was therefore used to measure the elemental composition of the same SWNTs as Raman and to quantify the amount of functionality introduced to the SWNT.

Chapter 2. SWNT Induced Decomposition of Peroxides: Experimental

2.1 Materials

o-Dichlorobenzene (ODCB, Fisher) was used as received. Recycled ODCB was washed once with aqueous sodium thiosulfate, once with water, then once with 2M NaOH and again with water. It was further washed with saturated sodium bicarbonate, once more with water, once with saturated sodium chloride, and then the organic layer was dried over anhydrous magnesium sulfate. It was gravity filtered to remove the drying agent, then distilled at one atmosphere over calcium hydride. For degassed runs, the oxygen was removed using three freeze-pump-thaw cycles and the ODCB stirred under nitrogen. Nitrobenzene (NB, Acros) was washed once with 2M NaOH, once with 2M HCl, then twice with water. It was dried over anhydrous calcium sulfate, and it was gravity filtered to remove the drying agent. It was distilled under reduced pressure over anhydrous calcium sulfate and stored under nitrogen. Diethyl ether (Fisher) was distilled from sodium immediately prior to use. Hydrogen peroxide, 50% in water (Aldrich) was used as received. Trifluoroacetic anhydride (TFA, Aldrich) was distilled at one atmosphere over P_2O_5 and stored under nitrogen. Phthaloyl chloride (Aldrich) was distilled under reduced pressure and stored under nitrogen. Benzoyl peroxide (BP, Luperox A98, Aldrich) was determined to be 99%+ pure by iodometric titration, and it was used as received. p-Methoxybenzoyl peroxide (pMBP) was available in the laboratory, prepared by a literature procedure.[30] Iodometric analysis showed a purity of >99%. Phthaloyl peroxide (PhP) was prepared according to literature procedures[36] and purified to 99%+ by multiple recrystallizations. Trifluoroacetyl peroxide (TFAP) was

prepared according to a literature procedure and stored as a solution of peroxide in trifluoroacetic acid.[43] All three were stored at –20 °C. The single-walled carbon nanotubes used for non-degassed titration measurements were produced and purified in the Rice Carbon Nanotechnology Laboratory using the HiPCO (high-pressure carbon monoxide) reactor,[44] batch number 164-2. SWNTs used for degassed measurements were produced and purified the same way, batch number 162-8.

2.2 Methods

2.2.1 Synthesis of Phthaloyl Peroxide

Greene's synthesis was used to make phthaloyl peroxide.[36] A 500 mL three-necked round-bottom flask equipped with a magnetic stir bar, a 100 mL addition funnel, a glass stopper and a nitrogen purge was charged with 16 g (0.193 mol) of anhydrous sodium carbonate and 350 mL of dry diethyl ether. The flask was cooled to 0 °C in an ethylene glycol bath maintained at 0 °C with an external chiller. Hydrogen peroxide in dry diethyl ether (65 mL, 2.23 M, 0.145 mol) was added at 0 °C. The ethereal peroxide was prepared by the extraction of 50% hydrogen peroxide with diethyl ether followed by repeated drying of the organic layer over anhydrous magnesium sulfate. Distilled phthaloyl chloride (20 mL, 0.138 mol) was added to the addition funnel and introduced to the flask dropwise with stirring over the course of 20 minutes. When the addition was complete, the addition funnel was removed and replaced with a glass stopper. The flask was allowed to stir at 0 °C for 72 hours. The solution was vacuum-filtered and the filter cake containing crude peroxide was washed with 250 mL of cold water. The filtrate was

washed two times with saturated ammonium sulfate, once with water, twice with 10%

sodium bicarbonate, again with water, and finally once with saturated sodium chloride.

The organic layer was dried over anhydrous magnesium sulfate. The solvent was

removed on a rotovap and the crude peroxide combined with the washed filter cake. The

combined material was recrystallized from dry dichloromethane three times (1 g

peroxide/ 5 mL solvent) to afford ~5 g (~22% yield) of 99% pure phthaloyl peroxide, as

determined by iodometric titration.

2.2.2 Synthesis of Trifluoroacetyl Peroxide

Trifluoroacetyl peroxide was synthesized using the procedure published by

Krasutsky.[43] A 50 mL, single-necked round bottom flask equipped with a stir bar and a

10 mL addition funnel was charged with 13.9 mL of distilled trifluoroacetic anhydride

(100 mmol) and 7 mg of potassium trifluoroacetate (0.047 mmol). The flask was cooled

to 0 °C in an ice bath, and 1.6 mL 50% H_2O_2 (0.9 g, 26 mmol) was added to the addition

funnel. The peroxide was added dropwise to the solution with stirring. After the addition

was complete, the reaction was stirred for an additional 10 min. The resulting solution

gave ~3 molar TFAP in trifluoroacetic acid. The exact concentration was determined by

iodometric titration.

2.2.3 Iodometric Titration of Peroxides

The analysis of peroxides was performed using a modification of the iodometric

titration method published by Nozaki.[45] Sodium iodide (~ 0.5 g) was added to a 250 mL

Erlenmeyer flask followed by 10 mL of acetic anhydride. The solution was swirled to dissolve the salt (did not fully dissolve). Peroxide was added either as a pure material or as a solution to test and swirled for 30 min to ensure all of the peroxide reacted with the sodium iodide. For purity measurements, 70 mL of water was added and the solution titrated to a clear endpoint with sodium thiosulfate (0.07 M nominal concentration, standardized with potassium periodate). For decomposition runs, 40 mL of water was added before titration. A 1% starch solution was added immediately before reaching endpoint for purity measurements. The two-phase nature of decomposition runs decreased the utility of starch indicator, and it was typically not used in those cases.

2.2.4 Determination of Peroxide Decomposition: Pressure Measurement

To a 25 mL single-necked round-bottomed flask was added: 1-10 mg SWNTs, 10 mL ODCB, and a pressure apparatus that included a pressure transducer (MKS Baratron, 0-1000 torr range) connected to a chart recorder, a rotary valve, and a rotatable transfer spoon. Benzoyl peroxide (70-80 mg) was added to the transfer spoon and the spoon was installed in the apparatus. The flask was lowered into an oil bath at 80 °C and equilibrated. After equilibration, a vacuum of 15 in of Hg was applied to the apparatus via the rotary valve and the valve closed to seal the system. The chart recorder was zeroed and the spoon rotated to add the peroxide to the solution. The reaction was stirred for two hours and the pressure rise monitored with the chart recorder. After two hours, the reaction was stopped and the final pressure recorded.

2.2.5 Determination of Peroxide Decomposition: Iodometric Titration

A stock solution of 100 mg/L SWNTs in ODCB was made by adding 100 mg purified SWNTs to 1L of ODCB. The solution was bath sonicated for 18h. The appropriate quantity of stock solution (10-50 mL) was added via a volumetric pipette to a 100 mL, single-necked, round-bottom flask equipped with a magnetic stir bar. Enough ODCB was added to bring up the total volume to 50 mL. The resulting solution contained 1-5 mg of SWNTs, and was bath sonicated for an additional 15 minutes to enhance the dispersion of the SWNTs. For degassed runs, the flask was then flushed with nitrogen for 10 minutes and placed in an oil bath at the desired temperature (40-90 °C) under nitrogen. For non-degassed runs or for runs in the presence of bubbling O_2, the flask was simply placed in the oil bath open to air. For runs using BP, pMBP, or PhP, 0.3 mmol of the desired peroxide was added in one portion (0.006 M final concentration). For TFAP, the exact concentration was determined (solution of TFAP in TFA) using iodometric titration, and 0.3 mmol peroxide was added dropwise (~20 second addition) via an adjustable pipette. For degassed runs, the flask was then sealed with a nitrogen line. For non-degassed runs, the flask was left open. For runs in the presence of bubbling O_2, a glass tube was placed in the flask and pure oxygen bubbled through the solution during the run. After stirring for 1 hour, the solution was vacuum filtered through a 0.2 μm Teflon filter (Whatman, 47 mm diameter, polypropylene backed) that was moistened with absolute ethanol into a 250 mL sidearm flask containing sodium iodide and acetic anhydride for titration. The flask was rinsed with 5 mL acetic anhydride (also filtered) and the filtered SWNTs further rinsed with an additional 5 mL of acetic anhydride. The filter holding the SWNTs was removed, dried in air, and stored in a 20 mL scintillation

vial for further analysis. The dark yellow-brown solution in the flask was swirled for 30 min, and then 40 mL water was added. The two-phase mixture was titrated using the iodometric method.

2.2.6 Raman Microscopy

A Renishaw inVia Raman Microscope was used to acquire the Raman spectra. Samples were prepared by cutting a piece of double-sided tape of ~ 1 cm x 0.5 cm. The tape was mounted to a 2.5 cm x 7.6 cm glass slide and the teflon filter containing the SWNTs was pressed on the tape. The tape removed a section of SWNTs that were then analyzed in the spectrometer using 780 nm and 633 nm lasers.

2.2.7 X-Ray Photoelectron Spectroscopy

A Physical Electronics Quanteras XPS was used for all XPS analyses. A monochromated Al source was used, and the typical analysis area was 100 x 100 µm. When possible, the high-power (200 W) mode was used to improve signal. Otherwise the 40W mode was used. The pass energy was 23.6 eV and the step size was 0.1 eV. Samples were prepared by first drying the teflon filter under vacuum to remove all solvent. A rectangular area of ~ 1 cm x 0.5 cm was cut out of the center of the filter, with extreme care exercised to ensure that no contact was made with the analysis area. The sample was then mounted in the XPS sample holder and analyzed in the instrument.

Chapter 3. SWNT Induced Decomposition of Peroxides: Results and Discussion

3.1 Peroxide Decomposition Rate

Initial studies of the decomposition of peroxides examined the evolution of carbon dioxide produced when benzoyl peroxide (BP) decomposed in the presence of pristine, purified HiPCO single-walled carbon nanotubes (SWNT)s[44,46] at 80 °C. The pressure change over two hours was measured with a pressure transducer in solutions containing only BP and o-dichlorobenzene (ODCB) and solutions containing BP, SWNTs, and ODCB. The results are summarized in Tables 1 and 2.

Table 1. Pressure rise of BP/ODCB solution (control)

Peroxide (mg)	SWNTs (mg)	Time (h)	Starting Pressure (in. Hg)	Pressure Rise (in. Hg)
78	0	2	15	0.72
77	0	2	15	0.61
79	0	2	15	0.68
			Average	0.67

Table 2. Pressure rise of BP/SWNTs/ODCB solution

Peroxide (mg)	SWNTs (mg)	Time (h)	Starting Pressure (in. Hg)	Pressure Rise (in. Hg)
74	5	2	15	1.04
75	5	2	15	1.22
74	5	2	15	1.12
			Average	1.13

It was observed that the pressure change was 68% higher when SWNTs were present, even though less peroxide was used than in the control. This result confirmed that induced decomposition did take place, but it was difficult to measure the rate of decomposition accurately.

The inaccuracy of the decomposition measurement was the result of a number of limitations of the pressure apparatus. First, the measured pressure change was subject to error from the vapor pressure of the ODCB itself. Non-uniformity in the temperature of the upper part of the apparatus led to changes in the pressure in the vessel. Second, very small leaks would show as pressure increases but were difficult to identify (large leaks were quite obvious). Third, the rotatable spoon was several inches above the flask, and the joint was a narrow 14/20 joint. Thus, solid peroxide would sometimes stick to the walls of the apparatus instead of making it into the solution. Finally, the pressure transducer itself was not sensitive enough to differentiate between slightly different runs (e.g., one with 1 mg SWNTs and one with 2 mg SWNTs).

Two additional problems were apparent. One, different decomposition mechanisms generate different measured pressure changes with the same amount of peroxide decomposition. Unimolecular homolytic cleavage (thermolysis) generates two

CO_2 molecules per peroxide decomposed,[36] but induced decomposition via the proposed single electron transfer (SET) would generate only one, leading to large errors in decomposition measurement if both mechanisms are operative. The pressure measurement method was unable to differentiate between them. Second, and perhaps even more important, the rotating spoon was completely unsuitable for liquid peroxides. Trifluoroacetyl peroxide (TFAP) was one of the peroxides of interest, and it is best handled as a solution in trifluoroacetic acid. For these reasons, another approach was required.

Iodometric titration was chosen to replace pressure monitoring as the method to measure the extent of peroxide decomposition. Using a variation of iodometric titration developed by Nozaki[45] for quantitative analysis of organic peroxides, the residual peroxide left after a reaction was accurately determined. The decomposition mechanism would not affect the amount measured, and reactions would not need to take place inside a sealed flask, allowing liquids as well as solids to be added to the solutions.

Measurements of decomposition rates using the titration method confirmed initial results obtained with the pressure apparatus. At 80 °C in 10 mL ODCB, BP was consumed three times faster in 2 hours (79% peroxide consumed) when 5 mg SWNTs were present than when no SWNTs were present (25% peroxide consumed). Several screening experiments were conducted to examine the effects of temperature and functionality. These results are summarized in Tables 3 and 4.

Table 3. Effect of temperature on BP decomposition (in 10 mL ODCB)

Temp (°C)	Time (h)	SWNTs (mg)	Peroxide consumed (%)
25	2	0	6
25	2	5	4
40	24	0	0
40	18	5	19
80	2	0	25
80	2	5	79

Table 4. Effect of SWNT functionality on BP decomposition (in 10mL ODCB)

Temp (°C)	Time (h)	SWNTs (mg)	Functionality	Peroxide consumed (%)
80	2	5	Phenylated	52
80	2	5	Dodecylated	53

As expected, minimal decomposition was seen at 25 °C whether SWNTs were present or not. Surprisingly, at 40 °C some decomposition was observed with SWNTs present although only at very long run times. Interestingly, no decomposition at all was observed in the control run at 40 °C. This result was probably attributable to small errors in titration or measured weights as none of these initial runs were performed in duplicate.

The phenylated and dodecylated SWNTs[7,47] were expected to be less effective electron donors than pristine SWNTs because they have more sidewall defects and a weaker extended pi electron system. As expected, the use of functionalized SWNTs reduced the amount of induced decomposition by around 50%. The decomposition rate was indifferent to functionality type. However, they clearly retain some of their electron

donating capacity as they still produce substantial decomposition compared to the control.

It has been reported that the irradiation of SWNTs in the presence of H_2O_2 resulted in the disappearance of the characteristic near-infrared (NIR) fluorescence of the SWNTs.[23] In order to determine if the decomposition of BP could be photochemically induced in the presence of SWNTs, the reaction was irradiated with a 500W quartz halogen lamp through a water filter. No increase in the decomposition rate was observed. Given that the lifetimes of excited SWNTs are very short,[48] such a result was to be expected.

Having established that induced decomposition indeed took place, and that it was sensitive to temperature and SWNT type, several other control experiments were performed to ensure that the observed effect was produced by the SWNTs and not an impurity. In particular, purified HiPCO SWNTs contain residual iron,[44] measured by TGA in batch 164-1 to be ~1.5% by weight. Iron was present in a miniscule amount (~ 75 micrograms in 5 milligrams of SWNTs) in the peroxide reactions, so it was quite unlikely that it would cause these rate accelerations. Furthermore, the iron is encapsulated by a layer of carbon, such that X-Ray Photoelectron Spectroscopy (XPS) never detected iron in any purified SWNT sample. XPS detected iron in raw SWNT samples (1-2 atomic %, or 4-8% by weight), so the technique was able to identify iron when present. Interference from residual iron, though unlikely, still needed to be ruled out. Therefore, iron was tested to determine if it accelerated the decomposition of BP. The results are shown in Table 5.

Table 5. Effect of Iron on BP Decomposition

Iron Type	Amount	Temp (°C)	% Peroxide consumed
Iron Powder	2 mg	80	15.8
Fe (II)	2 μg	80	14.3
Fe (III)	2 μg	80	20.6
Fe (II)	2 mg	80	89
Fe (III)	2 mg	80	92
Blank Control		80	25

Iron in powder form (2 mg), 50 μg Fe(II), and 50 μg Fe(III) all produced similar results as the blank control. The Fe(II) and (III) used were as iron chlorides. When the amount of Fe(II) or (III) was increased to 2 mg iron, a very large increase in decomposition rate was seen, to the extent that nearly all of the peroxide was consumed. However, these two experiments are highly unrealistic as they contain far more iron mass than the SWNT experiments. They were merely included to verify that iron can induce decomposition, just not at the level contained by purified SWNTs. Furthermore, as the purification process subjects SWNTs to repeated oxidation, it is quite unlikely that the iron present is anything other than iron (II) or (III) oxide. As the iron powder almost certainly has at least a monolayer of oxide on the surface, iron oxide clearly cannot cause the observed acceleration. Additionally, if the carbon layer on the iron is too thick to be detected by XPS analysis (analysis depth of at least 60 Å), then it is surely too thick to allow any interaction between the iron and the peroxide.

Having established that iron was not involved in the decomposition, a very sensitive peroxide was examined, trifluoroacetyl peroxide (TFAP). The trifluoromethyl groups of TFAP are highly electron-withdrawing, leaving the O-O bond very electron

deficient. TFAP is known to be accelerated by benzene,[35] and known to undergo SET,[33] so if the mechanism of induced decomposition were a single-electron transfer then TFAP should be more sensitive to SWNTs than BP.

Initial runs of TFAP in ODCB at 25 °C showed a large decomposition rate in the blank control. Approximately 27% of the TFAP was consumed in only 45 minutes, and 70% was consumed at 50 °C (1 h). TFAP was apparently so sensitive that ODCB itself was a good enough electron donor to induce decomposition. Nitrobenzene (NB) was chosen as a much more electron-poor solvent, and blank control runs confirmed that TFAP was much more stable in NB, with only about 7-8% consumption observed in 1 h at 50 °C. When 5 mg of SWNTs were present, 75% of the peroxide was consumed in 1 h. These results were comparable to the BP results at 80 °C and 2 h, clearly showing the high sensitivity of the TFAP to induced decomposition.

A final control experiment was run using H_2O_2. The possibility existed that the synthesis of TFAP left some unreacted H_2O_2 in solution, and that this material may be responsible for some of the extreme sensitivity shown by TFAP. However, when 50% (aqueous) H_2O_2 was added at a comparable level, essentially no decomposition was observed over 1 h. Therefore, if any H_2O_2 had still been present, it was not the cause of the increased sensitivity.

The next step was to determine the dependence of the decomposition of BP and TFAP on the SWNT concentration. The results are summarized in Table 6.

Table 6. Decomposition rates with increasing amounts of SWNTs

Temp (°C)	Peroxide	Solvent	Time (h)	SWNT (mg)	% Peroxide Consumed
80	BP	ODCB	1	0	12
80	BP	ODCB	1	1	32
80	BP	ODCB	1	2.5	42
80	BP	ODCB	1	5	45
80	BP	ODCB	1	10	50
50	TFAP	NB	1	0	7
50	TFAP	NB	1	1	71
50	TFAP	NB	1	2.5	65
50	TFAP	NB	1	5	75

Surprisingly, for both BP and TFAP, increasing the SWNT concentration made very little difference in the consumption rate. In particular, the decomposition rate of TFAP was essentially flat with respect to the SWNT concentration. Given that the concentration of peroxide was much higher than that of SWNTs (~10 mg oxygen per run), the reaction was under excess peroxide, not excess SWNT conditions. Therefore, the most likely cause was that the SWNTs were not fully debundled.

In solution, SWNTs do not exist as discreet tubes but rather as bundles of tubes held together by strong Van der Waals interactions.[7,49] If the concentration of the SWNTs in ODCB is too high, very large bundles may form. If large bundles form, then interior tubes become unavailable for reaction with peroxides, and the decomposition is controlled by available surface area, not by mass. If that is the case, then an increase in SWNT concentration will likely result in an increase in bundle size, and no effective increase in available surface area.

To deal with the bundling issue, the solutions were diluted by a factor of 10. Instead of using 10 mL of solvent with each run, 50 mL of solvent would be used. Furthermore, rather than weighing out a set amount of SWNTs per each run, a stock solution would be made, sonicated, and diluted to the appropriate concentration. This approach provided two major benefits. One, the SWNTs should debundle much better, with no variances in bundling between runs. Two, the measurement of SWNTs in any given run would be far more accurate, as well as more easily duplicated.

Using the finalized method, a series of decomposition runs with BP was made with each reaction containing 0 to 5 mg SWNTS. Five runs were made and averaged at each concentration. The results are shown in Figure 5.
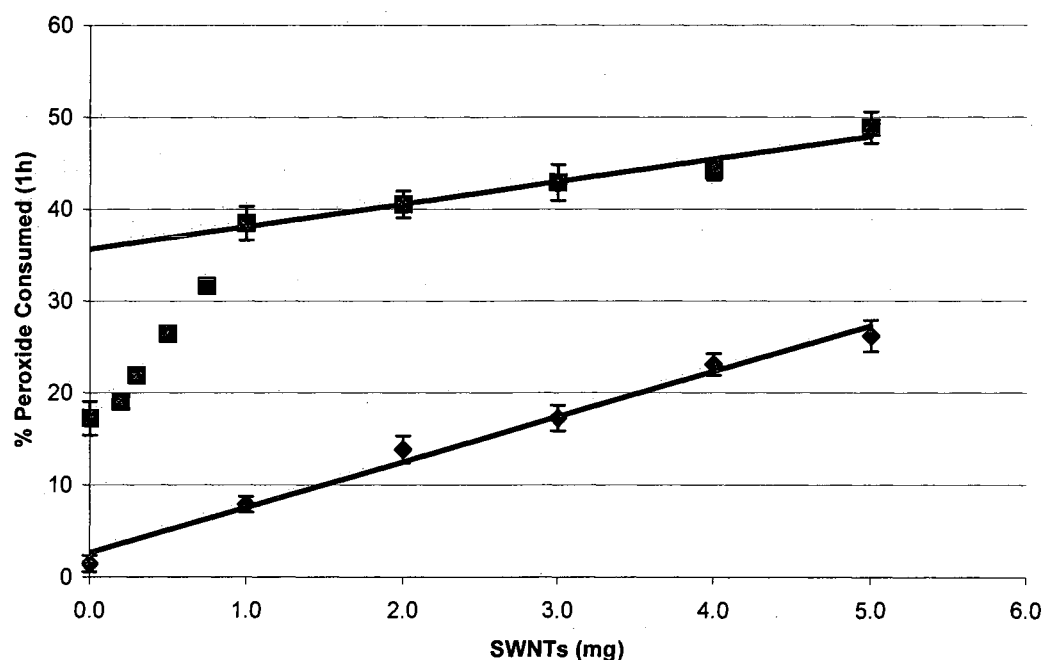
Figure 5. Decomposition of 0.3 mmol BP in 1 hour in 50 mL ODCB at 80 and 90 °C with SWNTs. 80 °C data in black diamonds, 90 °C data in black squares.

When no SWNTs are present at 80 °C, only 1.4% of the BP is consumed in 1 hour. This value was somewhat lower than that reported for benzene solvent in the literature,[29,30] so a control of BP in benzene was run for comparison. The decomposition in benzene was ~ 6% in 1 hour, similar to literature values. Clearly, ODCB does not induce BP thermolysis as much as benzene. The decomposition rate of BP at 80 °C increases linearly with increasing SWNT concentration (Slope 4.92, r^2=0.988). However, at 90 °C, much higher (17%) thermal decomposition is observed without SWNTs. There is then a steep rise until the SWNT concentration reaches 1 mg, after which the rate increases linearly with increasing SWNTs up to 5 mg (slope 2.44, r^2=0.958).

The steep rise between 0 and 1 mg was unexpected. Initially, BP decomposition rates were measured in 1 mg increments. First, a blank control with no SWNTs was run, followed by runs with 1 mg, 2 mg, etc. up to 5 mg. The SWNT runs produced a line that clearly did not intersect the y-axis close to the value of the control. It was necessary, therefore, to test SWNT concentrations at 0.2, 0.3, 0.5, and 0.8 mg to determine the behavior of the reaction at concentrations below 1 mg SWNTs. These very low SWNT levels required a more dilute stock solution than 100 mg/L, so a stock solution of 10 mg/L was prepared. Two runs were made at each concentration, rather than five. The steep rise observed is probably a curve rather than a linear increase, but the curvature is likely lost in the larger error in that region than in the others. The error is the result of fewer data points and smaller concentrations of SWNTs (at such low concentrations, SWNTs may debundle better, increasing surface area and increasing decomposition rate acceleration).

With BP data as a baseline, *p*-methoxybenzoyl peroxide (pMBP) was examined. pMBP is more electron-rich at the O-O bond, owing to the presence of the electron-donating methoxy groups present on the ring.[30] pMBP is also more susceptible to thermolysis than BP. pMBP is believed to be less stable than BP as a result of increased internal dipole-dipole repulsion.[30] BP already has an internal dipole present with the negative end at the O-O bond. The electron donating methoxy groups increase the partial negative charge on each oxygen, increasing the internal repulsion and lowering the activation energy for thermolysis. Therefore, it was expected to be less susceptible to induced decomposition than BP. The results are shown in Figure 6.

Figure 6. Decomposition of 0.3 mmol pMBP in 1 hour in 50 mL ODCB at 70 and 80 °C with SWNTs. 70 °C data in black diamonds, 80 °C data in black squares. Grey squares show BP at 80 °C for reference.

The greater thermolysis rate at 80 °C of pMBP alone compared to BP alone is readily apparent in Fig. 2: 15.8% vs 1.4%. It was desirable to reduce the thermolysis rate in order to obtain a curve without the steep initial rise. Therefore, the reaction temperature was lowered to 70 °C.

The general trend is similar for pMBP as in BP. At 70 °C, with minimal (4.7%) thermal decomposition, pMBP exhibits a linear increase in induced decomposition with increasing SWNT concentration (slope=3.41, r^2=0.997). As expected, the slope is somewhat lower than BP at 80 °C, but the two are close. At 80 °C, pMBP also displays the very steep initial slope, until at 1 mg and higher SWNT concentration it again becomes linear (slope 2.59, r^2=0.977). At the higher temperature, the slope is higher than BP at 90 °C, but still similar. Again, data points taken between 0 and 1 mg show an initial steep rise followed by a linear increase with increasing SWNT concentration up to 5 mg SWNTs.

The data are considerably different for phthaloyl peroxide (PhP). PhP is similar electronically to BP and therefore should exhibit a similar thermal response.[36] However, the O-O bond is confined into a roughly planar configuration owing to the cyclic nature of the peroxide. This restriction results in a considerable amount of lone pair-lone pair repulsion between the two oxygens and hence a considerable amount of strain in the molecule. This strain leads to a greatly increased sensitivity to induced decomposition,[36,37,38] and so PhP was expected to be very sensitive to SWNT concentration.

The results are shown in Figure 7.
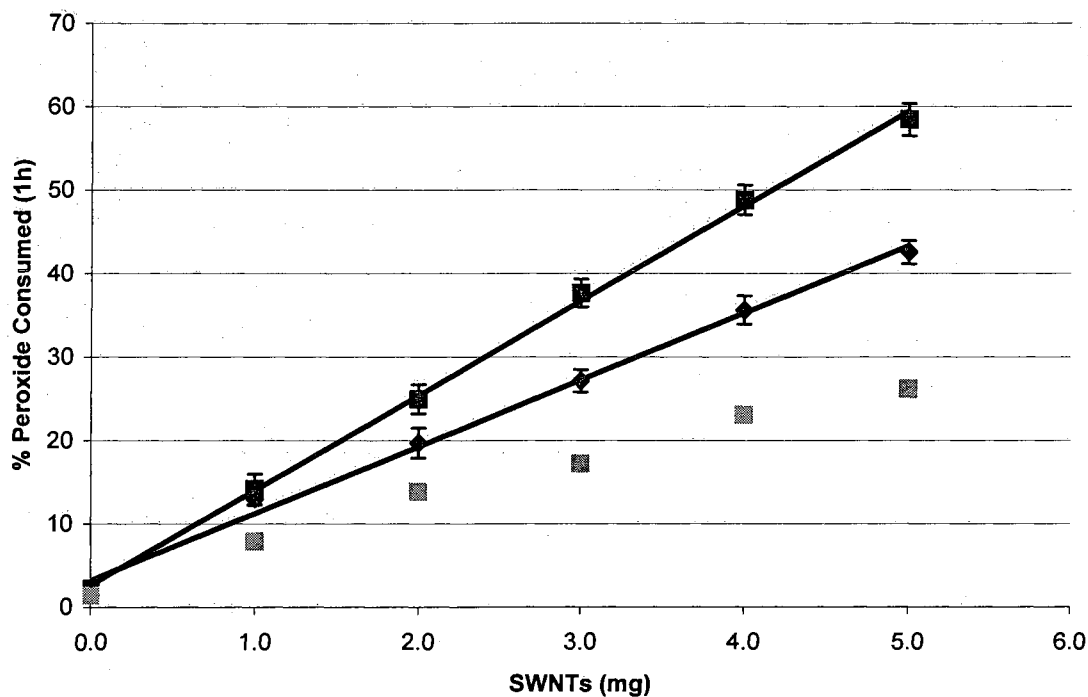
Figure 7. Decomposition of 0.3 mmol PhP in 1 hour in 50 mL ODCB at 70 and 80 °C

with SWNTs. 70°C data in black diamonds, 80 °C data in black squares. Grey squares

show BP at 80°C for reference.

The graph clearly shows that PhP is much more sensitive than either BP or

pMBP. At 70 °C and 80 °C, it displayed very little thermal decomposition (1.5 and 2.2%,

respectively), and therefore showed none of the nonlinearity seen in BP or pMBP at

higher temperatures (where a substantial amount of thermal decomposition occurred).

PhP exhibited a linear increase in decomposition with increasing SWNTs (slope=8.01,

r^2=0.994 at 70°C and slope=11.35, r^2=0.999 at 80°C). The slope of PhP at 80 °C, 11.35,

is approximately 2.3x greater than the slope of BP at 80°C, 4.93. Very interestingly, PhP

is the only peroxide to show an increase in sensitivity (as measured by slope) at higher

temperature. An increase in temperature was expected to cause an increase in sensitivity,

but this result was not seen in BP or pMBP at the temperatures studied. However, it must be noted that only PhP compares two temperatures with minimal thermal decomposition at either one. It appears that thermolysis of the peroxides alone masks the increase in sensitivity, and this effect will be discussed later.

Trifluoroacetyl peroxide (TFAP) was the final peroxide to be examined. As noted earlier, it was initially run in NB because TFAP proved to be quite sensitive to the ODCB solvent. However, a couple of problems became apparent with NB. First, the pale yellow color of NB made detection of the endpoint difficult. Second, NB was a much better solvent than ODCB for the I^{3-} anion in the titration, so it was more difficult to titrate the two-phase solution accurately. Third, and most important, it was found that SWNTs are not stable as a suspension in NB over time. In as little as three days, a substantial amount of NB would react in an unknown fashion with the SWNTs, resulting in a greatly darkened solution and the SWNTs became coated with some NB-based material. The SWNTs would gain as much as 80% of their own weight through this process.

Because of the problems with NB, ODCB was used as the solvent and the increased decomposition simply tolerated. It was found that the thermolysis could be reduced by a dropwise addition of the peroxide solution to the reaction. Thus, the 25-35% decomposition initially observed in the blank control was reduced to 19.8% at 50 °C. The results are shown in Figure 8.
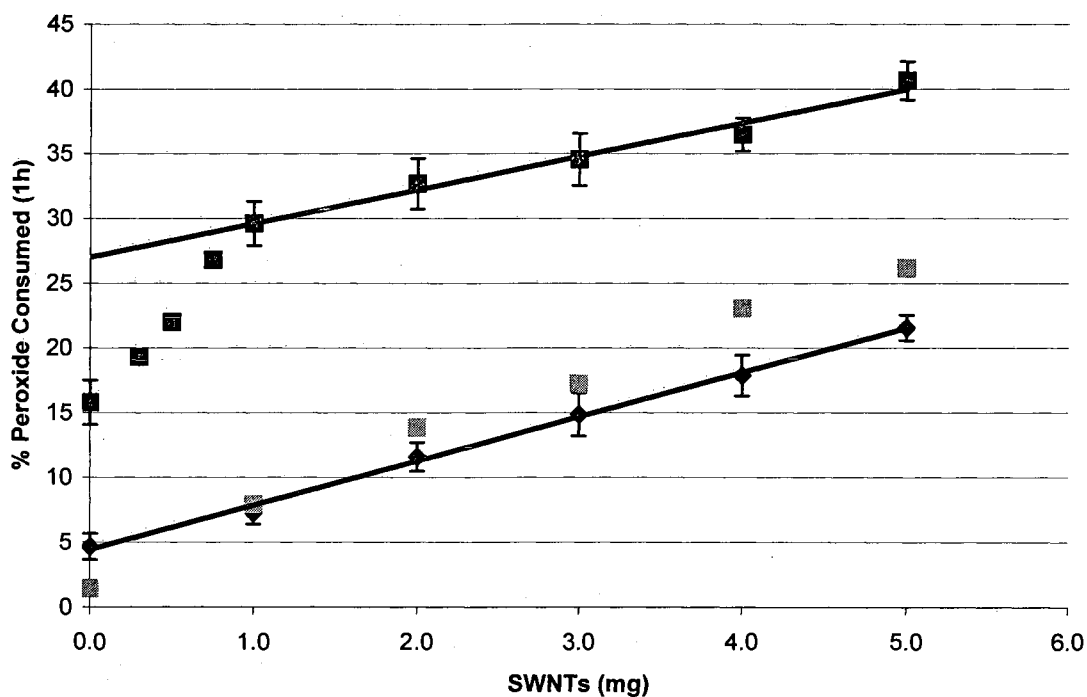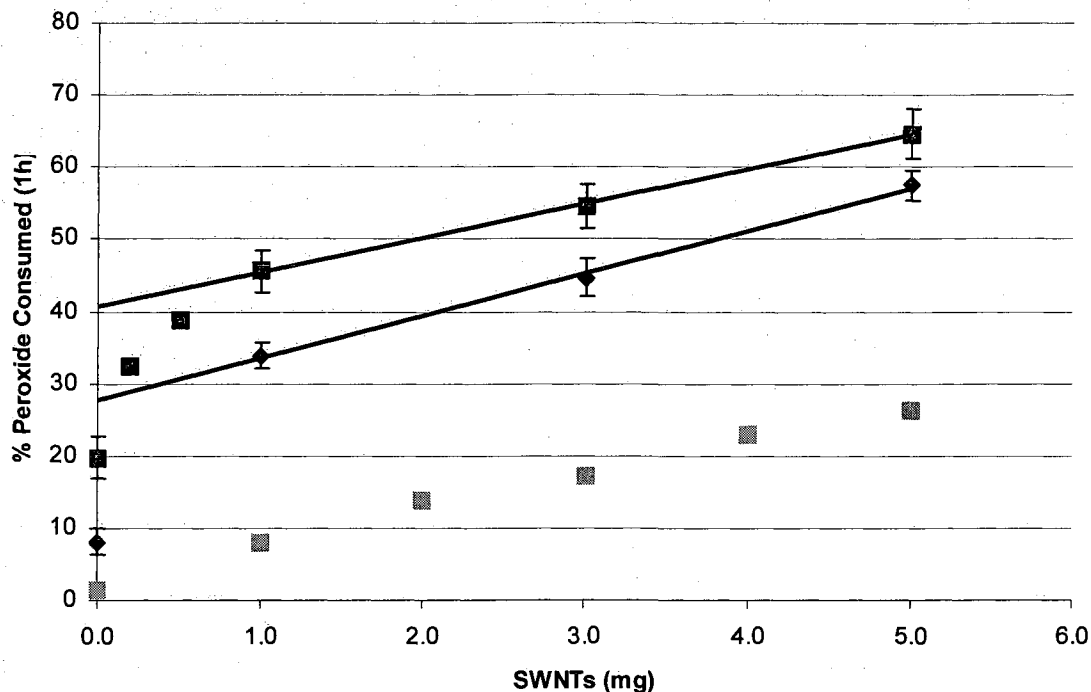
Figure 8. Decomposition of 0.3 mmol TFAP in 1 hour in 50 mL ODCB at 40 and 50 °C

with SWNTs. 40 °C data in black diamonds, 50 °C data in black squares. Grey squares

show BP at 80 °C for reference.

TFAP was substantially more sensitive to SWNTs than either BP or pMBP,

although not quite as sensitive as PhP. However, TFAP was studied at much lower

temperatures (40 °C and 50 °C) than any of the others, owing to its temperature

instability. As seen previously, the substantial thermal decomposition (8.1 and 19.8 % at

40 °C and 50 °C, respectively) led to a steep initial rise in decomposition from the blank

control up to a concentration of 1 mg SWNTs followed by a linear increase in peroxide

decomposition with increasing SWNT concentration up to a concentration of 5 mg

SWNTs. The reason TFAP exhibited no purely linear decomposition curve was that

TFAP underwent too much thermolysis at either temperature employed to avoid the

nonlinear region. This region was measured with two points at 50 °C; there was no

obvious benefit to measure it at 40 °C.

3.2 SWNT Characterization

In order to determine if the SWNTs that had been subjected to peroxide were

functionalized, the SWNTs were analyzed by Raman Microscopy and X-ray

Photoelectron Spectroscopy (XPS). Raman Microscopy is commonly used to determine

primarily the qualitative degree of functionalization of the SWNT sidewall,[6,11,40,41]and

XPS can be used to measure the elemental composition. The two bands used in Raman

Microscopy are the so-called D (diamond) band and the G (graphite) band. The D band is

related to the sp^3 carbons, hence the diamond name, and the graphite band is related to

the sp^2 carbons, hence the graphite name. The ratio of the two (D/G, expressed here as a

percentage) gives an indication of the amount of sp^3 carbons that have been generated on

the sidewall. Analyses were performed with both 780 nm and 633 nm excitation lasers.

The 780 laser primarily excites semiconducting SWNTS, while the 633 nm laser excites

both semiconducting and metallic SWNTs. Examples of the Raman spectra are shown in

Figures 9-12.
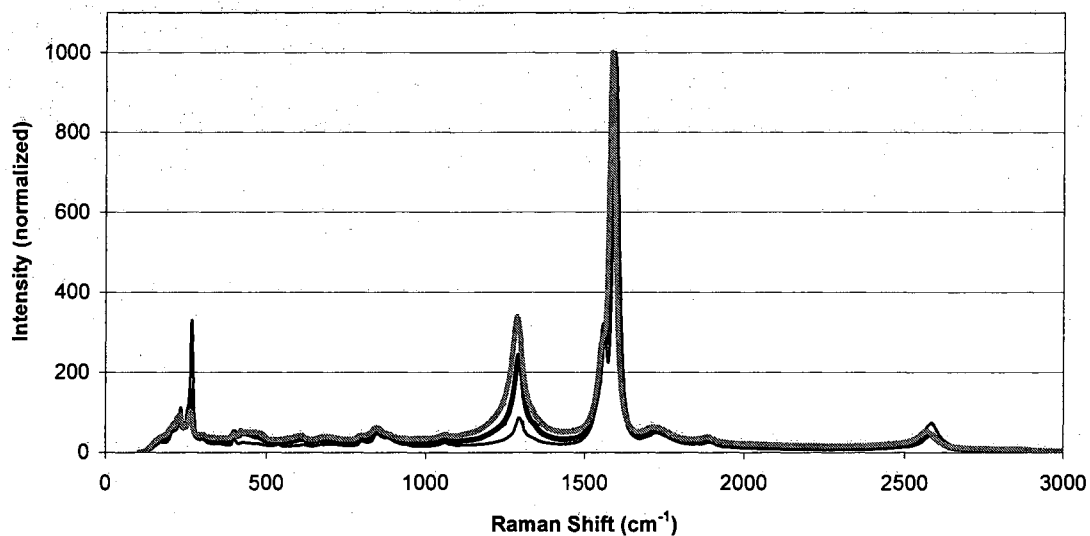
Figure 9. Raman spectra of PhP-treated SWNTs (top, thick gray line) and BP-treated SWNTs (middle, thick black line) vs control (untreated) SWNTs (bottom thin black line). D-band at ~1295, G-band at ~1590.
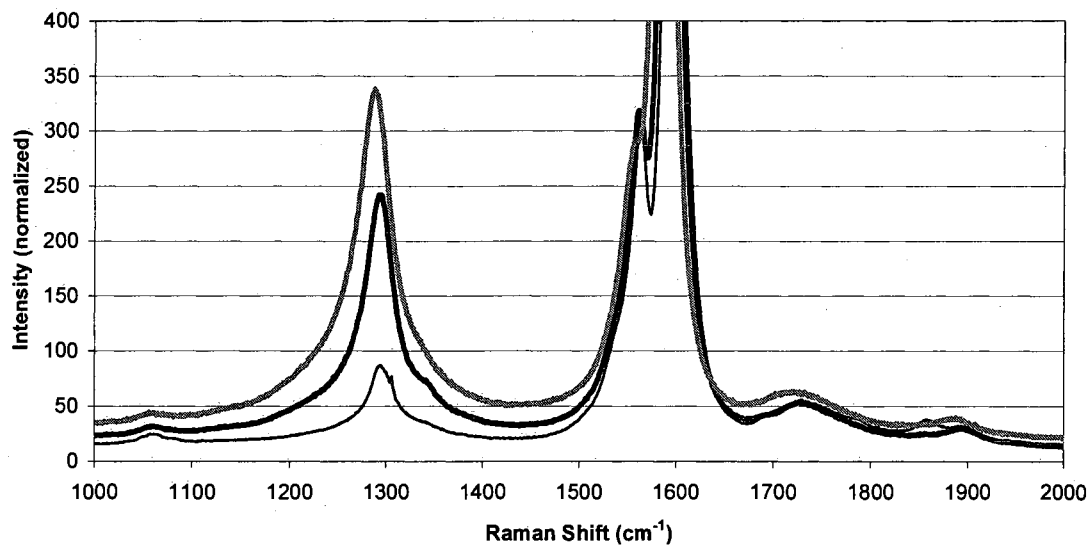
Figure 10. Enlarged view of D and G-band region of Fig. 9. PhP-treated SWNTs (top, thick gray line) and BP-treated SWNTs (middle, thick black line) vs control (untreated) SWNTs (bottom black line).
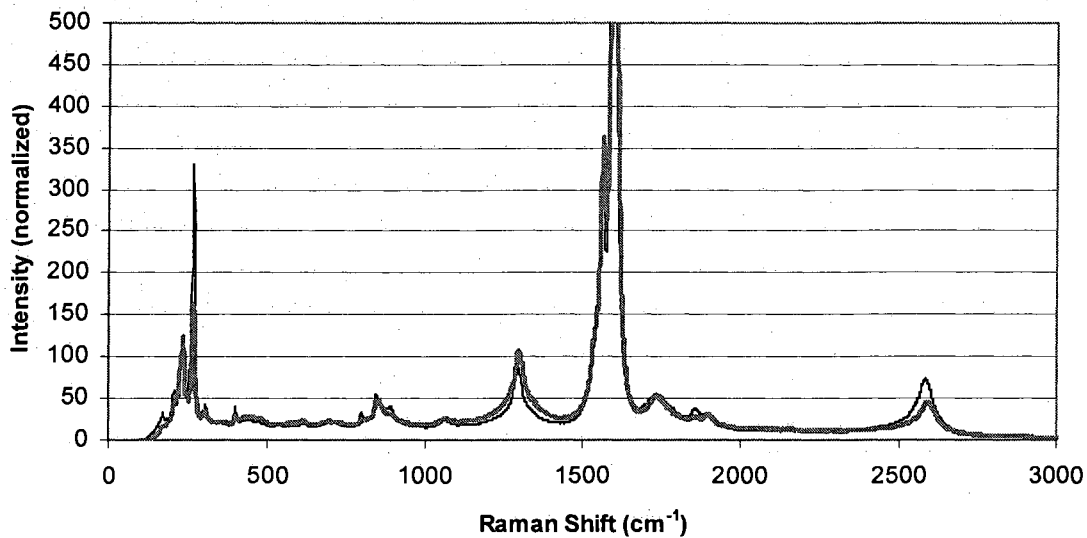
Figure 11. Raman spectra of TFAP-treated SWNTs (thick gray line) vs control

(untreated) SWNTs (black line). D-band at ~1295, G-band at ~1590.
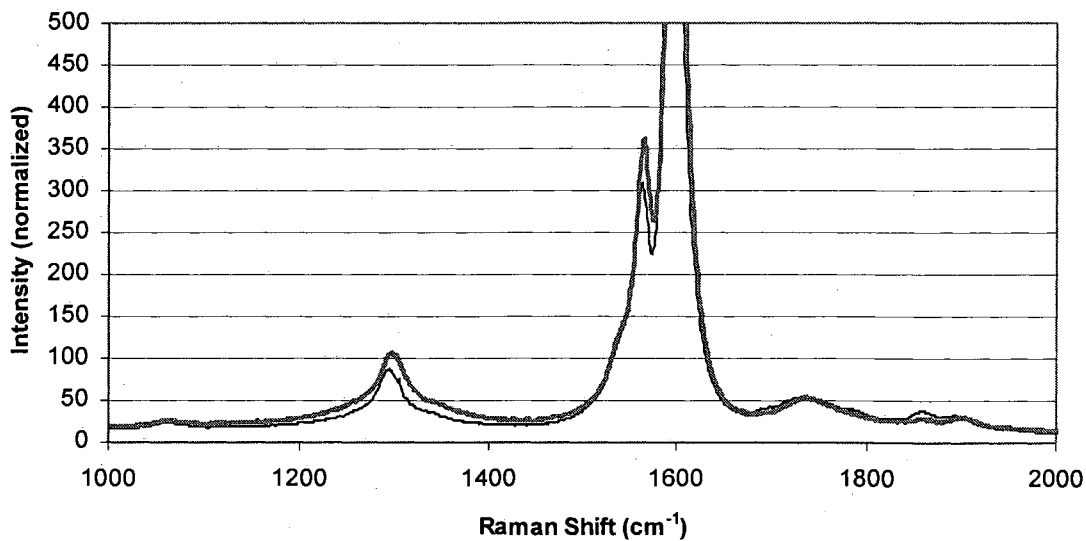
Figure 12. Enlarged view of D and G-band region of Fig. 11. TFAP-treated SWNTs (gray

line) vs control (untreated) SWNTs (black line).

An increase in D/G (as measured by peak height) was seen from 9% in the control to 24% in the BP treated sample, to 24% in the pMBP sample (not shown in the spectra), and to 34% in the PhP sample. Peak height, though commonly used, does not reflect the large amount of broadening seen in the D band. If the peak area was used instead, the ratio increased from 12% in the control to 35% BP, 37% pMBP, and 58% PhP. These increases are accompanied by a decrease in the shoulder peak on the G-band. These results strongly indicate that the peroxides functionalized the SWNTs to a degree that is in rough correspondence with their decomposition rate.

The exception was TFAP. In spite of a very large decomposition rate, TFAP exhibited essentially no change in the D/G band. This result was initially surprising, although closer examination of the literature suggests it should not have been. Those using perfluoroalkyl iodides or those using perfluoroazo compounds to functionalize SWNTs obtained low incorporation levels.[9,10] When using TFAP as a trifluoromethylation reagent, Sawada[35] recorded yields of 70% or lower, even with electron-rich substrates, an excess of TFAP, and running the reaction to complete peroxide consumption. When electron-poor substrates were used, the yield fell to below 20%. It appears, therefore, that trifluoromethyl radicals are simply less reactive than phenyl radicals, possibly due to the greater stability of the fluorinated radical as compared to nonfluorinated analogs.[33]

XPS analysis of the SWNTs is shown in Table 7.

Table 7. Elemental composition (Atomic %) of peroxide treated SWNTs

	Blank Control	BP, 80 °C	pMBP, 80 °C	PhP, 80 °C	TFAP, 40°C
Carbon	94.6	89.8	91.6	80.4	92.8
Oxygen	4.4	9.5	7.3	18.7	5.2
Chlorine	1	0.7	1	0.9	1.3
Fluorine	0	0	0	0	0.7

The XPS data indicate that all SWNTs were functionalized to some degree. As expected, the PhP exhibited the highest level, followed by BP, pMBP, and even some fluorine was seen in SWNTs treated with TFAP. Apparently the Raman method is not sensitive enough to pick up this low a level of functionalization (~1 CF_3 group per 400 carbons). What were not expected were the high levels of oxygen seen. PhP and pMBP both would be expected to cause an oxygen increase because both resultant radicals contain oxygen, but neither BP nor TFAP should contain oxygen in their resultant radicals. Three possibilities exist to explain the discrepancy. First, the carboxyl radical may attack the SWNT before losing CO_2. Second, the carboxylate anion may add back in to the cation on the SWNT. Third, the SWNT radical cation may react with oxygen in solution. Of the three possibilities, attack by the carboxyl radical on the SWNT and addition of the carboxylate anion to the SWNT are the easiest to determine. In either case, the resulting product would contain an ester functionality, and this functionality is identifiable by XPS. Therefore, to determine which route (or routes) took place, the XPS carbon 1s spectra of the SWNTs were closely examined.

The C1s spectra of PhP, BP, TFAP, and untreated SWNTs are shown in Figures 13 and 14.
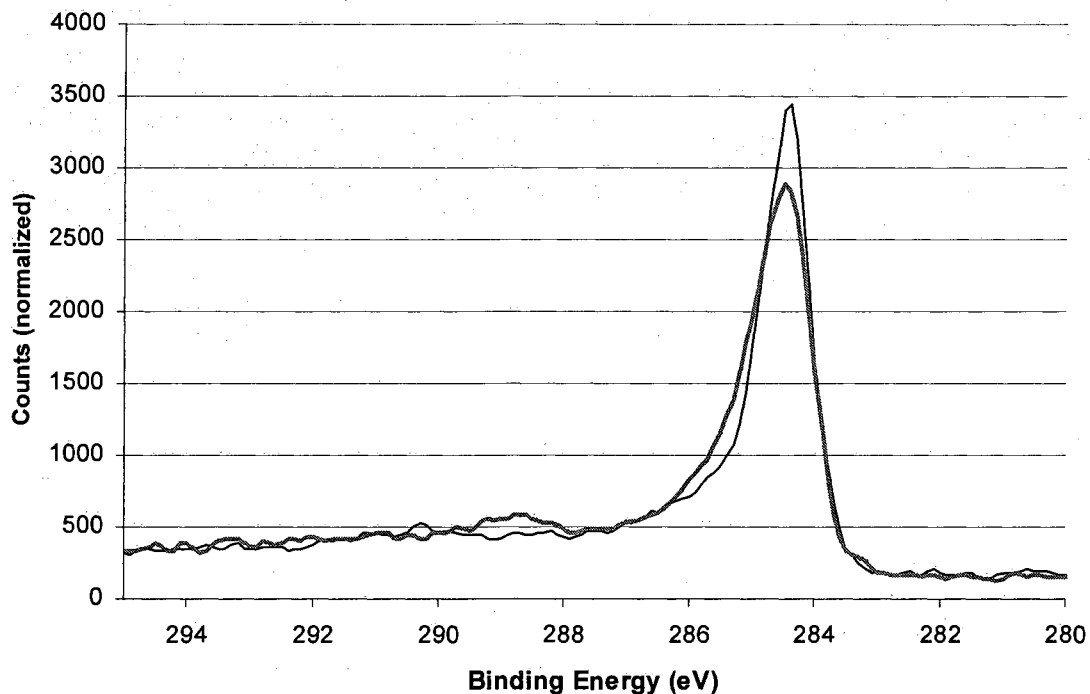
Figure 13. XPS of the C1s region of PhP-treated SWNTs (thick gray line) vs control

(untreated) SWNTs (thin black line)

Since the carboxylate anion from PhP is tethered to the aryl radical, then the ester must

be seen in the spectrum if the radical attacks the SWNT. The spectrum of the PhP sample

clearly showed a peak at 289 eV, consistent with an ester group, and consistent with

expectations. Contrast the spectrum of PhP in Fig. 13 with the spectra of BP and TFAP in

Figure 14.
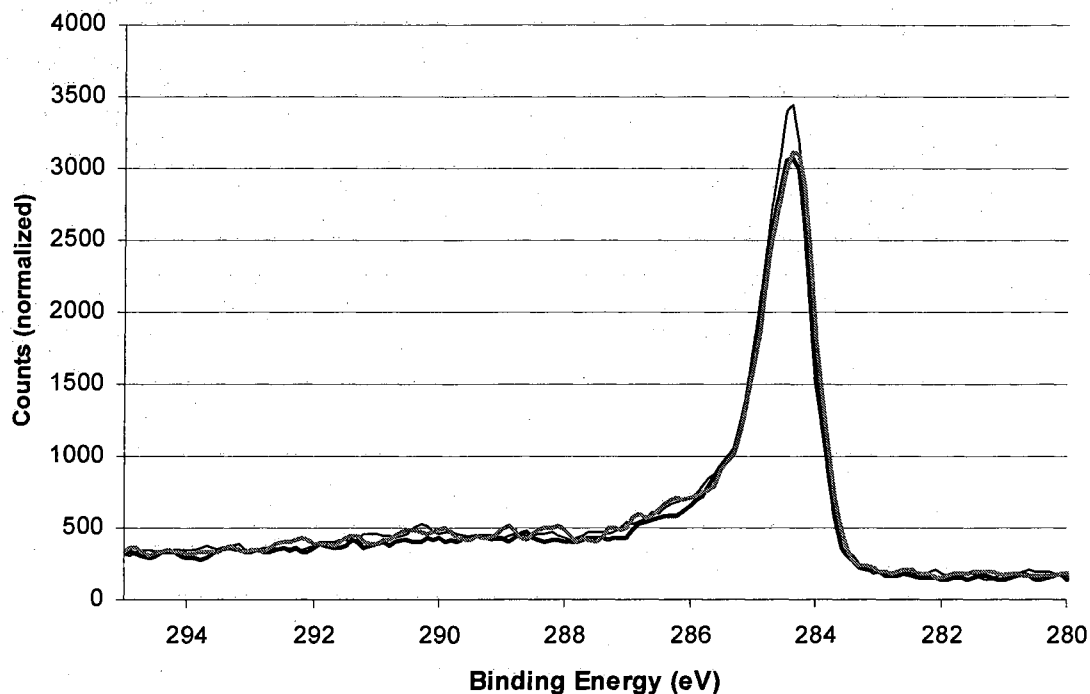
Figure 14. XPS of the C1s region of BP-treated SWNTs (thick black line) and TFAP-treated SWNTs (thick gray line) vs control (untreated) SWNTs (thin black line)

Neither BP nor TFAP treated SWNTs exhibit any peak at 289 eV. Since the level of functionality in TFAP SWNTs was quite low, one might naturally expect that the peak was too small to detect, but certainly a peak should be seen in the case of BP. Therefore, it appears that neither the carboxyl radical nor the carboxylate anion were responsible for the oxygen increase, leaving dissolved oxygen as the remaining possibility.

To determine if oxygen in solution was the cause of the excess oxygen in the XPS data, runs of BP, pMBP, and PhP were made in both fully degassed ODCB and in oxygen-rich ODCB, produced by sparging gaseous oxygen into the reaction flask continuously during the reaction. The titration results are seen in Figures 15-17.
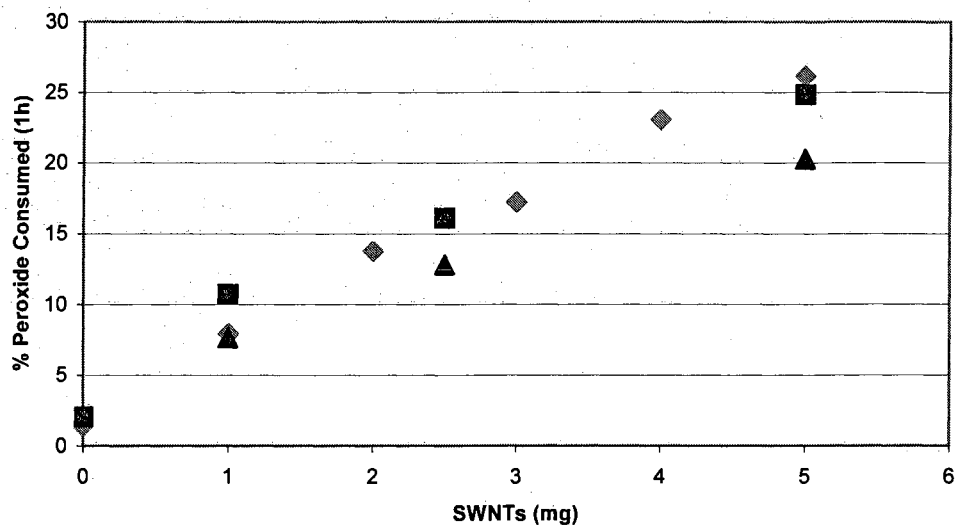
Figure 15. BP decomposition at 80 °C with SWNTs in degassed and oxygenated solvent. Degassed ODCB (black squares), oxygenated ODCB (black triangles), and original non-degassed ODCB (gray diamonds).
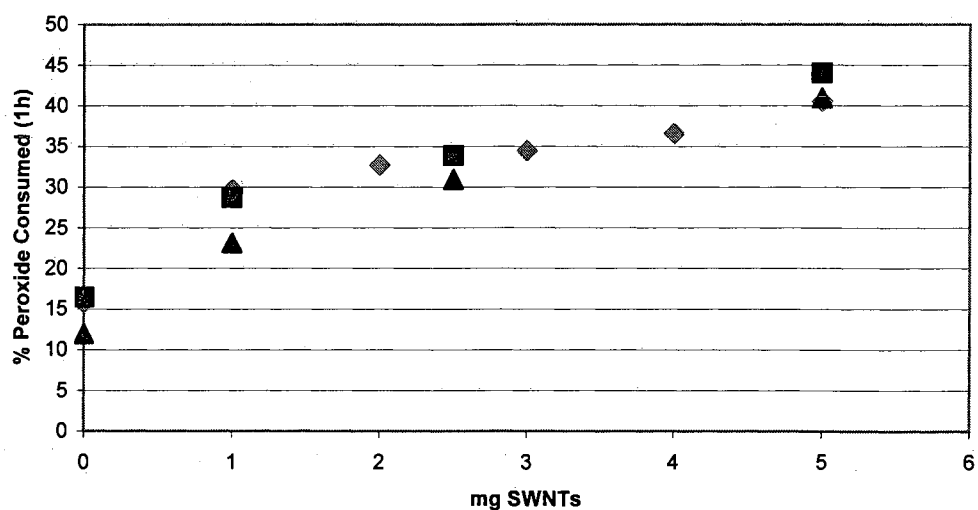
Figure 16. pMBP decomposition at 80 °C with SWNTs in degassed and oxygenated solvent. Degassed ODCB (black squares), oxygenated ODCB (black triangles), and original non-degassed ODCB (gray diamonds).
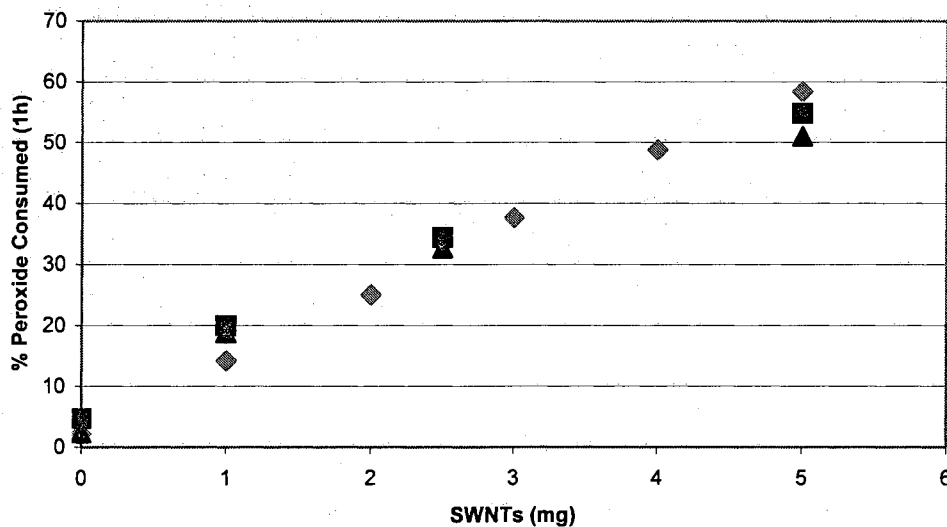
Figure 17. PhP decomposition at 80 °C with SWNTs in degassed and oxygenated solvent. Degassed ODCB (black squares), oxygenated ODCB (black triangles), and original non-degassed ODCB (gray diamonds).

These runs were made with a different batch of SWNTs (162-8) because the original batch had run out. All are single-point runs. The decomposition trends are the same as before, except that the new batch of SWNTs was slightly less effective at inducing decomposition. The apparent lower level of consumption in the oxygenated runs was probably the result of the oxygen interfering slightly with the titration (dissolved oxygen can oxidize I⁻ in solution).[39]

XPS results of the degassed vs oxygen runs clearly showed a difference in the amount of oxygen present, shown in Table 8.

Table 8. XPS of SWNTs from degassed ODCB runs vs SWNTs from oxygenated ODCB runs

SWNTs (mg)	Peroxide	Atomic % Oxygen in Radical	Atomic % Oxygen	
			Degassed ODCB	Oxygenated ODCB
1.0	BP	0	3.3	8.5
2.5	BP	0	4.1	8.9
5.0	BP	0	4.0	8.3
1.0	pMBP	12.5	4.8	9.5
2.5	pMBP	12.5	5.2	9.9
5.0	pMBP	12.5	5.6	10.0
1.0	PhP	22.2	11.1	16.1
2.5	PhP	22.2	11.3	15.8
5.0	PhP	22.2	13.2	16.2

As a blank control, 5 mg SWNTs were stirred in 50 mL ODCB (not degassed) using the same protocol as before but omitting the peroxide. The oxygen level in the blank control was 4.4%. The atomic % of oxygen in the radical is calculated by the number of oxygen atoms divided by the total number of non-hydrogen atoms (XPS cannot detect hydrogen so it is ignored in XPS analyses). For the degassed runs, the oxygen level remained flat with increasing SWNTs in BP, increased slightly in pMBP, and increased substantially in PhP, consistent with the oxygen level of the attacking radical and the % consumption of peroxide. Notably, the oxygen level in oxygenated runs was relatively flat in pMBP and PhP (as well as in BP) from 1 to 5 mg SWNTs. This result is perfectly sensible: more SWNTs led to more decomposition, but then there were more SWNTs available for functionalization, so the amount of functionalization itself should have remained flat.

However, when oxygen was present, the oxygen level shot up for all runs, approximately 4-5% higher than the degassed equivalent. Thus it appears clear that dissolved oxygen in the solvent becomes incorporated into the SWNTs, most likely through direct reaction of the SWNT radical cations with the dissolved oxygen. It is possible that the phenyl or trifluoromethyl radical reacts with the oxygen first, forming a peroxy radical that subsequently attacks the SWNT. However, as it has been shown that SWNTs do not inhibit the autooxidation of cumene,[32] this route is not considered likely.

The Raman data from the deoxygenated XPS samples are shown in Table 9.

Table 9. Raman D/G ratios of SWNTs from degassed runs at 780 and 633 nm excitation. Data at 780 nm for pMBP are missing because of equipment failure.

		D/G ratio	
Peroxide	SWNTs (mg)	780 nm	633 nm
Blank		11.9	7.6
BP	1	16.3	14.3
BP	2.5	21.1	13.5
BP	5	19.9	13.8
pMBP	1	N/A	7.7
pMBP	2.5	N/A	8.7
pMBP	5	10.1	7.2
PhP	1	30.5	27.4
PhP	2.5	29.0	23.6
PhP	5	28.0	27.5

As with the XPS data, Raman data show similar functionalization levels regardless of the SWNT concentration. The Raman data clearly show that BP functionalizes SWNTs more

than pMBP. In fact, the D/G ratios of pMBP indicate no change from the blank control, although XPS data (Table 8) do show an increase in oxygen, indicating some degree of functionalization. The Raman method does not appear to be sensitive enough to pick up this lower level of functionalization. This result is in contrast with earlier data from the non-degassed runs. Those runs indicated that BP and pMBP functionalized SWNTs to a similar degree. However, as the degassed runs have been made with a different batch of SWNTs, the answer is very likely a difference in the SWNTs themselves. The second batch of SWNTs was slightly less reactive than the first, so it is not surprising that pMBP, the more electron-rich peroxide, was less reactive toward the SWNTs than BP.

Since the functionalization level was generally flat with a fixed peroxide concentration and increasing SWNT concentration, the functionalization level with fixed SWNT concentration and an increasing peroxide concentration was examined. The Raman results are shown in Table 10.

Table 10. Raman D/G ratios of SWNTs from degassed runs at 780 and 633 nm excitation. Data at 780 nm for pMBP are missing because of equipment failure.

Peroxide	Amount of Peroxide (mmol)	D/G ratio	
		780 nm	633 nm
Blank	0	11.9	7.6
BP	0.15	17.7	14.1
BP	0.33	21.1	13.5
BP	0.6	23.0	16.2
pMBP	0.15	13.8	9.7
pMBP	0.3	N/A	8.7
pMBP	0.6	24.9	17.2
PhP	0.15	31.4	29.3
PhP	0.3	29.0	23.6
PhP	0.6	35.4	25.9
TFAP	0.15	9.0	6.3
TFAP	0.3	9.2	6.3
TFAP	0.6	9.0	5.6

BP and pMBP both exhibited a general increase with increasing peroxide concentration. PhP appeared to show a slight increase at 780 nm but it was essentially flat (within experimental error) at 633 nm. The PhP-treated SWNTs are quite highly functionalized even at low peroxide levels, and as shown earlier, functionalized SWNTs are less effective at induced decomposition, thus reducing the impact of additional peroxide. Furthermore, the relatively poor sensitivity of Raman spectroscopy may have had an impact as well. TFAP, as before, shows no increase over the blank, the D/G ratio flat within experimental error. The trifluoromethyl radical is simply not as reactive as the

phenyl radical, and Raman is not sensitive enough to detect low levels of

functionalization.

The XPS data, shown in Table 11, tell a similar story.

Table 11. XPS of SWNTs from degassed runs

	BP		pMBP		
	2.5 mg SWNTs		2.5 mg SWNTs		
Amount of Peroxide (mmol)	Carbon	Oxygen	Carbon	Oxygen	
0.15	94.3	4.1	90.3	3.9	
0.3	94.2	4.1	92.5	5.2	
0.6	94.4	4.0	89.6	8.2	
	PhP		TFAP		
	2.5 mg SWNTs		2.5 mg SWNTs		
Amount of Peroxide (mmol)	Carbon	Oxygen	Carbon	Oxygen	Fluorine
0.15	88.2	10.4	92.6	4.5	1.4
0.3	86.8	11.3	92.1	4.3	2.5
0.6	80.7	17.5	91.8	4.4	2.6

As seen before, when the solvent is degassed the oxygen level of the BP treated SWNTs

and the TFAP treated SWNTs remained close to the control, i.e. 4.4% oxygen. The XPS

data clearly showed an increase in oxygen level, and therefore an increase in functionality

in the two oxygen containing peroxides, pMBP and PhP, with increasing peroxide level.

TFAP even shows a slight increase in fluorine level, demonstrating that even though it is

much less reactive, it still functionalized the SWNTs to some degree.

More interesting is the information contained in the XPS C1s spectra, shown in Figures 18 and 19.
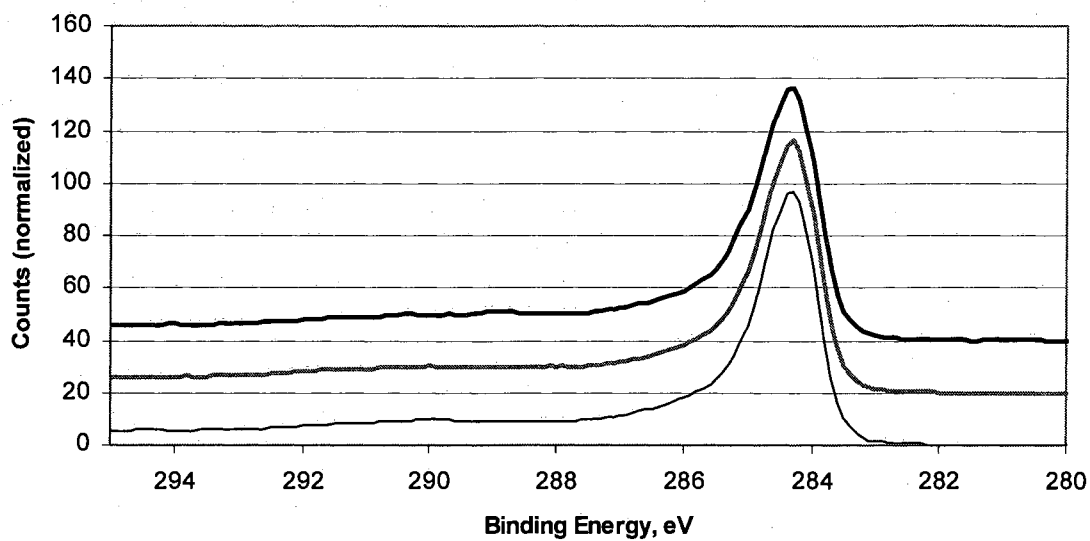
Figure 18. Offset C1s XPS spectra of BP-treated SWNTs (top, thick black line) and TFAP-treated SWNTs (middle, thick gray line) vs control (untreated) SWNTs (bottom, thin black line)
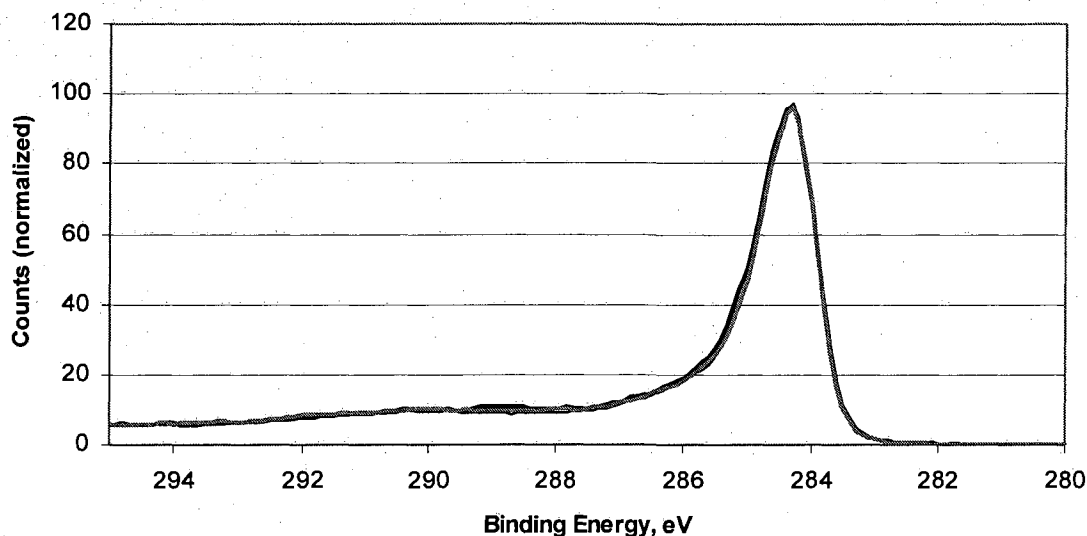
Figure 19. Overlay C1s XPS spectra of BP-treated SWNTs (thick black line) and TFAP-treated SWNTs (thick gray line) vs control (untreated) SWNTs (thin black line)

Neither the BP nor TFAP exhibit any substantial peak at 289 eV, indicating no ester present in the functionalized SWNTs. BP shows a tiny hint of a peak, possibly indicating a very slight amount of carboxylate anion added to the SWNT cation, but certainly nothing conclusive. In all other respects, both curves are identical with the blank control. One might expect to see a peak at 292 eV in TFAP treated SWNTs arising from the CF_3 carbon, but 2.6% fluorine only translates into about 0.8% carbon. This carbon level is probably too little to see in the C1s spectrum, especially considering the broad peak from about 288 eV to almost 293 eV that arises from the shake up electrons.

The XPS C1s spectra of pMBP and PhP treated SWNTs are shown in Figures 20 and 21.
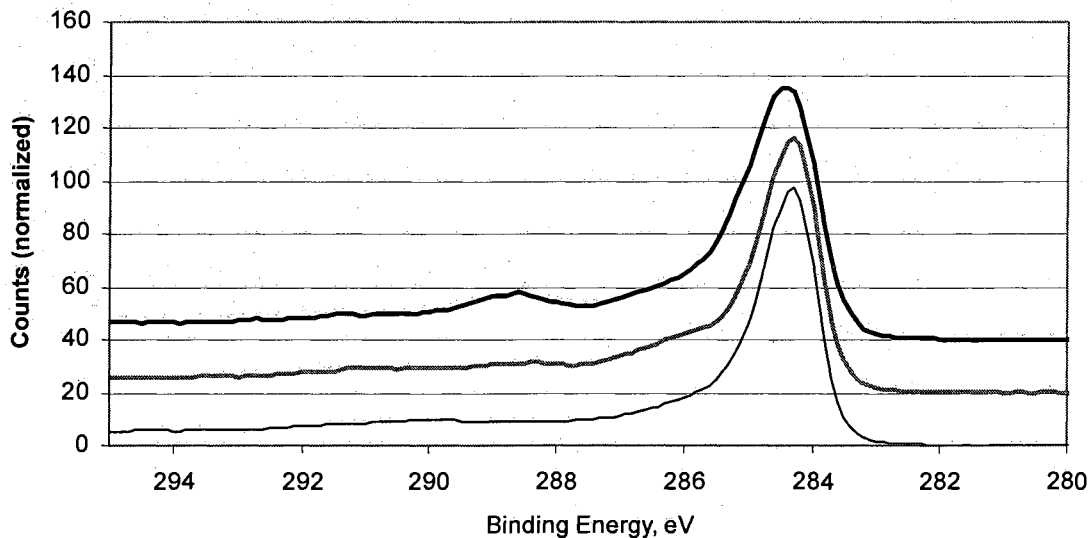
Figure 20. Overlay XPS C1s spectra of PhP-treated SWNTs (top, thick black line) and pMBP-treated SWNTs (middle, thick gray line) vs control (untreated) SWNTs (bottom, thin black line)
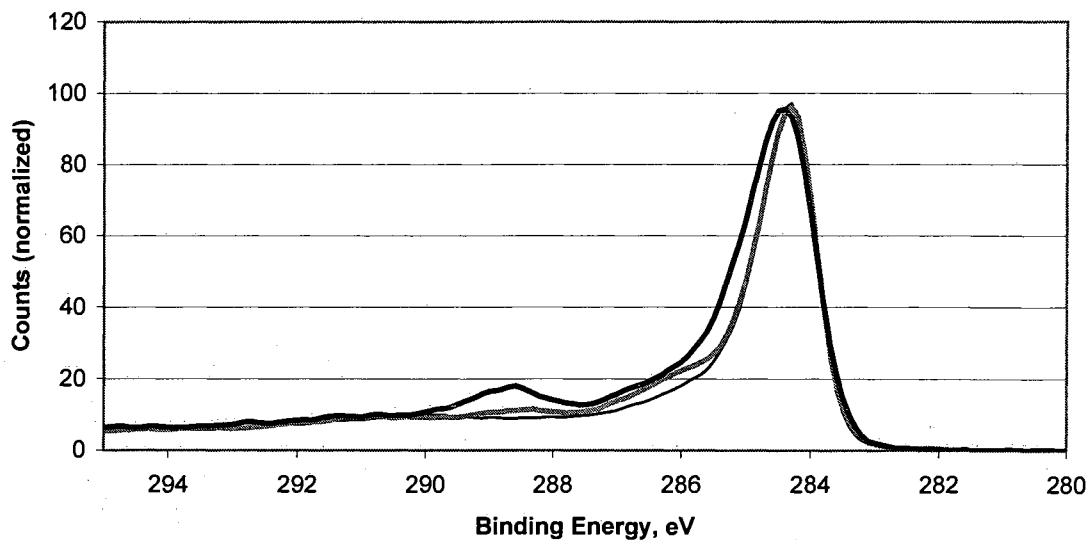
Figure 21. Overlay XPS C1s spectra of PhP-treated SWNTs (thick black line) and pMBP-treated SWNTs (thick gray line) vs control (untreated) SWNTs (thin black line)

pMBP and PhP-treated SWNTs exhibited very different spectra compared to the BP and TFAP-treated SWNTs. In the case of pMBP treated SWNTs, there was a distinct shoulder at 286-287 eV that originated from the two ether carbons (one from the methyl carbon of the methoxy group and one from the ring carbon where the methoxy group attaches). There was also a small peak at 289 eV, very similar to the tiny peak in the BP SWNT spectrum. As with BP, this peak suggests that a small amount of carboxylate anion may add to the SWNT cation, but it is again not conclusive and at best an infrequent occurrence. PhP exhibits a number of different features, most notably the ester peak at 289 eV, but also a large shoulder at around 285.5 eV. The 289 eV peak arises from the carbonyl carbon of the ester group, and the 285.5 eV shoulder arises from the alpha carbon next to the carbonyl. The most important feature, however, is the presence of the shoulder at about 287 eV. This is the proper energy for an ether-type carbon in an ester. This peak is conclusive evidence that the tethered carboxylate anion adds to the SWNT cation and forms a lactone. If it did not cyclize, the free carboxylate group should remain open as the free acid, and a peak at 287 eV would not be seen. Since the peak was observed, the carboxylate anion must have esterified, and the only species present that one may reasonably expect to do so is the SWNT cation.

Chapter 4. SWNT Induced Decomposition of Peroxides: Conclusions

SWNTs induce the decomposition of bis-acyl peroxides via a single electron transfer (SET) mechanism. Studies with electron-rich aromatics and C_{60} have concluded that this is the operative mechanism in acyl peroxide decomposition.[34,50] Benzene accelerates the decomposition of perfluorinated peroxides such as TFAP by a factor of 2.7 to 4.2.[35] Calculation of the energy levels of the antibonding molecular orbitals has shown that they are reduced compared to nonfluorinated compounds. As a result, they are excellent electron acceptors. Similarly, studies of PhP with styrene and polynuclear aromatics[38] and studies of aryl diazonium salts with SWNTs[6] also support the SET mechanism. The proposed mechanism is that SWNTs reduce bis-acyl peroxides to radical anions, which immediately undergo O-O bond scission. The carboxyl radical quickly loses CO_2 followed by attack of the radical on the SWNT radical cation. In the case of TFAP, there is very likely a high degree of recombination of the trifluoromethyl radicals to form C_2F_6, which is subsequently lost.[35] The subsequent path depends on the initial peroxide used. For the cyclic peroxide PhP, the path appears fairly certain, as shown in Figure 22.
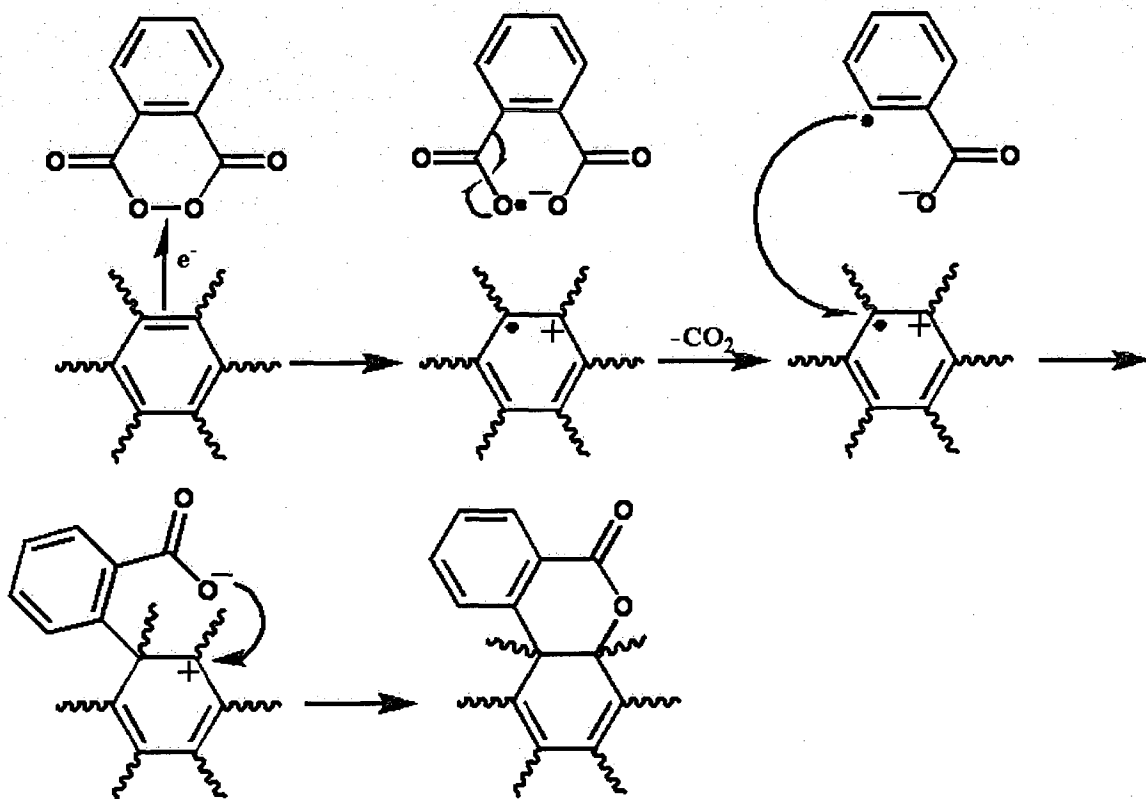
Figure 22. Induced decomposition pathway of PhP

For clarity the SWNT sidewall is shown as a single aromatic ring. After attack of the aryl radical, the tethered carboxylate group adds to the cation and forms a lactone. It is possible that the presence of the carboxylate group enhances the ability of the radical to attack the SWNT. The electrostatic attraction between the anion and the SWNT cation may serve to keep the radical in close proximity to the SWNT, increasing the functionalization efficiency of the radical. The XPS spectra, especially the presence of the ester and ether-type carbon signals, strongly support this conclusion.

For acyclic peroxides, the pathway for C_{60} has been established by Yoshida.[50] With SWNTs it is not as clear what happens to the carboxylate anion. It may add to the SWNT cation and remain as the ester or the ester may be hydrolyzed to the alcohol. The

carboxylate may not recombine with the SWNT at all and end up as a byproduct. The absence of an ester-type carbon in the C1s spectra from the XPS strongly suggests that it does not end up as the ester, at least not in any substantial amount. This result also argues against hydrolysis to the alcohol, as not only is there no work-up as there is in the C_{60} case, but the lack of an increase in oxygen in the degassed samples (for BP and TFAP) further indicates that there is no added functionality.

Likewise, in the acyclic case the fate of the SWNT cation is undetermined, especially when TFAP is the peroxide. If the solvent is not degassed, then the radical cation may react with the oxygen present in solution. It cannot be proven whether the peroxide radical or the SWNT radical cation reacts with the oxygen. However, the amount of dissolved oxygen incorporated into the SWNT is fairly constant across all of the peroxides tested (BP, pMBP, and PhP- degassed/ oxygenated runs of TFAP were not made). One would expect that if the peroxide radical attacked oxygen and then attacked a SWNT, then sensitive peroxides such as PhP should incorporate more oxygen than less sensitive peroxides like BP. Furthermore, in the case of TFAP, an increase in fluorine should be observed. Given that PhP, with the highest percent decomposition, shows a similar oxygen increase to the other peroxides upon switching from degassed to oxygenated solvent, and given that TFAP shows no increase in fluorine when non-degassed solvent is used, reaction of oxygen with the SWNT radical cation seems more likely. It should be noted that the SET mechanism is probably not the sole mechanism, as radicals are known to attack SWNTs.[7-11]

The degrees of acceleration of the decomposition of these peroxides by SWNTs are in line with expectations based on electronic and steric factors.[30,35,36] The sensitivity

increases as pMBP<BP<<TFAP=PhP. Both the electron-poor TFAP and the sterically strained PhP exhibited much higher sensitivity to induced decomposition. It is somewhat difficult to compare PhP and TFAP as the solvent sensitivity of TFAP necessitates a lower operating temperature, but they are quite close. In all cases, the decomposition is linear with respect to SWNT concentration above 1 mg SWNTs/ 50mL solvent.

The behavior of the peroxides below 1 mg/ 50 mL is particularly interesting. If there is no or minimal thermal decomposition, then the curve is linear from 0 through 5 mg SWNT concentration. At temperatures high enough to cause unimolecular thermolysis, the curve changes dramatically. The low concentration region, below 1 mg, shows a much steeper slope than the slope above 1 mg, and is likely not truly linear. In contrast, above 1 mg the decomposition curve is linear and comparable to the decomposition curve from reactions where minimal thermolysis takes place. This phenomenon is probably coupled to the odd observation that the slope of the linear region decreases at higher temperatures for these peroxides.

In the situation where thermolysis is negligible, the only decomposition pathway present is via the induced SET mechanism. An increase in reaction temperature should increase the sensitivity of the peroxide to induced decomposition. Thus, when the temperature is increased, if thermolysis does not increase substantially at the higher temperature, the slope of the curve should steepen. An example of this behavior is PhP, whose slope increases from 8 to 11 going from 70 °C to 80 °C. The situation becomes markedly more complex when a change in temperature introduces thermolysis. First, a second decomposition pathway is now available. Second, and far more important, this pathway drastically increases the concentration of radicals in solution. All of these

peroxides are known to autoinduce;[30,35,36] thus, a small increase in unimolecular thermolysis can lead to a large increase in overall decomposition (thermolysis + autoinduced). When a very small amount of SWNTs are added, the effect on the thermal pathways is negligible and the induced decomposition merely adds to the others (total rate=thermolysis + autoinduced + SWNT induced). As the concentration of SWNTs increases, two new effects begin to show. One, more peroxide decomposes via SWNT induction, reducing the concentration of peroxide and reducing the unimolecular thermolysis rate; and two, the SWNTs act as radical scavengers, lowering the overall concentration of radicals in solution. Since autoinduction is dependent on the concentration of radicals in solution, the presence of the SWNTs begins to reduce the autoinduction effect. The data suggest that the reduction of the autoinduction effect occurs at around 1 mg SWNTs/ 50 mL, giving a transition to a smooth linear region. This process also explains the drop in the slope at higher temperatures. At lower SWNT concentrations, the autoinduction effect artificially increases the apparent decomposition rate, and at higher concentrations the effect is essentially absent. Thus the overall slope is reduced, and a large initial increase is observed.

Chapter 5. Non-covalent SWNT Encapsulation Into Water-Soluble PEG-eggs: Background and Literature Review

SWNT nanoparticles have attracted attention as potential therapeutic agents, either as molecular transporters or as thermoablation targets. As transporters, SWNTs can carry biologically active compounds into cells. Molecules that have been carried into cells include peptides and proteins, [51,52] as well as larger molecules such as DNA for gene delivery. [53,54] *In vivo* studies indicate that the functionalized SWNTs are cleared via the renal system. [55] This process requires the SWNTs to be water soluble, and this solubility is normally achieved by covalently functionalizing the SWNTs. In some instances, the SWNTs may be noncovalently functionalized, as in the case of transporting some oligonucleotides that are freed by endosomal rupture. [55] As thermoablation targets, the SWNTs are simply heated by near-infrared (NIR) radiation resulting in cell death. [53] NIR radiation from 700-1,100 nm is not absorbed by biological systems, but this radiation is strongly absorbed by SWNTs. [53] This difference in absorption can be exploited to selectively kill cells, using the SWNT as a target.

Regardless of use, SWNTs used in biological systems must be water soluble to function properly. Covalent functionalization, while useful, has several limitations. Carboxylic acids and sulfonic acids are the most common groups for imparting water solubility. Unfortunately, these side groups are subject to charge screening *in vivo*, where the negatively charged ions are "screened" by cations, reducing the effective concentration of the negatively charged species. [56] This screening of the side chains results in bundling of the SWNTs. [1,47,49] Additionally, covalent functionalization disrupts

the extended pi system of the nanotube, greatly affecting its electronic properties. In particular, heavy functionalization of a SWNT results in the loss of the NIR fluorescence.

To maintain the desired electronic properties, therefore, noncovalent functionalization is required. As discussed in the background chapter on peroxides, noncovalent modification involves the wrapping of the SWNT with a polymer or oligomer without chemically attaching the molecule to the nanotube. The polymer or oligomer is held in place by pi-stacking or Van der Waals forces.[4] This approach to modification leaves the extended pi-system of the SWNT intact, preserving the SWNTs electronic properties. The wrapping molecule will modify some of the physical properties of the tube. The most commonly desired physical modification is to put the normally water-insoluble nanotubes into aqueous solution.[4,5]

There are a number of materials available for the noncovalent functionalization of SWNTs. Surfactants such as sodium dodecylsulfate[4,57] are commonly used, as are a number of polymeric materials such as polystyrenesulfonate or polyvinylpyrrolidone.[4] Poly(ethylene glycol) (PEG) is an attractive polymer for achieving biocompatible, noncovalently functionalized water-soluble SWNTs. Although PEG by itself is not capable of noncovalently functionalizing SWNTs,[4] when modified with an appropriate endgroup or polymer block it can be successfully used. Polythiophene-terminated PEG is an example of an endgroup-modified PEG-based polymer,[58] and poloxamers, diblock copolymers of PEG and polypropylene oxide, are examples of block polymer- modified PEG.[1]

The compatibility of PEG in biological systems is well known, and it has been shown to protect or "shield" nanoparticles *in vivo*.[59,60,61] As such, it prevents uptake by

the reticuloendothelial system, increasing the amount of time the material remains in tissues. In addition to the shielding effect, PEG also increases the perceived size of the nanoparticle, thus reducing renal filtration and further increasing circulation times *in vivo*.[15] However, poloxamer-encapsulated SWNTs are not suitable for *in vivo* use. The polymer is easily and rapidly displaced by blood sera proteins, eventually resulting in accumulation of the SWNTs in the liver.[62] To combat this displacement, a new PEG-based encapsulation was developed,[6] the "PEG-egg". Figure 23 shows a schematic of the PEG-egg.
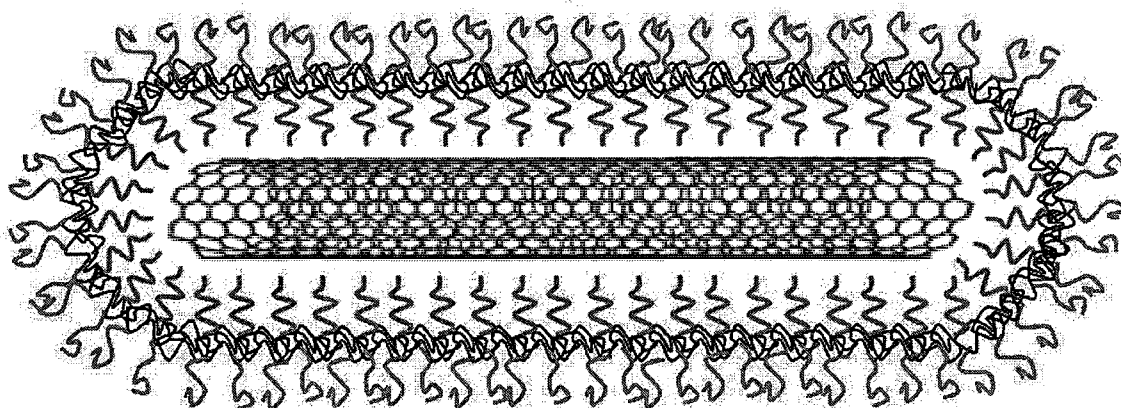
Figure 23. PEG-egg structure: SWNT in center, PS block in gray (inner layer), PAA block in black (middle layer), and PEG block in light gray (outer layer)[1]

PEG-eggs are SWNTs non-covalently encapsulated by a triblock copolymer of PEG-poly(acrylic acid)-polystyrene (PEG-PAA-PS). The polystyrene block provides the necessary endblock to permit encapsulation of the SWNT,[4] and the PEG block provides the water solubility, biocompatibility and biostability.[63,64] The center PAA block provides a means for crosslinking the micelle to prevent displacement of the polymeric shell by

proteins. These PEG-eggs are based on materials and structures developed by Wooley[65] and Taton.[66] In both cases, they used amphiphilic block copolymers in a solvent/nonsolvent system to generate micelles that were subsequently fixed by crosslinking the outer shell.

Wooley constructed what she described as "shell cross-linked knedel-like structures" (SCK's).[65] These structures were two-layered nanospheres based on a diblock copolymer, polystyrene-block-poly(acrylic acid) (PS-PAA), which was made by sequential anionic polymerization. Thus, styrene was first polymerized at −78°C using sec-butylithium as the initiator. After the polymerization was complete, the living polstyryl anions were modified with 1,1-diphenylethylene to moderate their reactivity. After modification, t-butyl acrylate was added to polymerize the final block. The resulting diblock was purified and the t-butyl groups hydrolyzed in toluene with p-toluenesulfonic acid. The polymer was dissolved in tetrahydrofuran (THF) and formed controlled-spherical micelles when water was slowly added. The micelles were easily deformed by drying or adsorption, but when the micelles were crosslinked with a carbodiimide activator and a diamine crosslinker they formed stable, non-deformable water-soluble spheres.

Taton used the same polymer to make similar structures but extended it to include micelles with SWNTs encapsulated in the center of the micelle.[66] Using dimethylformamide (DMF) as solvent, he suspended SWNTs in a DMF/polymer solution by ultrasonication. Water was added slowly to promote micellization, as in the formation of SCK's. The SWNT-encapsulated micelles were not isolable until they had been

crosslinked like the SCK's. At this point, the SWNTs became completely trapped within the micelle and could be recovered and redissolved in water.

The approach taken by Wang[1] built upon these structures. By adding a PEG chain to the PAA end of the diblock, a micelle could be created that had all of the advantages of Taton's micelles plus the biological advantages of the PEG. Furthermore, with a PEG outer shell, a high degree of crosslinking could be achieved without the danger of micelle-micelle crosslinks forming.[67]

The required polymer, PEG-PAA-PS was similar to the polymers synthesized by Tang[68] and Niu.[69] Tang synthesized a methoxy-terminated PEG (MPEG) copolymer with a poly(2-(dimethylamino)ethyl methacrylate) middle block and a poly(2-(diethylamino)ethyl methacrylate) terminal block while Niu synthesized a MPEG-copolymer with a polystyrene middle block and a poly (acrylic acid) terminal block. Both used atom transfer radical polymerization (ATRP)[70,71] to synthesize the required polymer, and both started with a bromine terminated MPEG macroinitiator as developed by Chen.[72]

ATRP proceeds by the mechanism shown in Figure 24.[70]

$$R\text{-}X \ + \ M_t^n\text{-}Y \ / \ Ligand \xrightleftharpoons[k_{dead}]{k_{act}} R^\bullet \ + \ X\text{-}M_t^{n+1}\text{-}Y \ / \ Ligand$$

k_p monomer k_t termination

$$R\text{-}Br \ + \ CuBr\text{-}L \xrightarrow{k_{act}} R^\bullet \ + \ CuBr_2\text{-}L \qquad \textbf{Initiation}$$

$$R^\bullet \ + \ Monomer \xrightarrow{k_p} R\text{-}P_{(n)}{}^\bullet \qquad \textbf{Propagation}$$

$$R\text{-}P_{(n)}{}^\bullet \ + \ Monomer \xrightarrow{k_p} R\text{-}P_{(n+1)}{}^\bullet \qquad \textbf{Propagation}$$

$$R\text{-}P_{(n)}{}^\bullet \ + \ CuBr_2\text{-}L \xrightarrow{k_{deact}} R\text{-}P\text{-}Br \ + \ CuBr\text{-}L \qquad \textbf{Deactivation}$$

$$R\text{-}P_{(n)}{}^\bullet \ + \ R\text{-}P_{(m)}{}^\bullet \xrightarrow{k_t} R\text{-}P_{(X)}\text{-}R \qquad \textbf{Termination}$$

Figure 24. Reaction sequence for ATRP. The top line shows the generic reaction sequence; the bottom lines show the individual steps (with copper as the metal)

In the reactions used by Tang and Niu, a bromine-terminated macroinitiator reacts with copper (I) bromide in solution with N,N,N',N',N"-pentamethyldiethylenetriamine (PMDETA) as the metal ligand. The metal complex is oxidized by the macroinitiator through a one-electron process to $Cu(II)Br_2$, generating a radical on the initiator. The radical then adds to a monomer in solution, initiating chain growth. The newly created chain either reacts with an additional monomer, extending the length of the chain, or it reacts with the oxidized $Cu(II)Br_2$, again through a one-electron process, reducing the metal complex to $Cu(I)Br$ and regenerating the bromine terminal functionality, now on a lengthened polymer chain. The lengthened chain can reenter the process by oxidizing another metal complex through the transfer of the terminal bromine, thus continuing the cycle.

The reaction scheme used by Wang[1] is shown in Figure 25.
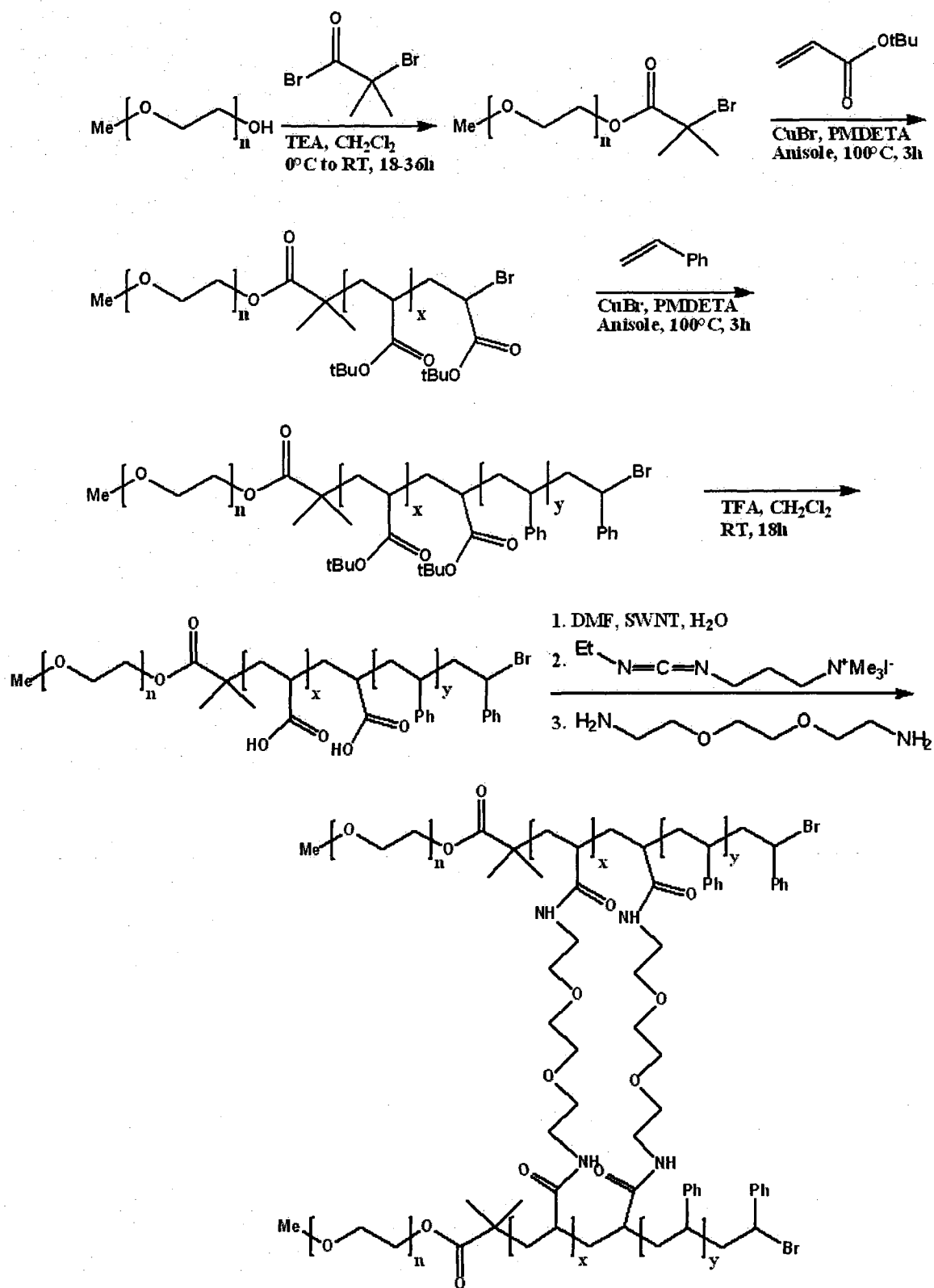
Figure 25. Synthesis of the triblock copolymer and crosslinking into a PEG-egg

Wang[1] used the same macroinitiator as Tang and Niu, but simply reversed the order of Niu's polymerization. The PAA block was synthesized first, followed by the PS block, both via ATRP. However, since acrylic acid is not polymerizable by ATRP,[70] *t*-butyl acrylate (tBA) was substituted as a synthon and hydrolyzed to the acid after the polymerization of both blocks. Thus, MPEG-PtBA-PS was synthesized followed by hydrolysis of the PtBA block with trifluoroacetic acid (TFA) to unveil the desired MPEG-PAA-PS polymer. As with the formation of Taton's micelles, the polymer was dissolved in DMF with SWNTs and sonicated, and water was added dropwise to form the micelles. The micelles were then crosslinked with a carbodiimide and diamine crosslinker at a stoichiometric ratio of acid groups to activator/crosslinker.

The resulting PEG-eggs were tested for NIR fluorescence, biological compatibility, and stability.[1] They were observed to retain their intrinsic NIR fluorescence, as opposed to covalently functionalized SWNTs.[73,74] The PEG-eggs were also tested against a blood protein, bovine serum albumin (BSA). NIR fluorescence measurements showed no difference between PEG-eggs exposed to the BSA protein and those that were unexposed, even after more than 7 days, indicating that the polymer shell was not displaced by the protein. Furthermore, the crosslinked eggs could be dried and resuspended, and they did not flocculate upon addition of tetrahydrofuran (THF) to an aqueous solution. Uncrosslinked eggs, however, flocculated immediately. Crosslinked eggs were also slower to oxidize in the presence of Fe(III) than uncrosslinked eggs, as measured by fluorescence quenching experiments. Finally, biological testing indicated no

acute cytotoxicity of the crosslinked eggs as 95% of the cells survived the presence of the eggs at 33 ug/mL.[1]

Unfortunately, the PEG-eggs have proven difficult to make. The synthesis of the triblock copolymer was very troublesome and the only polymer made was MPEG17-PAA35-PS14. More material was needed to develop PEG-eggs as a potential anticancer agent through thermablation. There may be advantages in testing different block lengths, especially in the polystyrene and PEG blocks. Control over the polymerized block lengths is therefore highly desirable. Furthermore, it was desirable to make PEG-eggs with MPEG-45 rather than MPEG-17, but the triblock could not be made with MPEG-45 as a macroinitiator. The objectives of this thesis, therefore, were fourfold: 1) identify the problems with the methodology that prevented reproduction of the synthesis; 2) optimize the methods to provide control over the polymerized block lengths; 3) expand the methodology to include PEG45 as a starting material; and 4) produce a sufficient quantity of material for further biological testing.

Chapter 6. Non-covalent SWNT Encapsulation Into Water-Soluble

PEG-eggs: Experimental

6.1 Materials

The poly(ethylene glycol) macroinitiators, 750 and 2000 molecular weights, were prepared by literature procedures.[72] Methoxy-PEG-OH (MPEG-OH, 750 and 2000 MW, Aldrich) was used as received. Dichloromethane (DCM, Fisher) was distilled over calcium hydride at one atmosphere and stored under nitrogen. 2-Bromoisobutyryl bromide was distilled under vacuum (0.1 mm Hg) and stored under nitrogen. Triethylamine (TEA) was distilled over anhydrous calcium sulfate at one atmosphere and stored under nitrogen. Anisole (Aldrich) was washed three times with one-half volume of 2M NaOH, then twice with water. It was dried over anhydrous calcium chloride, and then gravity filtered to remove the drying agent. It was distilled from sodium under vacuum (0.1 mm Hg). Toluene (Fisher) was distilled over P_2O_5 at one atmosphere. t-Butyl acrylate (tBA, Aldrich) was extracted three times with 1M NaOH, then washed three times with water. It was dried over anhydrous magnesium sulfate and gravity filtered to remove the drying agent. It was then passed through a column of activated, basic alumina, 150 mesh (Aldrich) and distilled under vacuum (0.1 mm Hg). Styrene was passed over a column of activated, basic alumina, 150 mesh (Aldrich) and distilled under vacuum (0.1 mm Hg). Anisole, toluene, t-butyl acrylate, and styrene were degassed using three freeze-pump-thaw cycles. Anisole and toluene were stored under nitrogen; t-butyl acrylate, and styrene were stored under nitrogen at -20 °C. Copper (I) bromide (Aldrich)

was purified by stirring with glacial acetic acid (5 g/50 mL) for 18 hours. It was vacuum filtered and washed with ethanol and diethyl ether. It was further purified with a second cycle, then dried under vacuum overnight and stored under nitrogen. N,N,N',N',N"-Pentamethyldiethylenetriamine (PMDETA, Aldrich) was purified by distillation under vacuum (0.1 mm Hg) and stored under nitrogen. Trifluoroacetic acid (TFA, Aldrich), 1-[3-(dimethylamino)propyl]-3-ethylcarbodiimide methiodide (EDC, Aldrich), and 2,2'-(ethylenedioxy)diethylamine (Aldrich) were used as received. Purified single-walled carbon nanotubes, batch number 162-8, were produced and purified in the Rice Carbon Nanotechnology Laboratory using the HiPCO (high-pressure carbon monoxide) reactor.[44] Raw SWNTs, batch number 109.3, were produced in the same laboratory.

6.2 Methods

6.2.1 Synthesis of the MPEG-Br Macroinitiator (750 and 2000 MW PEG)

The macroinitiator is synthesized using a slightly modified literature procedure developed by Chen.[72] To a 250 mL, three-necked round-bottom flask equipped with a magnetic stir bar, a 50 mL addition funnel, a nitrogen purge, and a rubber septum was added: 13.4 g (17.9 mmol) ~750 MW MPEG-OH and 130 mL of dry dichloromethane. The solution was cooled to 0 °C with stirring in a chilled ethylene glycol bath. After 15 minutes, 5.0 mL (3.6 g, 35.7 mmol, 2 equiv) distilled triethylamine was added via syringe. The solution was stirred for 5 min, during which 4.4 mL (8.2 g, 35.7 mmol, 2 equiv) distilled 2-bromoisobutyryl bromide in 50 mL dry dichloromethane was added to the addition funnel. The bromide solution was added dropwise with stirring over

approximately 20 minutes. After addition, the flask was removed from the bath and allowed to warm to room temperature while stirring. The solution was stirred at room temperature for 18 hours, and then vacuum filtered to remove precipitated byproduct. The filtrate was poured into 150 mL water and stirred for 4 hours. The layers were separated and the organic layer was stored. The aqueous layer was extracted twice with 150 mL DCM, and the organic layers were added to the stored organic layer. The combined organic layers were washed once with 1M HCl, once with 1M NaOH, and dried over anhydrous magnesium sulfate. The solvent was removed on a rotovap to yield the crude bromoester oil. The oil was dissolved in 300 mL diethyl ether and the solution placed in a -20 °C freezer overnight. The crystallized product was recovered by vacuum filtration, and purity checked by NMR. If the NMR spectrum indicated the presence of water (peak at δ 2.005), the bromoester was redissolved in dry DCM and run over a column of activated, basic alumina (150 mesh). The solvent was removed on a rotovap and the pure product (10 g, 85%, remainder lost in workup) stored under nitrogen. ^{1}H NMR 1.94 (-C(C$\underline{H}_3$)$_2$-, s, 6H), 3.38 (C$\underline{H}_3$-O-, s, 3H), 3.55 (CH$_3$-O-C$\underline{H}_2$-CH$_2$-O-, m, 2H), 3.66 (-O-C$\underline{H}_2$-C$\underline{H}_2$-O-, s, 4nH), 3.74 (-O-C$\underline{H}_2$-CH$_2$-O-C(=O)-, m, 2H), 4.32 (-O-CH$_2$-C$\underline{H}_2$-O-C(=O)-, m, 2H). For 2000 MW PEG, the procedure is modified as follows: 2.4 equivalents of TEA and bromide are used instead of 2, and the reaction is stirred for 36 hours instead of 18. The crystallized 2000 MW bromoester typically does not need drying over alumina. The pure product (11 g, 50%, remainder lost in workup) is also stored under nitrogen. ^{1}H NMR 1.94 (-C(C$\underline{H}_3$)$_2$-, s, 6H), 3.38 (C$\underline{H}_3$-O-, s, 3H), 3.55 (CH3-O-C$\underline{H}_2$-CH$_2$-O-, m, 2H), 3.66 (-O-C$\underline{H}_2$-C$\underline{H}_2$-O-, s, 4nH), 3.74 (-O-C$\underline{H}_2$-CH$_2$-O-C(=O)-, m, 2H), 4.32 (-O-CH$_2$-C$\underline{H}_2$-O-C(=O)-, m, 2H). Typical ^{1}H NMR spectra of both 750 MW

and 2000 MW macroinitiators are in Appendix A. Spectra of both may contain residual DCM (5.32 s).

6.2.2 Synthesis of MPEG-PtBA-Br Diblock (750 and 2000 MW PEG)

A highly modified version of Wang's procedure is used.[1] A 50 mL, three-necked round-bottom flask equipped with a magnetic stir bar, a nitrogen purge, a glass stopper, and a rubber septum was charged with 1.0 g (1.1 mmol) 750 MW MPEG macroinitiator and 40 mg (0.28 mmol, 0.25 equiv) purified copper (I) bromide. The flask was evacuated and backfilled with nitrogen 3 times to remove all oxygen. 9.3 mL of purified, degassed anisole (0.12 M solution) was added via syringe. The amount of t-butyl acrylate to be added depends on the desired block length, as the monomer concentration is used to control the block length. These run conditions result in a conversion of ~75% of the tBA, so a block length of 30 tBA units calls for 40 equiv of tBA in the reaction. Thus, 6.5 mL (5.7 g, 44 mmol, 40 equiv) was added to the flask via syringe. The solution was lowered into an oil bath at 100°C. 116 µL (96 mg, 56 mmol, 0.5 equiv) of PMDETA was immediately added via syringe. After the addition of the PMDETA, the CuBr went into solution and the solution turned amber. After stirring for 3 hours, the flask was removed from the oil bath and cooled under nitrogen. When the reaction was close to room temperature and had turned an olive green, the flask was opened to air and stirred for 30-40 minutes. The solution turned a dark green and most of the catalyst precipitated as a very dark green solid. The solution was then filtered through a column of activated, basic alumina (150 mesh), wet with toluene, to remove the catalyst. The flask was rinsed with 10 mL of toluene that was then added to the alumina column. The polymer was eluted

with 100 mL of toluene, and the solvents and unreacted monomer removed on a rotovap. The polymer was redissolved in DCM and concentrated on the rotovap. The polymer was then dried under high vacuum (0.1 mm Hg), the residual DCM causing the polymer to foam, speeding drying. ^{1}H NMR 1.44 ((CH_3)$_3$-C- + -CH_2-CH(C(=O)-OtBu)-, br s, 9xH + 2xH), 2.22 (-CH$_2$-CH(C(=O)-OtBu)-, br s, xH), 3.38 (CH_3-O-, s, 3H), 3.65 (-O-CH_2-CH$_2$-O-, s, 4nH). For 2000 MW MPEG macroinitiator, the procedure is modified to use 0.3 equiv CuBr instead of 0.25 equiv and to use 0.6 equiv PMDETA instead of 0.5 equiv. Typical ^{1}H NMR spectra of both 750 MW and 2000 MW PEG diblock polymers are in Appendix A. Spectra of both polymers may contain residual anisole (3.81 s, 6.9 m, 7.3 m) and DCM (5.32 s).

The PtBA chain length is estimated by integrating the peak at 3.38 (the methoxy terminal group) and setting it to a value of 3. The number of tBA units added is calculated by integrating the peak at 1.44 ppm and dividing by 11. This peak contains the hydrogens of the t-butyl group as well as 2 polymer backbone hydrogens. The third backbone hydrogen, the one attached to the carbon bearing the ester is seen at 2.22. That peak can be used as a comparative measure as it should equal approximately the number of tBA monomer units added to the chain.

6.2.3 Synthesis of MPEG-PtBA-PS Triblock (750 and 2000 MW PEG)

The same procedure was followed as in the synthesis of the MPEG-PtBA-Br with the following modifications. A 50 mL, round-bottom three-necked flask was charged with 0.5 equiv or 1 equiv CuBr depending on the styrene block length desired. For a 10-15 block length, 0.5 equiv. is used, and for 20 or greater block length, 1 equiv. is used.

The flask was evacuated and backfilled with nitrogen 3 times to remove all oxygen, as before. The molecular weight of the MPEG-PtBA-Br was calculated from NMR. The MPEG-PtBA-Br was placed in a single necked flask and purged with nitrogen. The polymer was then dissolved in the appropriate amount of purified, degassed anisole to produce a 0.06 M solution (typical polymerization: 2 g of 5000 MW polymer, 0.40 mmol, and 6.7 mL anisole). The solution was transferred to the 50 mL flask via syringe. The equiv. of PMDETA used is equal to 2x equiv. CuBr used. The actual block length is again controlled by monomer concentration, 0.5 equiv. CuBr yielding ~20 % conversion and 1 equiv. of CuBr yielding ~40% conversion. The polymer was synthesized at 100 °C for 3 hours as before, and recovered as before as well. ^{1}H NMR 1.44 ((C$\underline{H}_3$)$_3$-C- + -C$\underline{H}_2$-CH(C(=O)-OtBu)-, br s, 9xH + 2xH), 2.22 (-CH$_2$-C$\underline{H}$(C(=O)-OtBu)-,br s, xH), 3.38 (C$\underline{H}_3$-O-, s, 3H), 3.65 (-O-C$\underline{H}_2$-C$\underline{H}_2$-O-, s, 4nH), 6.57 (*o*-aromatic $\underline{H}$ on styrene, br m, 2yH), 7.20 (*m,p*-aromatic $\underline{H}$ on styrene, br m, 3yH). Typical ^{1}H NMR spectra of both 750 MW and 2000 MW PEG triblock polymers are shown in Appendix A. Spectra of both polymers may contain residual anisole (3.81 s, 6.9 m, 7.3 m) and DCM (5.32 s).

The PS chain length is estimated by integrating the peak at 3.38 (the methoxy terminal group) and setting it to a value of 3. The PS chain length is calculated by integrating the entire aromatic region and dividing by 5. If residual anisole solvent is present, then the NMR peak at 3.81 (methoxy of the anisole) may be used to correct the aromatic region. Multiply the area of the methoxy peak by 1.66 (3H/methoxy, 5H/aromatic ring), subtract the result from the total aromatic integration, and then divide by 5.

6.2.4 Hydrolysis of MPEG-PtBA-PS to MPEG-PAA-PS

Modified procedure by Wang.[1] The MPEG-PtBA-PS polymer was dissolved in sufficient dry DCM to produce a 0.02 M solution in a 50 mL, single-necked, round-bottom flask equipped with a magnetic stir bar. Trifluoroacetic acid was added to the solution (10 mol TFA/ mol tBA groups), and the flask was sealed under nitrogen. The solution was stirred for 18 hours at room temperature, and then the solvent and TFA were removed under vacuum. The recovered brittle polymer was used without further purification. ^{1}H NMR (DMSO) 1.68 (-C$\underline{H}_2$-CH(C(=O)-OH)-, br s, 2xH), 2.36 (-CH$_2$-C$\underline{H}$(C(=O)-OH)-, br s, xH), 3.38 (C$\underline{H}_3$-O-,s, 3H), 3.65 (-O-C$\underline{H}_2$-C$\underline{H}_2$-O-, s, 4nH), 6.57 (o-aromatic $\underline{H}$ on styrene, br m, 2yH), 7.20 (m,p-aromatic $\underline{H}$ on styrene, br m, 3yH). Typical ^{1}H NMR of both 750 MW and 2000 MW PEG triblock polymers are shown in Appendix A.

6.2.5 Non-covalent Encapsulation of SWNTs into PEG-eggs

Wang's method of producing the PEG-eggs was used.[1] The procedure is the same for both 750 and 2000 MW PEG polymers. 10-75 mg of polymer, 1 mg purified or raw SWNTs, and 2 mL dimethylformamide (DMF) was added to a 20 mL scintillation vial. The vial was tip sonicated at 5 watts for 1 min, followed by the dropwise addition of 18 mL water with continuing sonication. After the addition was complete, 1-[3-(dimethylamino)propyl]-3-ethylcarbodiimide methiodide (EDC, 1 mol/ mol AA groups) was added to the suspension to activate the carboxylic acid groups. The solution was shaken and a cloudy ppt formed. To this mixture was added 2,2' (ethylenedioxy)diethylamine (0.5 equiv diamine/ equiv EDC) to crosslink the activated

acid groups. The cloudy suspension immediately turned a uniform, nearly clear black. The crude solution was centrifuged starting at 3000 x g (5000 RPM/ T-1250 rotor) to remove impurities. The supernatant was subsequently centrifuged at successively higher g forces (12,000, 27,000, 58,000), recovering the pellet each time and redissolving it in water, resulting in a series of purified PEG-egg solutions.

6.2.6 Gel-permeation chromatography (GPC) Analysis

GPC measurements were performed on a Waters 717 GPC equipped with a Styragel HR 1 column (7.8 mm x 300 mm) and a refractive index (RI) detector. The solvent was tetrahydrofuran (THF).

6.2.7 Fluorescence of PEG-eggs

Near-IR fluorescence of the aqueous PEG-egg solutions was measured on a NS1 NanoSpectralyzer. The excitation frequencies were 659 and 785 nm.

Chapter 7. Non-covalent Encapsulation of SWNTs into PEG-eggs:

Results and Discussion

7.1 Polymerization of Triblock Copolymer

Attempts by several students to duplicate the work reported by Wang[1] had run

into consistent failure at the styrene polymerization step. *t*-Butyl acrylate (tBA) was

easily added to the macroinitiator, but the subsequent styrene polymerization resulted in

no addition of monomer. The first attempts to resolve the problem focused on using the

published conditions with highly purified materials.

The macroinitiator, monomethoxy-terminated PEG esterified with 2-

bromoisobutyryl bromide (MPEG-Br) to generate a tertiary alkyl bromide, was made

following the literature procedure.[72] Subsequent polymerizations with tBA proved to be

highly disappointing. Typical products had 10-20 tBA units in the polymer (as

determined by NMR) rather than the 35 to 85 monomer units previously achieved, even

with 100 equivalents of monomer present. Several attempts were made with different

batches of macroinitiator, but little change was seen.

It was noted, however, that all of the polymerizations were a very dark brown,

almost black, and by the end of the run a substantial amount of a black precipitate coated

the walls of the reaction flask. This precipitate was thought to be dead catalyst, either

oxidized or in an insoluble complex. The first attempt to determine the cause centered on

the tBA used in the polymerization. Though purified, tBA was suspected of containing a

small amount of acrylic acid, possibly formed during storage. Acrylic acid is known to

complex with CuBr, hence the use of tBA as a synthon in place of acrylic acid.[70] Thus,

tBA was added via syringe to the reaction dropwise very slowly over the course of 2 h. It was thought that if the problem was acrylic acid in the tBA, then slow addition during the reaction might slow down the precipitation of catalyst. Unfortunately, no change in precipitation was observed and no improvement in polymerization was seen.

The next modification was to alter the order of addition. Originally, the macroinitiator and CuBr were placed in a sealed flask and flushed with nitrogen. A solution containing the anisole, tBA, and N,N,N',N',N''-pentamethyldiethylenetriamine (PMDETA) was added. Two different sequences were tried, both adding all three components separately. The first sequence added anisole, followed by PMDETA, followed by tBA. The second reversed the sequence of tBA and PMDETA, adding the latter last. Although neither sequence made much difference, adding the PMDETA last seemed to improve the yield slightly. However, black precipitate still developed in the flask during both runs.

Since the problem appeared to be primarily associated with the catalyst, a run was made with 3 equivalents catalyst rather than 1 equiv. This change had a huge impact as the monomer incorporation shot up to 50. This result made it apparent that the poor monomer incorporation was the result of too low a concentration of active catalyst in the reaction flask.

However, it was not known why the catalyst was precipitating out of solution. It was not oxidation, as oxidized catalyst is bright green and these solutions were a dark brown, almost black. Furthermore, all of the reagents were degassed and purified (verified by NMR), so no oxygen should have been present to oxidize the CuBr. The only remaining possibility was the macroinitiator.

A second peak had been noticed in the NMR at about 2.005 ppm. Water was not originally suspected as the source of this peak as water normally appears in $CDCl_3$ at about 1.56 ppm. Furthermore, it was sharp, not broad, as might be expected if the peak were water and was hydrogen bonded to the PEG of the macroinitiator. The peak did not match any of the starting materials, however, and the macroinitiator preparation had no apparent byproduct that would produce such a peak. The preparation of the macro initiator used an aqueous workup, so water was a definite possibility.

To determine if the peak was water, the macroinitiator was further purified to remove as much water as possible. The standard preparation called for one drying step over magnesium sulfate. However, if water was the contaminant then one drying step was obviously insufficient to remove all of the water from the macroinitiator. Therefore, two approaches were used to dry the macroinitiator further. The first approach was to dissolve it in dichloromethane (DCM) and dry repeatedly over magnesium sulfate. The only material that should be removed by repeated magnesium sulfate treatment was water. If the unknown peak were a contaminant other than water then the contaminant would not be removed. Even if magnesium sulfate was fairly inefficient at removing the water, repeated drying sequences should at least reduce the water in the macroinitiator. The second approach was to dissolve the macroinitiator in DCM and run the solution over a column of activated, basic alumina. This method was expected to be much more effective than magnesium sulfate drying, and it had the added benefit of possibly removing the unknown if it did not prove to be water.

Both procedures removed the peak at 2.005. The magnesium sulfate approach was indeed less effective, but one could watch the steady disappearance of the peak in the

NMR spectrum after each drying step. The alumina approach was much more effective. Alumina treatment generally reduced the water peak to zero in one step, even when the water level was quite high (~3 waters/chain). Apparently the water was associated closely enough with the PEG chain to shift the NMR peak, but not in such a way as to broaden the peak.

With the unknown peak established as water, calcium chloride was tried as a drying agent instead of magnesium sulfate to see if it might be more effective. The macroinitiator was then dried further over an alumina column. Polymerizations improved somewhat, adding between 25 and 35 monomer units, and the black precipitate disappeared. However, this level of incorporation was still much less than expected or desired, and whitish solids at the bottom of the flask were now observed.

Unlike the previous black precipitate, these solids were apparent from the start of the reaction. They were first suspected of being catalyst that was not coordinated and dissolved in solution. However, additional PMDETA did not bring the solids into solution, and this possibility was discarded. Since the white solids were not observed previously and the only change to the procedure involved the macroinitiator, the macroinitiator was the most probable source of the solids. Using the original preparation, the macroinitiator obtained was a thick oil; using the new preparation it was a pasty solid. This change in appearance was believed to be the result of removing the water, but when the macroinitiator was redissolved in DCM, white solids remained in the flask. Calcium chloride appeared to passing through both the filtration step and the alumina column drying step. The preparation was then modified back to using magnesium sulfate as the

drying agent and simply using more drying agent and longer drying times to minimize the amount of water leading into the alumina drying step.

When the macroinitiator was finally pure, polymerizations now resulted in much higher monomer incorporation. Results of several different runs with different tBA concentrations are shown in Table 12.

Table 12. tBA monomer incorporation at differing monomer concentrations.

Run No.	Equiv. tBA	Number of monomer units added	Conversion (%)
1-053-01	50	40	80
1-054-01	100	78	78
1-057-01	50	35	70
1-058-01	100	70	70
1-059-01	50	25	76
1-060-01	100	45	68

The monomer incorporation of the polymerization averaged between 70% and 80% of the monomer originally present, as determined by NMR. This level of incorporation was not only much higher than obtained previously, but it was much more consistent. None of the reactions exhibited any black precipitate or any white solids.

With the tBA polymerization apparently solved, the polymerization of styrene was attempted next. Using Wang's conditions,[1] all of the polymers in Table 12 were polymerized with styrene. Unfortunately, none of them incorporated styrene at a level noticeable in the NMR spectrum. Only the polymerization with 1-060-01 showed even a hint of incorporation.

The failure of the polymers to add styrene was puzzling. Ionic polymerization of styrene had been reported to be impossible, but polymerization of styrene onto the MPEG-PtBA-Br polymer was clearly possible. Not only had the polymerization been reported in the literature[1,75,76,77] but an early attempt was made (prior to elimination of water) to "one-pot" the triblock by adding styrene after 3 hours. The NMR of that reaction showed substantial incorporation of styrene, but the NMR also showed a great deal of unreacted tBA. If unreacted tBA was present, the styrene was undoubtedly incorporated as a random copolymer with tBA, not as a block polymer. The fact that styrene did incorporate in the reaction, however, indicated a problem with the current polymer or the current conditions.

The most likely cause of the failure was believed to be a problem with the MPEG-PtBA chain ends. Atom transfer radical polymerization proceeds in a fairly simple way as described in the background section. In this particular case, CuBr abstracts a bromine from the macroinitiator and is oxidized to $CuBr_2$, leaving a tertiary radical. This radical then attacks a tBA monomer, adding it to the initiator and producing a secondary radical. The secondary radical then can attack another tBA monomer, or it can reduce the $CuBr_2$ to CuBr and terminate as a secondary alkyl bromide. The secondary bromide can then reenter the cycle by losing the bromine atom to another CuBr, oxidizing the copper to $CuBr_2$ as before. However, if the chain end does not reduce $CuBr_2$ to CuBr and terminate with bromine, then the chain end will be unable to reenter the cycle. These dead (or unreactive) chain ends will also not be able to polymerize styrene in the final step either.

A number of possibilities were considered. First, the chains could undergo chain-chain termination by combining with each other. This possibility was not considered

likely as the concentration was 0.08 M and it is difficult to combine two large chains in this manner. Second, the terminal bromine could be lost through a side reaction[78,79] (S_N2 substitution of bromine by the nitrogen of the ligand; the reaction is run at 100 °C for 3 hours). Third, the radical could be terminated through some unknown mechanism.

To address these possibilities, the method for tBA polymerization was altered. Two approaches were used. In the first approach, the reaction temperature was reduced to minimize the probability of loss of bromine to side reactions. In the second, the temperature was maintained at 100 °C but the catalyst loading was reduced from 1 equiv. CuBr to 0.5 equiv., reducing the concentration of radicals in solution and therefore reducing radical termination reactions. Reducing the reaction temperature to 60 °C from 100 °C in the first approach resulted in minimal polymerization, so the temperature was increased to 80 °C. At 80 °C, both approaches yielded similar results. The reduced temperature run added about 40 tBA monomers (40% conversion) and the reduced catalyst run added about 45 monomers (45% conversion). More importantly, both polymers successfully added styrene in a subsequent polymerization. The reduced catalyst approach was more effective, yielding a chain length of about 20 styrene units. The polymer made via the reduced temperature route only yielded about 15 styrene units, but 15 monomers added is still a marked improvement over the zero addition seen previously.

To determine if the styrene conversion could be improved further, additional reactions were run at 80 °C/ 0.5 equivalents (or 50%) catalyst and at 100 °C/ 0.25 equivalents (or 25%) catalyst. The reactions at 80 °C/ 0.5 equivalent CuBr averaged about 29 tBA monomers and the reactions at 100 °C/ 0.25 equivalent CuBr averaged

about 37 tBA monomers. Subsequent styrene polymerizations of the diblock polymers (all styrene polymerization run at 100 °C) were similar, averaging about 30 styrene units for diblock polymer made at 80 °C/ 0.5 CuBr versus about 34 for diblock polymer made at 100 °C/ 0.25 CuBr.

These results strongly indicate that the primary problem was not a side reaction of the terminal bromide, but undesirable termination reactions of the radical. One possible termination route was chain-chain termination. In order to determine if chain-chain termination took place, the GPC trace of a high-conversion dead MPEG-PtBA diblock was compared to a diblock that polymerized styrene well. The triblock made from the diblock was included in the comparison. The result is shown in Figure 26.
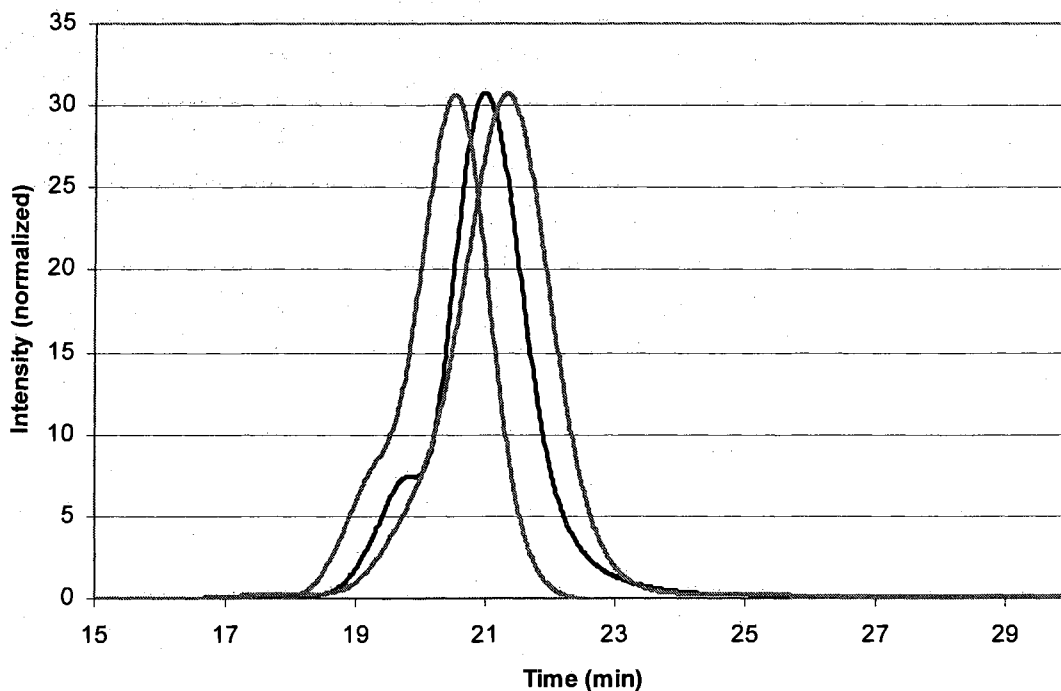
Figure 26. GPC trace of a high- conversion (80%) dead (unreactive) diblock copolymer

(black) vs an active diblock copolymer (right gray line) and subsequent triblock (left gray

line)

The dead diblock and live diblock are both made from 750 MW PEG, and have a

similar PtBA chain length (though not identical- chain length is 40 monomer units on the

dead diblock and 37 monomer units on the live diblock as determined by NMR). There is

a small high MW tail on the dead diblock and the peak molecular weight is slightly

higher than the live diblock (even accounting for the somewhat longer PtBA chain).

However, the high MW tail is nowhere near as large as would be expected if chain-chain

termination were a primary contributor to chain end death. Furthermore, the peak MW of

the dead diblock is not enough higher than that of the live diblock to account for chain-

chain termination. Chain-chain termination should approximately double the MW of the polymer. If chain-chain termination were occurring to a large enough extent to kill the polymer, then the GPC trace should show a predominant high MW peak, one that occurs at a much higher MW (probably close to the observed high MW tail peak, around 19.8 minutes) than the peak of the live diblock. Clearly, chain-chain termination was not the primary cause of chain end death; therefore, some other radical termination mechanism must be responsible.

Both the reduced catalyst and the reduced temperature approaches worked because both lowered the number of radicals in solution. The reduced catalyst works better as it puts an obvious upper limit on radical concentration. The reduced temperature slows the rate of formation of the radical but it has a higher absolute limit on the radical concentration, especially if it also slows the regeneration of the bromide end group from the radical and $CuBr_2$. The higher limit leads to more dead chain ends and fewer chains available to polymerize styrene, evidenced by the lower styrene conversion. Reducing the temperature also slows the addition of the radical to the monomer, impacting the overall efficiency of the polymerization, evidenced by lower tBA chain length. Therefore, reduction of the catalyst concentration was chosen as the primary approach to improving and optimizing the polymerization, and the reaction temperature was kept at 100 °C.

The one drawback of reducing the amount of catalyst was that the reaction slowed substantially, and as a result, conversion of tBA to polymer was less than desired, generally in the 30-40% range. Such a low conversion led to an unfortunate amount of monomer waste. Purification of the monomer involves washing steps as well as a distillation step and is time-consuming. Furthermore, the purified monomer must be

degassed. Thus, ways of improving the conversion were explored. The first attempts were to run the reaction in neat tBA (still at 100 °C), and do away with the anisole solvent completely. This approach had the added benefit of simplifying recovery and purification of the polymer as anisole is difficult to remove from the product. Eliminating anisole necessitated a further drop in catalyst concentration, as initial attempts at 0.25 equiv catalyst resulted in so much conversion that the polymer solidified in the flask. The catalyst loading was lowered to 10% (0.1 equivalent) and the reaction stayed as a solution. However, conversion in 3 hours at this low a level of catalyst was even worse (about 20%) at least in material that remained fluid enough to stir. Even more troubling, the polydispersity of the polymer was larger (~1.25 vs 1.15 for runs in anisole) and worse still, tBA was beginning to polymerize thermally, evidenced by a very high MW peak in the GPC trace. Furthermore, the very low levels of catalyst made the reaction difficult to control, as small changes in catalyst level led to large changes in tBA chain length. This method was clearly not satisfactory, and so other alternatives were explored.

The next approach was simply to increase the polymerization time. Reactions with both 750 MW macroinitiator (18 PEG monomers, or PEG-18) and 2000 MW macroinitiator (45 PEG monomers, or PEG-45) were compared at 3 and 4 hours (25% catalyst for PEG-18 and 30% catalyst for PEG-45, 50 equivalents tBA; PEG-45 requires slightly more catalyst owing to its longer length and hence slower polymerization rate). Longer times only showed a minor improvement in conversion, from about 30% to about 35%. With a target of 60-70% conversion, even a six-hour reaction time would not be enough, and very long reaction times were not desirable.

The primary cause of the low conversion was a slowdown in the rate of polymerization produced by the low concentration of radicals when using low catalyst levels. Increasing the monomer to polymer ratio clearly could lead to higher conversions (the first neat polymerization formed a gel), but solvent was still needed. The next approach, therefore, was to increase the concentration of the macroinitiator in solution. The primary risk with increasing the macromonomer concentration was an increase in chain-chain termination. However, given the size of the growing diblock and the comparative difficulty in getting two long chain ends together, chain-chain termination was not expected to be a problem.

The macroinitiator concentration was initially increased from 0.08 M to 0.16 M. A switch was also made to toluene as solvent to make the recovery of the diblock easier, and the catalyst was lowered slightly to 15-20%. Unfortunately, runs in toluene proved as difficult to control as in neat tBA. Small changes in catalyst level produced big changes in PtBA chain length. Initial runs at 15% catalyst produced diblocks with only 10-12 monomer units of tBA. Increasing the catalyst loading from 15% to 20% resulted in PtBA chain lengths of over 40 monomer units. In addition, some tBA thermal polymerization was seen again. Although toluene had been used successfully in other ATRP systems,[70] it was obviously not suitable for polymerizing tBA, necessitating a return to anisole as the solvent.

With anisole as solvent, polymerizations were run at 0.16 M macroinitiator, and 25% and 30% catalyst (PEG-18 and PEG-45, respectively) with 50 equivalents of tBA. Conversions now approached 80%, a major improvement over previous reactions. The resultant polymers were able to polymerize styrene effectively, but it was still somewhat

difficult to control the polymerization accurately. A macroinitiator concentration of 0.16

M resulted in a fairly viscous solution, and this viscosity may have been a factor in the

difficulty in controlling the reaction. It appeared that whenever reaction conditions were

near limits, whether it was catalyst concentration, monomer concentration (neat runs) or

solution viscosity, the reaction became more difficult to control. Therefore, the

macroinitiator concentration was dropped by about 25%.

With the macroinitiator concentration reduced to 0.12 M, the catalyst was set at

25% and 30% for MPEG-18 and MPEG-45, respectively. A series of reactions were run

with varying tBA concentrations. The results are shown in Table 13.

Table 13. Conversion of tBA in diblock polymerizations

Polymer Run No.	Macroinitiator	PEG mers	Equiv. tBA	tBA Monomers Added	Conversion (%)
1-158-01	1-156-01	18	50	34	68
1-159-01	1-144-01	45	50	34	68
1-160-01	1-156-01	18	40	30	75
1-161-01	1-157-01	45	40	29	72.5
1-180-01	1-162-01	18	40	25	62.5
1-181-01	1-157-01	45	40	30	75

As shown in the table, under these conditions the polymerization averages about 70%

conversion.

There was still some variability, but it was improved to the point that specific

block lengths could be targeted and reached by controlling the amount of tBA in the

reaction. Some of the variance is caused by different batches of macroinitiator. When the

same batch of macroinitiator is compared, the control improves. Therefore, if a given

block length is desired and the product is slightly off (25 monomers added instead of 30,

for example), the targeted length can be easily reached by using the same batch of

macroinitiator and altering the tBA concentration accordingly.

All of these MPEG-tBA block polymers proved highly effective at polymerizing

styrene. Obviously, all had large numbers of bromine-terminated chain ends. Therefore,

the reaction pathway that led to dead (non-bromine terminated) chain ends was either

minimized or stopped completely. However, since the reaction flask was evacuated and

purged with nitrogen, and all of the reaction components were purified, degassed, and

added under nitrogen, the side reaction causing the problem was not readily apparent.

The GPC data showed that chain-chain termination was not a notable contributor

to chain end death, so some other process must take place. The answer appeared to be in

the cool-down phase at the end of the tBA polymerization reaction. The original

procedure called for the reaction to be opened to air, cooled to room temperature, and

stirred for 2 hours. Under these conditions, any radicals in solution probably react very

rapidly with atmospheric oxygen. It takes less than 30 minutes for the CuBr to air oxidize

under these conditions, and nearly 15 minutes for the reaction to cool enough to only be

warm to the touch. Therefore, it should not be surprising that nearly all of the active

radicals can terminate with atmospheric oxygen rather than $CuBr_2$. Although some of the

radicals will terminate properly, regenerating the secondary bromide, the secondary

bromide can still reenter the catalytic cycle during the cooldown phase. Some of those

radicals will subsequently terminate with oxygen, further lowering the number of live

chain ends. Oxygen-terminated chains cannot reenter the cycle, and so oxygen

termination represents a sink that eventually captures most chain ends. As a result, simply lowering the amount of catalyst present put an upper limit on the number of chains that could terminate with oxygen (once CuBr is oxidized to $CuBr_2$ it cannot generate a new radical). This limit drastically reduced the number of dead chains, and the styrene polymerization worked immediately. The reduced temperature runs probably worked because they slowed the rate of radical formation, thus slowing down the rate of oxygen termination upon exposure to air during cooldown. However, these runs were less effective than reduced catalyst runs as there is no upper limit to the number of chains that may terminate. Instead, the runs depend on the reaction cooling down before all chains have oxygen terminated.

In an effort to further reduce the number of dead chain ends, the reaction was cooled under nitrogen at completion, and only opened to air after the flask was close to room temperature. Triblock polymers made in this manner showed an improvement in the styrene MW distribution, as shown by the shape of the high MW shoulder on the GPC trace of the triblock polymer. The GPC traces of two pairs of polymers are shown in Figure 27.
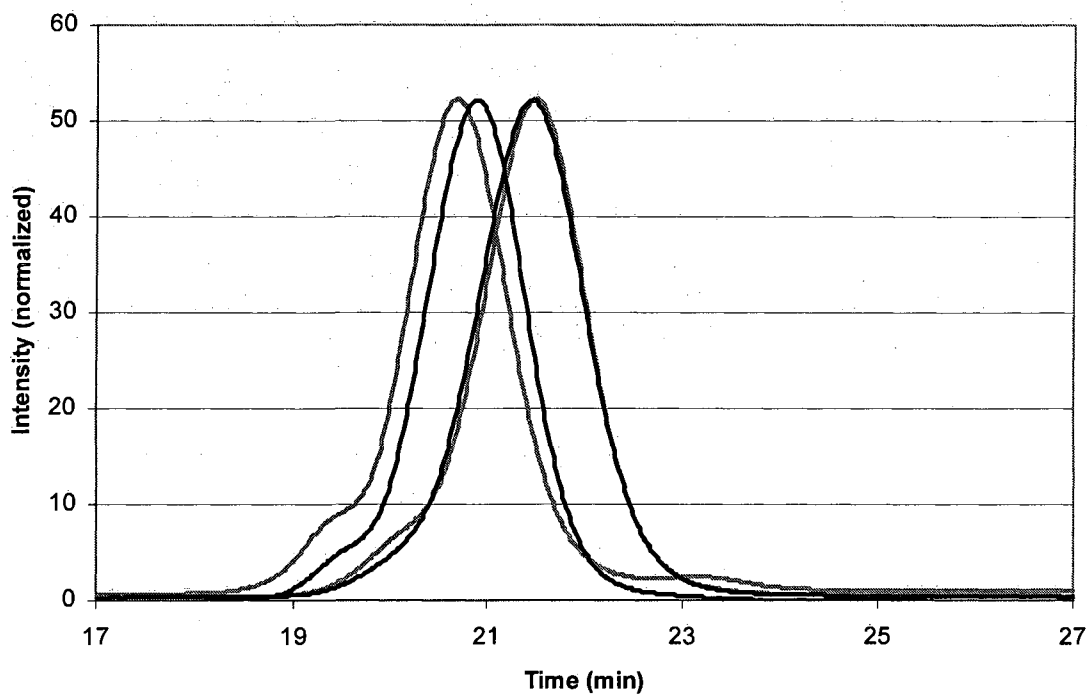
Figure 27. GPC traces of two diblock polymers (right black and right gray lines) and two triblock polymers (left black and left gray lines). The polymerization of one diblock (gray line) was cooled open to air, and the polymerization of the other (black line) was cooled under nitrogen. The higher MW triblock (gray line) was polymerized from the open-air cooled diblock and the other triblock (black line) was polymerized from the nitrogen-cooled diblock. The very small, low MW peak on the left gray line is MPEG-OH starting material.

The GPC curve shows two pairs of polymers; each pair consists of a diblock polymer and a triblock polymer made from that diblock. The diblock polymers in each pair were made under the same reaction conditions and are nearly identical in tBA chain length. The only difference between them was that the diblock used in the second pair

was cooled under nitrogen when it was made. The curves clearly show a reduction in the high molecular weight tail seen on the MPEG-PtBA-PS polymers. The reduction is not drastic, to be sure, but it is still an improvement. An attempt was made to add excess $CuBr_2$ to the solution at the beginning of the cooldown phase to improve the termination further, but the addition did not work, probably as a result of insufficient solubility of the $CuBr_2$. An attempt was made to overcome the insolubility by making a solution of $CuBr_2$/PMDETA in anisole to be added to the reaction as a solution, but it still was not sufficiently soluble.

Since the polymerization of the tBA was now well-controlled and produced diblock polymers that were highly effective at adding styrene, attention was turned to controlling the average block length of the polystyrene in the triblock polymer. The same basic approach to block length control used in tBA polymerizations can be applied to styrene polymerizations. The only difference is that since the diblock polymer is much longer than the original PEG macroinitiator, the concentration of the diblock must be reduced in solution to allow the polymer to unfold in solution and expose the reactive chain end. The reduction in concentration of the diblock, however, results in a decreased polymerization rate. Therefore, the catalyst concentration was increased to compensate for this rate reduction. An increase in catalyst concentration does not cause any problem, however, as there is no subsequent polymerization step and a terminal bromine is not required. Therefore, catalyst concentration can now be used as a method to control block length as well as monomer concentration by controlling the rate of polymerization. The results of the styrene optimization are shown in Table 14.

Table 14. Conversion of styrene in triblock polymerizations

Polymer Run No.	MPEG-PtBA-Br	Catalyst (% loading)	Equiv. Styrene	Styrene Monomer Units Added	Conversion (%)
1-164-01	1-153-01	100	50	21	42
1-165-01	1-152-01	100	50	20	40
1-175-01	1-155-01	100	50	19	38
1-176-01	1-154-01	100	50	17	34
1-166-01	1-153-01	50	50	15	30
1-167-01	1-152-01	50	50	14	28
1-173-01	1-155-01	50	50	8	16
1-174-01	1-154-01	50	50	12	24

The concentration of MPEG-PtBA-Br was set at 0.06 M. At 100% catalyst, the conversion of the styrene averaged 39%, and at 50% catalyst the conversion averaged 25%. The average of the 50% catalyst runs would be slightly higher except for one run of somewhat lower conversion. These reactions do give reasonable control over polystyrene block length; further fine-tuning of the length may be accomplished by varying the monomer concentration as in the PtBA case.

The final step in preparing the triblock copolymer is to hydrolyze the t-butyl ester groups to reveal the acid. The hydrolysis procedure used is the one reported by Wang,[1] described in the methods section. The only modification was to use 10 equivalents of trifluoroacetic acid (TFA) per tBA monomer added instead of 5. This increase was necessary because of the longer polymer chain lengths and the resulting need to lower polymer concentrations in DCM.

7.2 Formation and Testing of PEG-eggs

Triblock polymers made with MPEG-18 and MPEG-45 were used to form the PEG-eggs. The basic procedure as developed by Wang[1] was used to form the PEG-eggs. This step is quite straightforward, as described in the methods section. Small variances in the formation step do not seem to greatly affect the PEG-egg formation. Excessive sonication (more than 1 minute) prior to the dropwise addition of water may have a deleterious effect on the size of the eggs, but this effect has not been firmly established.

Eggs made from these triblock copolymers are stable in aqueous solution for at least several months. They can be removed from solution by centrifugation and the recovered pellet can be redissolved in pure water. A Peg-egg solution is shown in Figure 28.
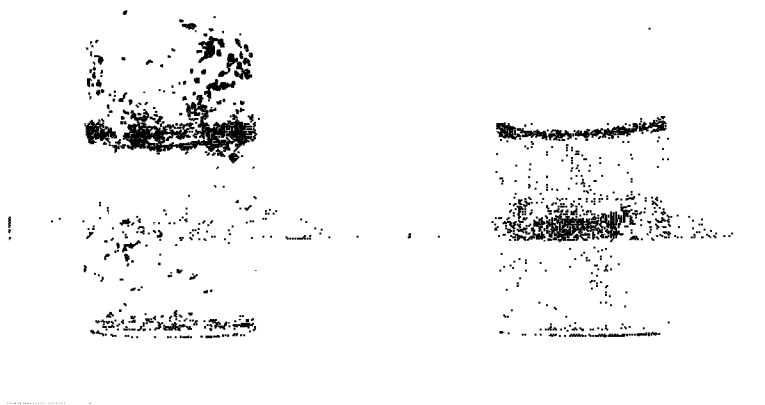

Figure 28. Photograph of raw SWNTs in water (left) vs PEG-eggs in water (right)

Initial fluorescence measurements made on these eggs showed them to be highly fluorescent, on par with SWNTs in the surfactant SDBS. A comparison of a PEG-egg and SDBS-suspended SWNTs is shown in Figure 29.
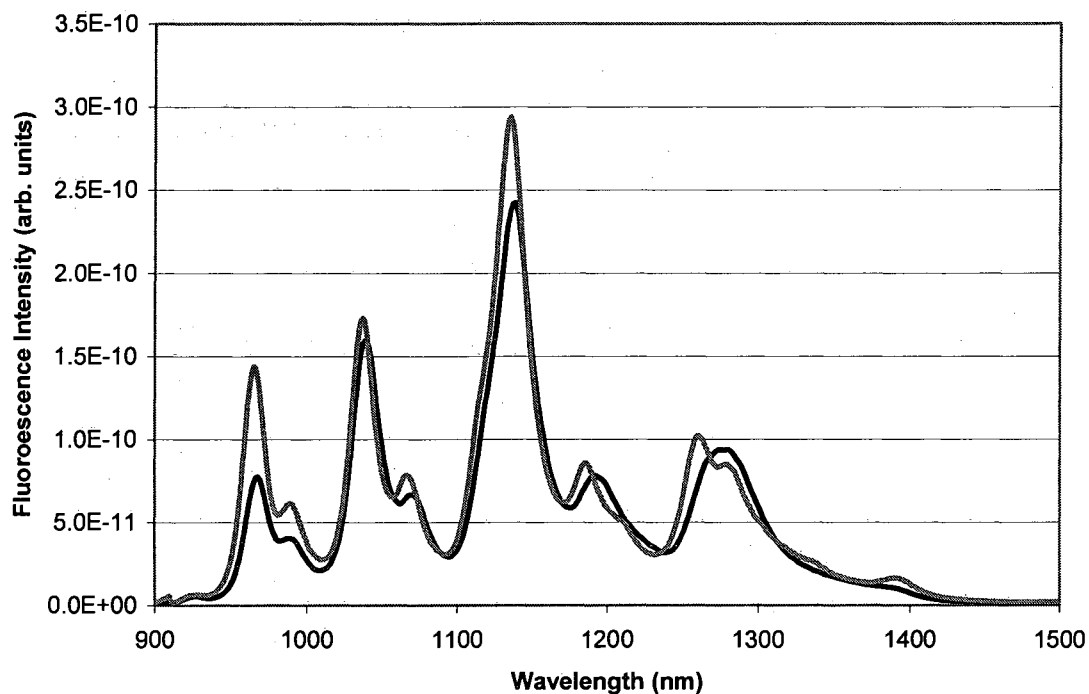
Figure 29. Fluorescence in aqueous solution (659 nm excitation) of SWNTs encapsulated by PEG-eggs (black line) vs SWNTs suspended by SDBS (gray line). Spectra corrected for SWNT concentration using absorbance values.

As can be seen in Figure 29, the fluorescence intensity of the SWNTs in PEG-eggs is as strong as the intensity of the SWNTs in SDBS. These same PEG-eggs were then tested for radiofrequency heating by Dr. Paul Cherikuri at M. D. Anderson and found to heat strongly under irradiation.[80] The SWNTs used in the PEG-eggs were

purified HiPCO SWNTS,[44] batch 162-8, the same as in the peroxide work. The SWNTs

in the SDBS suspension used for comparison were raw HiPCO SWNTs (unknown batch).

Purified SWNTs normally exhibit much worse fluorescence than raw SWNTs, owing to

the defects introduced in the purification process. Interestingly, there appears to be no

difference here between the purified SWNTS in PEG-eggs and raw SWNTs in SDBS.

Although the PEG-eggs fluoresced well, the majority of the material was heavy

enough to be removed by centrifugation at 12,000 x g. Only small amounts of the eggs

remained in solution at higher g forces. At first, it was believed that the material that

came out under lower g forces were bundled SWNTs encased by eggs, but the

fluorescence data proved that they were not bundled, otherwise they would not

fluoresce.[74] The next possibility was that the eggs were very large, owing to an excess of

polymer, and it was suspected that the reported polymer/SWNT ratio (50 mg polymer/ 1

mg SWNTs)[1] was much higher than it needed to be. Therefore, a new set of PEG-eggs

was made in an attempt to optimize the polymer/SWNT ratio. Two series of eggs were

made: one from a 17/29/12 PEG/PAA/PS triblock and one from a 45/35/11 PEG/PAA/PS

triblock. The ratio of polymer to SWNT was set by the ratio of PS to SWNT, as shown in

Table 15.

Table 15. PEG-egg formation: polymer to SWNT ratio

Triblock	Polymer (mg)	PS (mg, calculated)	SWNTs (mg)
17/29/12	52	15	1
17/29/12	35	10	1
17/29/12	17	5	1
45/35/11	76	15	1
45/35/11	51	10	1
45/35/11	25	5	1

The SWNTs used this time were raw HiPCO SWNTs, but the eggs were made as before. They were centrifuged at 3,000 x g, and the supernatant collected. The supernatant was centrifuged at 12,000 x g and the pellet redissolved in water. The redissolved PEG-eggs were analyzed for fluorescence.

The results of the 17/29/12 triblock based eggs are shown in Figure 30.
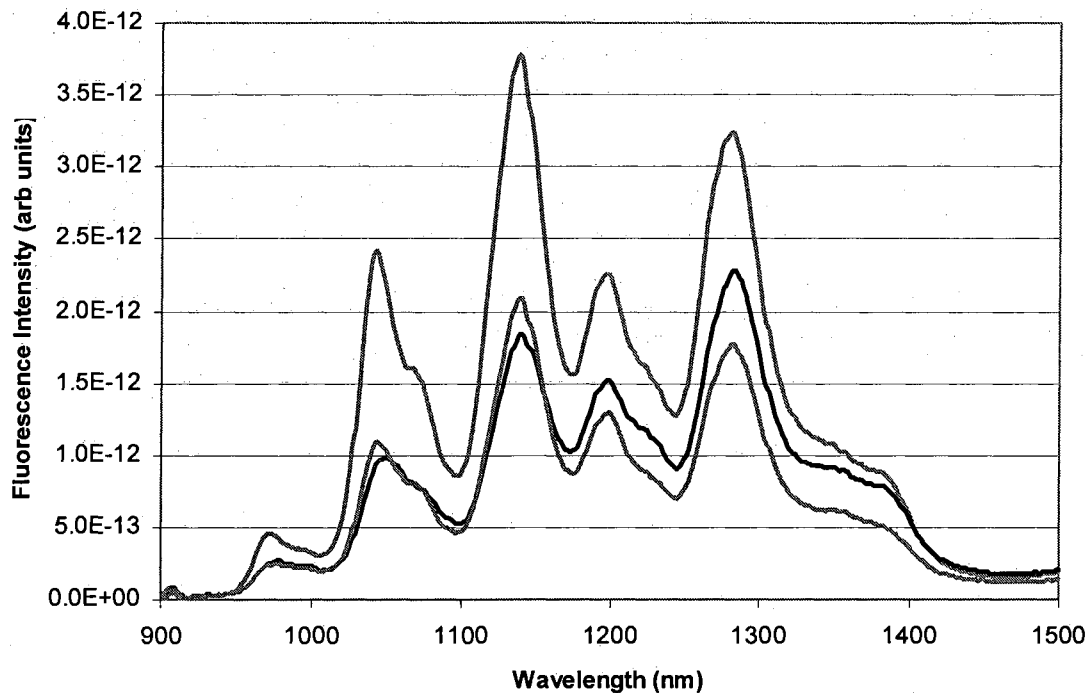
Figure 30. Fluorescence of SWNTs encapsulated by PEG-eggs (17/29/12 PEG/PAA/PS triblock) at different PS/SWNT ratios (15:1 mg PS/ mg SWNT top gray line, 10:1 black line, 5:1 bottom gray line). Spectra corrected for SWNT concentration using absorbance values.

The spectra show that the strongest fluorescence intensity comes from the eggs made with 15 mg of polystyrene. Interestingly, both the 10:1 and 5:1 polymer ratios showed the same fluorescence, about half that of the 15:1 eggs.

Figure 31 shows the fluorescent spectra of the 45/35/11 triblock based eggs.
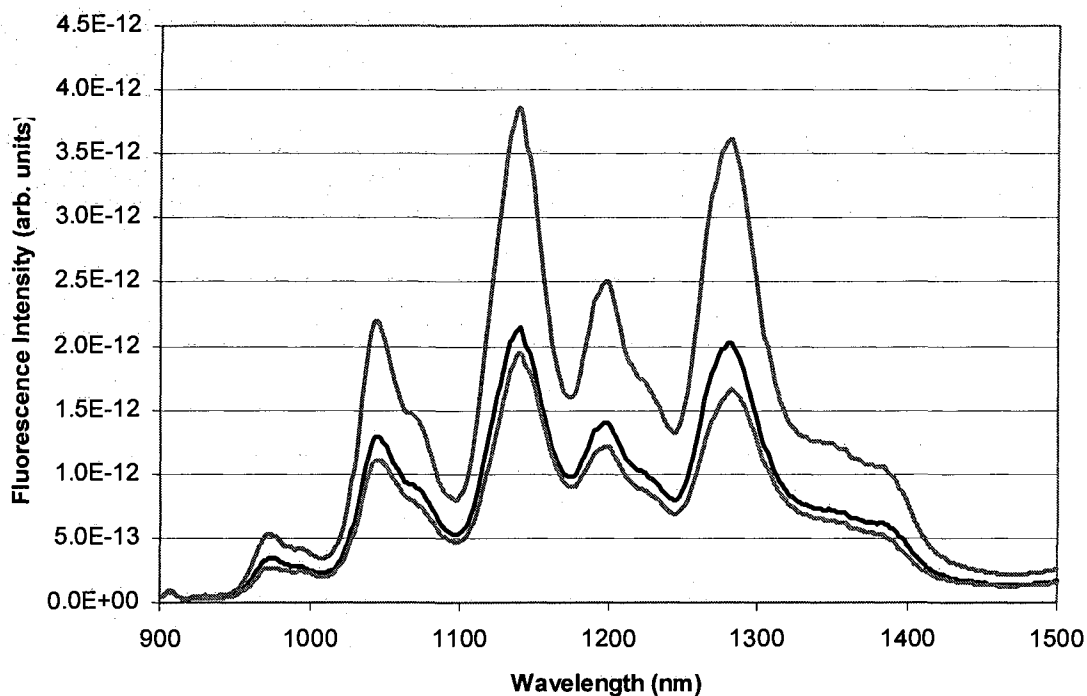
Figure 31. Fluorescence of SWNTs encapsulated by PEG-eggs (45/35/11 PEG/PAA/PS triblock) at different PS/SWNT ratios (15:1 mg PS/ mg SWNT black line, 10:1 top gray line, 5:1 bottom gray line). Spectra corrected for SWNT concentration using absorbance values.

This time, the maximum fluorescence occurred in the eggs made with a 10:1 ratio of polystyrene/ SWNTs. The 15:1 and 5:1 ratio materials exhibited similar fluorescence, about half the intensity of the 10:1. A comparison of the two PEG-egg samples with maximum fluorescent intensity is shown in Figure 32.
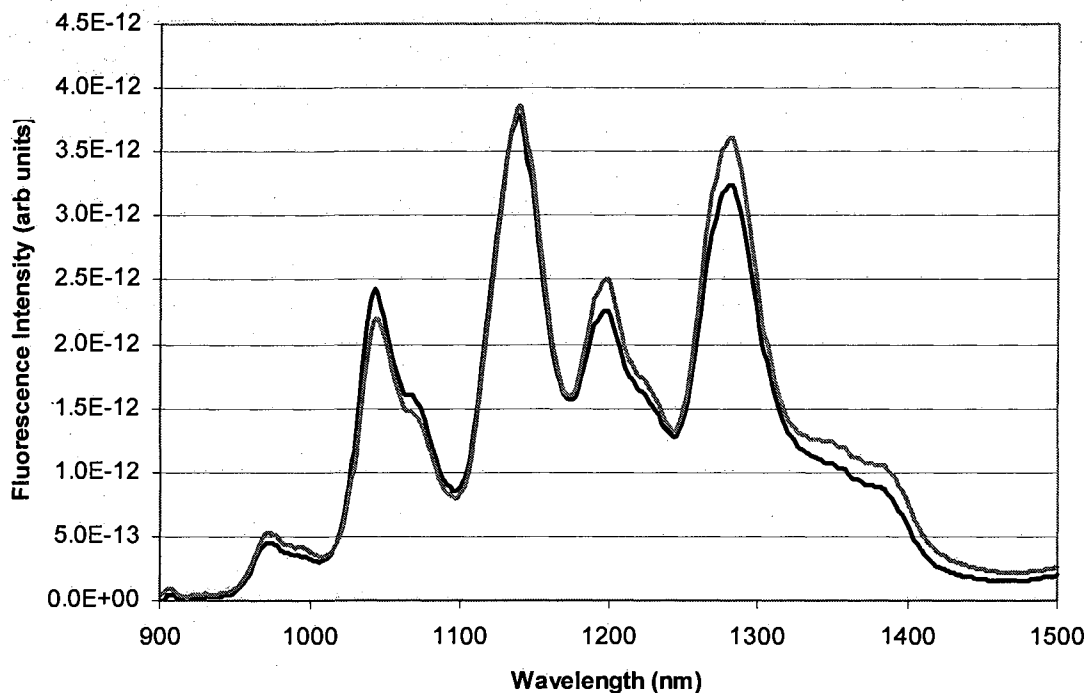
Figure 32. Fluorescence of SWNTs encapsulated by PEG-eggs: 17/29/12 triblock (black

line) at 15:1 vs 45/35/11 triblock (gray line) at 10:1. Spectra corrected for SWNT

concentration using absorbance values.

The fluorescence exhibited by the two different polymers is nearly identical,

although at different polymer/SWNT ratios. As the others were about half the intensity of

these, they are all approximately equal to each other as well. The reason that the

maximum fluorescence of the PEG-18 PEG-egg occurs at a different polymer/SWNT

ratio than the PEG-45 PEG-egg is not readily apparent. The total polymer/SWNT ratio by

weight is actually the same in the two samples, and that suggests that the total polymer

ratio may be as important as the styrene/SWNT ratio. Further work is needed to

determine the optimum ratios.

Chapter 8. Non-covalent Encapsulation of SWNTs into Water-Soluble

PEG-eggs: Conclusions

The primary problem in successfully polymerizing the styrene block of the triblock copolymer is the termination of the active radical through some pathway other than bromination with $CuBr_2$. GPC data showed that chain-chain termination was not a substantial contributor to active chain death. Literature reports also indicate that chain-chain termination is generally not an issue.[78] Atmospheric oxygen is the most likely cause of the loss of active chain ends. As soon as the catalyst concentration was reduced, the styrene polymerization worked very well. A reduction in catalyst concentration limits the number of chain ends that can terminate with oxygen, improving the performance of the diblock in the styrene polymerization. When the reaction is opened to air, active radicals may react with atmospheric oxygen, resulting in dead chains. More importantly, while the open flask is still hot, bromide-terminated chains can still react with CuBr in solution, generating new radicals that may then terminate with oxygen. In this way, oxygen termination acts as a sink, killing chains until all of the catalyst is consumed. Lowering the catalyst concentration puts an upper limit on how many chains can oxygen terminate, reducing the number of dead chains (at 25% catalyst, the maximum number of chains that can terminate is 25%).

Additionally, further improvements in the polymerization of styrene were obtained when the cooling step after tBA polymerization was conducted in an inert atmosphere. It is unclear if cooling the reaction under nitrogen would allow higher catalyst loadings to be used or not as this approach was not pursued. The reaction changes color (from amber to very light green) during the cooldown phase under

nitrogen, but it is not known if that is a reliable indicator that all of the radicals have terminated with $CuBr_2$. That reaction is faster than the initiation step,[75] but it will slow down as the reaction flask cools. In the absence of an excess of $CuBr_2$, some radicals may still be present when the flask is opened, depending on the temperature of the flask. If the reaction is completely cooled to room temperature, then all of the radicals should have terminated. In light of the fact that good conversions (70%) can be obtained at low catalyst levels, it does not appear to be necessary to try and run at higher catalyst levels.

The key to reducing the number of radicals was to reduce the amount of catalyst in solution. The need for high catalyst loading previously can be traced back to the loss of catalyst in the tBA polymerization. The presence of water in the reaction led to the formation of an insoluble CuBr complex, reducing the catalyst available for polymerization. It was not immediately clear why water should play such a significant role in the polymerization. Literature reports indicate that ATRP is not sensitive to water,[70] which is one of the benefits of using ATRP to make polymers. It is worth noting, however, that acrylic acid is a problem in ATRP[70] and will complex with the copper catalyst. That is why tBA is used as a synthon for acrylic acid, and PtBA is hydrolyzed to the acid in a final step after all polymerization steps are complete. It is possible that the water in the MPEG macroinitiator was hydrolyzing the tBA *in situ*. The reaction uses an excess of triamine ligand (2:1 ligand: CuBr), and it is conceivable that hydroxyl anions are formed from the interaction of the water and the amine. These hydroxyls could hydrolyze the acrylate to the acid, and the acid subsequently complexes with the CuBr. The acrylate would not need to hydrolyze to a large extent, only enough to remove substantial catalyst from solution. Hydrolysis of tBA should be fairly slow, and the

observed precipitation of the catalyst is not fast. It takes nearly 30 minutes at 100 °C before a noticeable amount of precipitate is seen on the walls of the flask. The hydrolysis of tBA to the corresponding acid is therefore a more plausible explanation than the possibility that water is directly deactivating the catalyst.

Now that water in the PEG macroinitiator is known to interfere with the polymerization, the problems with the original procedure can be explained. Precipitation of the macroinitiator from DCM with diethyl ether does not fully exclude water from the MPEG-18 macroinitiator, most likely because the PEG chain is too short to form well-defined, large crystals (the PEG-18 starting material is a very soft, almost greaselike solid). As a result, a large fraction of the MPEG-18 remains amorphous and water is retained within that region. The water then either directly or indirectly deactivates the catalyst by removing it from solution, necessitating a large amount of catalyst in the tBA polymerization. The amount of water is not consistent, however, so batches of MPEG-18 with less water will have excessive chain ends active when the reaction is opened to air, deactivating the chain ends. It appears that successful runs had just enough water to remove the right amount of catalyst to give decent tBA conversion, yet removed enough to leave sufficient chain ends active to polymerize styrene.

This sequence explains why the reaction was so difficult to duplicate. Batches of PEG with more water would not polymerize tBA well enough, and batches with too little water had excessive catalyst and yielded a polymer with dead chain ends so styrene could not be added to the chain. It also explains why the MPEG-45 never worked before. The longer chain of the MPEG-45 is able to crystallize into well-defined crystals and excludes water very well (the MPEG-45 starting material is a hard, solid granule). Most of the

time, NMR shows no water after the crystallization step. Therefore, tBA polymerizations with MPEG-45 macroinitiator invariably had excessive catalyst. Therefore, almost all of the chains would terminate with oxygen during the cooldown phase, leaving almost no chains with the secondary bromide required for styrene polymerization.

Once the problems synthesizing the triblock copolymer were resolved, it was a simple matter to optimize the conditions to control the PAA and PS block lengths. The key to reproducible control over the block lengths was to avoid conditions where small variations led to big changes in monomer conversion. Some of these variables, such as macroinitiator concentration, are set and will not be affected by an increase in scale. The main issue with macroinitiator concentration is the viscosity of the reaction solution and the ability of the macroinitiator (for tBA polymerizations) or the diblock polymer (for styrene polymerizations) to unfold and expose the reactive chain end. Moving to a larger scale will not make any difference in the behavior of the polymer in solution, and so it is unlikely that a different concentration will show any improvement.

The catalyst loading is a different situation. Typical tBA polymerizations used 34-48 mg of CuBr catalyst (25-30% catalyst loading based on macroinitiator). Variations in actual loading of 1 or 2 mg from weighing errors (the scale used for weighting catalyst only measured to 1 mg) or catalyst impurity represent only a 2-6% variance in catalyst concentration. However, if a catalyst loading of 10-15% is used, then a 1-2 mg variability in catalyst added becomes a 7-15% variance in catalyst concentration, enough to make a considerable difference in monomer conversion. If the reaction were scaled up by a factor of five, then that 7-15% variance drops back to only 2-3%. Therefore, when making the polymer on a large scale, lower catalyst loadings may produce improved yields of active

chain ends. It is possible, even probable, that a reduced catalyst loading at larger scales would result in a drop in polymerization rate, necessitating adjustments to the conditions to maintain acceptable monomer conversion. Thus, any attempt to scale up the reaction must consider these issues, realizing that optimum conditions in terms of catalyst loading and monomer concentration may need to be adjusted.

In addition to the ability to control the block length of the PAA and PS blocks, the resolution of the polymerization problem also enabled the incorporation of the longer chain MPEG-45 into the triblock copolymer. MPEG-45 macroinitiator requires slightly more catalyst to polymerize tBA effectively, owing to the much longer (3x) chain, but it otherwise behaves similarly to the MPEG-18 macroinitiator. Given that MPEG-45 does require more catalyst than MPEG-18 for efficient tBA polymerization, it is unlikely that lower catalyst levels could be used effectively in a scaled-up synthesis. At the styrene polymerization step and at the hydrolysis step, MPEG-45 based polymers behave essentially the same as their MPEG-18 counterparts. Therefore, any commercially available hydroxy-terminated MPEG should be usable in the polymerizations, thus giving complete control over all of the block lengths of the triblock copolymer.

The formation of the PEG-eggs themselves from the triblock polymer was never a problem. Once the triblock copolymer was available, PEG-eggs could be made reproducibly and in quantity. Minimal sonication was necessary to debundle and isolate SWNTs into individual eggs. The eggs remain stable for long periods of time; as of this writing, solutions of PEG-eggs in water have remained unchanged for over four months.

The PEG-eggs fluoresce as well as their SDBS-suspended counterparts. The ratio of polymer to SWNT in forming the PEG-eggs appears to have some role in the observed

fluorescence. The factors that are most important in obtaining maximum fluorescence are not yet clear. So far, the tested MPEG-18 based and MPEG-45 based triblock polymers gave nearly identical maximum fluorescence at essentially the same polymer/SWNT ratio. However, the ratio of the polystyrene/SWNTs between the two polymers was quite different, and the PAA block length, though similar, was not identical. Additional series of PEG-eggs made with different PS blocks need to be made and analyzed. Furthermore, series of PEG-eggs made with different PAA blocks (and constant PS blocks) need to be made and analyzed. Finally, the degree of crosslinking of the egg may play a small role, so a series of eggs with different crosslink densities should be explored as well.

It was expected that the most influential block as far as fluorescence intensity would be the polystyrene block. This block is responsible not only for wrapping the SWNT and protecting it from water exposure, but it also plays a role in debundling the SWNTs during egg formation by winding in between the individual tubes. Furthermore, although PS is not a conjugated polymer, the aromatic rings may quench the fluorescence to some degree. Thus, a shorter polystyrene block may prove desirable for several reasons. One, a shorter chain may have an easier time penetrating between the SWNTs in a bundle. Two, a shorter chain will be less able to wrap around an entire bundle, again encouraging better debundling of the tubes. Three, less polystyrene around the SWNTs minimizes any possible quenching of the fluorescence.

The observed results, however, do not show a clear answer. Both triblocks have short polystyrene blocks (12 styrene monomer units for the MPEG-18 based polymer and 11 styrene monomer units for the MPEG-45 based polymer), but the shorter PEG fluoresced better at a higher polystyrene/SWNT ratio. Clearly, the polystyrene/SWNT

ratio is not the only polymer parameter that is important. Triblock polymers with longer

styrene chains (20 monomer units) are currently being tested for fluorescence. Additional

studies on other MPEG-PAA-PS polymers with different block lengths should further

extend the understanding of the impact of different parameters on PEG-egg performance.

SUMMARY

The results presented in this thesis address two problems in the use of SWNTs in practical applications. The first problem is the lack of understanding of the interaction of peroxides with SWNTs, and the second problem is the difficulty in synthesizing a triblock coplymer for the manufacture of SWNT-containing PEG micelles. Peroxides may react with SWNTs in unexpected ways if the peroxide-SWNT interaction is misunderstood. Specifically, if SWNTs induce the decomposition of peroxides in complex systems, then improperly designed systems may not behave as intended. PEG-egg micelles have potential applications as therapeutic tools. However, they can only be useful if they can be made reproducibly and in quantity.

Peroxides are widely used in reactions with SWNTs and in SWNT-containing composites. Peroxides perform one of two primary functions in these systems. The first purpose is to functionalize SWNTs through modification of the SWNT sidewall. This modification may take place directly by attack of the peroxide generated radical or indirectly by attack of the peroxide generated radical on a secondary compound, creating a new radical that subsequently modifies the SWNT. The second purpose is to crosslink or to otherwise alter the system matrix or another matrix component. In the first study presented here, peroxides have been shown to undergo induced decomposition in the presence of SWNTs. This process has a substantial potential impact on SWNT-containing composite systems. The chosen peroxide, therefore, has an impact on the behavior and resulting products of the system. For example, if the desired outcome is to crosslink the matrix or initiate a second species, then peroxides that have a low sensitivity to SWNTs will be preferred. Peroxides such as BP or pMBP that have a lower induced

decomposition rate should be less likely to interact with the nanotube instead of the desired species. On the other hand, if the objective is for the peroxide to attack the nanotube preferentially, then SWNT-sensitive peroxides such as PhP are nearly ideal. It has a very low thermolysis rate at even 80°C, but when in contact with a SWNT, it decomposes very rapidly, producing a radical exactly where it is wanted- at the nanotube.

SWNTs have shown great promise as transporters of molecules or as thermablation agents for therapeutic use in biological systems. PEG-eggs are good materials for introducing water solubility and biological compatibility to SWNTs while preserving their intrinsic electronic properties, primarily fluorescence and susceptibility to RF heating. The second study in this thesis has shown how to overcome problems in the synthetic methodology that have prevented wider use and study of PEG-eggs. First, the ability to reproduce the synthesis on a reasonable scale provides a larger amount of available material for biological studies. Second, rather than being limited to one polymer set, the chain lengths of all three blocks may now be controlled. The PEG length is controlled by macroinitiator selection, and the PAA and PS blocks are controlled through polymerization conditions. The ability to control the polymerization opens up a pathway to optimizing the polymer for the purpose of maximizing the performance of the PEG-eggs. The solubility, the intrinsic fluorescence, and the interaction with biological systems (e.g. half-life *in vivo*) all may be affected by altering the chain length of the individual blocks. Therefore, the PEG-eggs can be tailored to suit the application as needed.
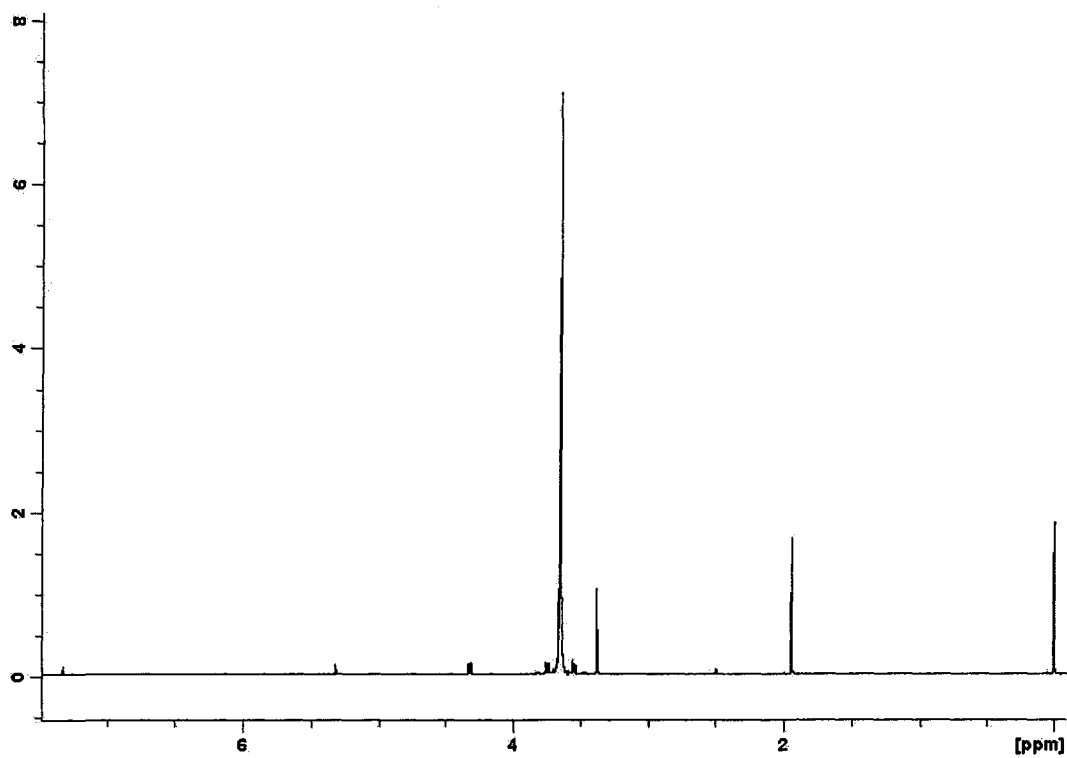
APPENDIX A: ^{1}H NMR spectra of PEG-egg polymers

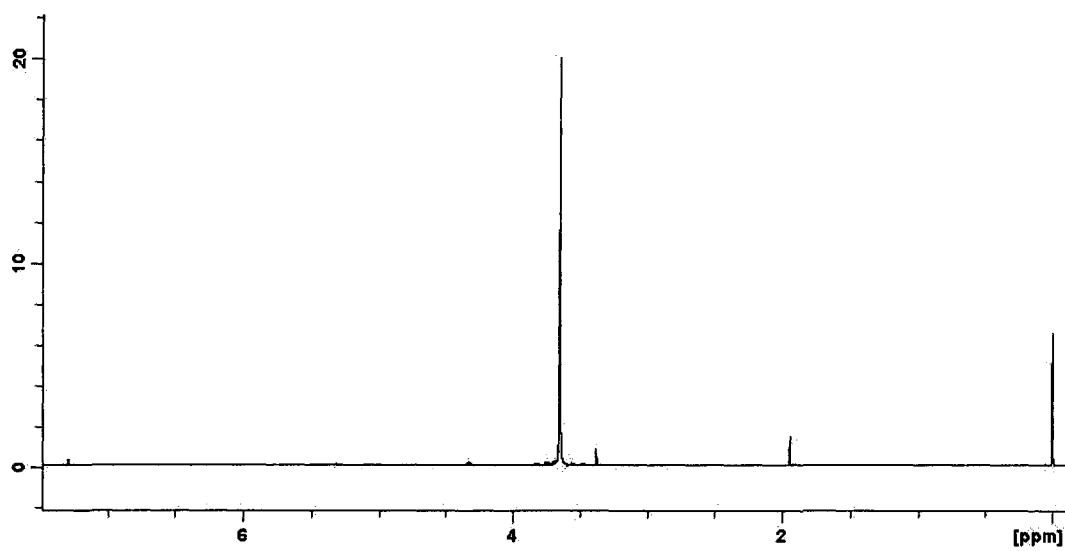Figure 33. ^{1}H NMR (CDCl$_3$) of 750 MW PEG MPEG-Br macroinitiator

Figure 34. ^{1}H NMR (CDCl$_3$) of 2000 MW PEG MPEG-Br macroinitiator

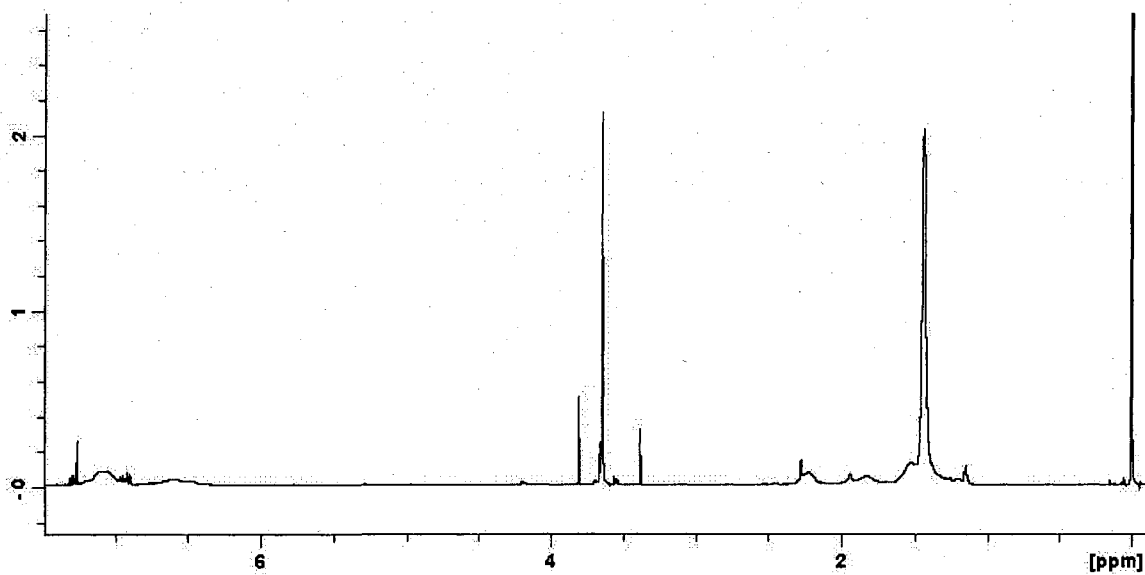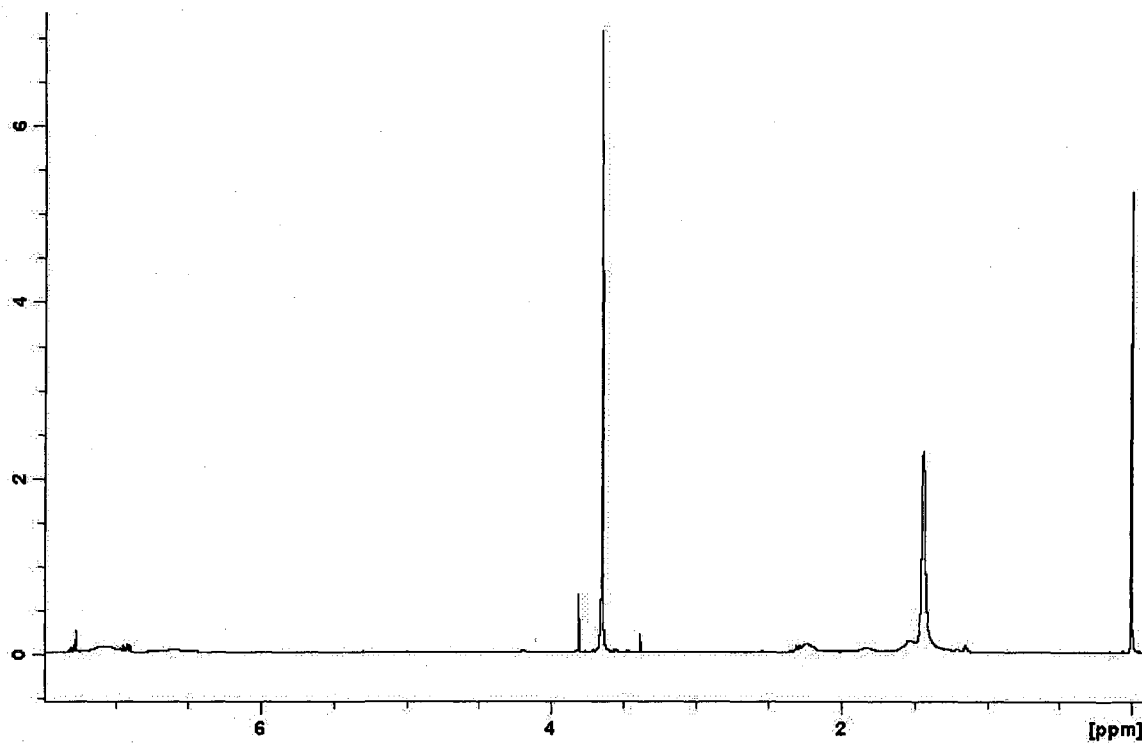Figure 35. ^{1}H NMR (CDCl$_3$) of 750 MW PEG MPEG-PtBA-Br diblock polymer

Figure 36. ^{1}H NMR (CDCl$_3$) of 2000 MW PEG MPEG-PtBA-Br diblock polymer

Figure 37. ^{1}H NMR (CDCl$_3$) of 750 MW PEG MPEG-PtBA-PS triblock polymer

Figure 38. ^{1}H NMR (CDCl$_3$) of 2000 MW PEG MPEG-PtBA-PS triblock polymer
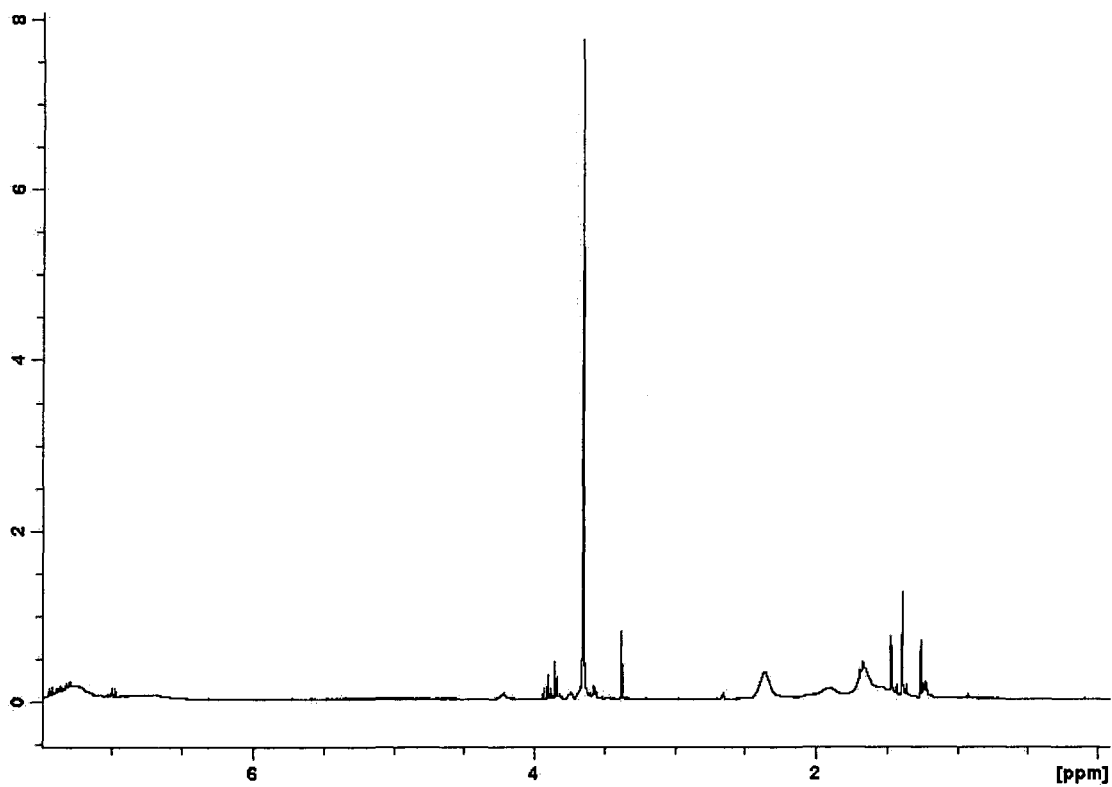
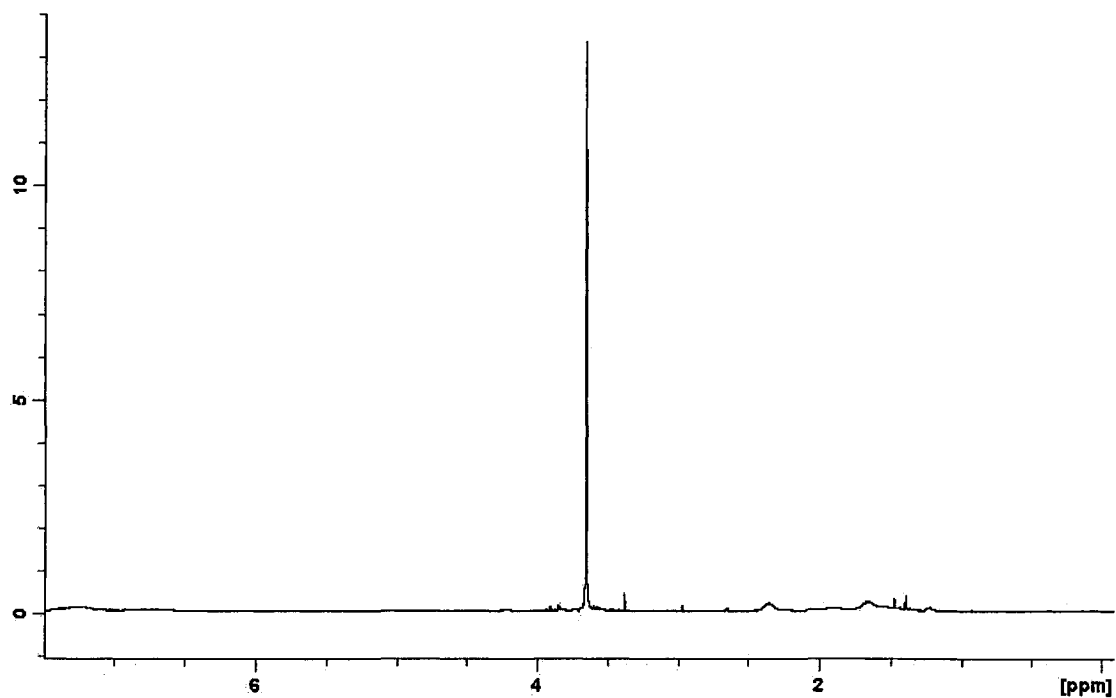Figure 39. ^{1}H NMR (DMSO-d$_6$)of 750 MW PEG MPEG-PAA-PS triblock polymer

Figure 40. ^{1}H NMR of 2000 MW PEG MPEG-PAA-PS triblock polymer

BIBLIOGRAPHY

[1] Wang, et. al., *Carbon*, 2007, *45*, 2388

[2] Figure courtesy Prof. Bruce Weisman

[3] Hirsch, A. *Angew. Chem. Int. Ed. Engl.* **2002**, *41*, 1853-1858.

[4] Hirsch, A.; Vostrowsky, O. *Top. Curr. Chem.* **2005**, *245*, 193-237.

[5] Tasis, D.; Tagmatarchis, N.; Bianco, A.; Prato, M. *Chem. Rev.* **2006**, *106*, 1105-1136.

[6] Dyke, C. A.; Stewart, M. P.; Maya, F.; Tour, J. M. *Synlett* **2004**, *1*, 155.

[7] Ying, Y.; Saini, R. K.; F., L.; Sadana, A. K.; Billups, W. E. *Org. Lett.* **2003**, *5*, 1471-1473.

[8] Lee, K. M.; Li, L.; Dai, L. *J Am. Chem. Soc.* **2005**, *127*, 4122-4123.

[9] Holzinger, M.; Vostrowsky, O.; Hirsch, A.; Hennrich, F.; Kappes, M.; Weiss, R.; Jellen, F. *Angew. Chem. Int. Ed. Engl.* **2001**, *40*, 4002-4005.

[10] Nakamura, T.; Ishihara, M.; Ohana, T.; Tanaka, A.; Koga, Y. *Chem. Commun.* **2004**, 1336-1337.

[11] Liu, J.; Rodriguez i Zubiri, M.; Vigolo, B.; Dossot, M.; Fort, Y.; Ehrhardt, J.-J.; McRae, E. *Carbon* **2007**, *45*, 885-891.

[12] Liu, J.; Rodriguez i Zubiri, M.; Dossot, M.; Vigolo, B.; Hauge, R. H.; Fort, Y.; Ehrhardt, J.-J.; McRae, E. *Chem. Phys. Lett.* **2006**, *430*, 93-96.

[13] Khare, B. N.; Wilhite, P.; Quinn, R. C.; Chen, B.; Schlingler, R. H.; Tran, B.; Imanaka, H.; So, C. R.; Bauschlicher, C. W.; Meyyappan, M. *J. Phys. Chem. B.* **2004**, *108*, 8166-8172.

[14] Qin, S.; Qin, D.; Ford, W. T.; Herrera, J. E.; Resasco, D. E.; Bachilo, S. M.; Weisman, R. B. *Macromolecules* **2004**, *37*, 3965-3967.

[15] Baibarac, M.; Baltog, I.; Lefrant, S.; Mevellec, J.Y.; Bucur, C. *Diamond and Related Materials* **2008**, *17*, 1380-1388.

[16] Homenick, C.M.; Sivasubramaniam, U.; Adronov, A. *Polymer International*, **2008**, *57*, 1007-1011.

[17] Peng, H.; Reverdy, P.; Khabashesku, V. N.; Margrave, J. L. *Chem. Commun.* **2003**, 362-363.

[18] Umek, P.; Seo, J. W.; Hernadi, K.; Mrzel, A.; Pechy, P.; Mihailovic, D. D.; Forro, L. *Chem. Mater.* **2003**, *15*, 4751-4755.

[19] Liang, F.; Beach, J. M.; Rai, P. K.; Guo, W.; Hauge, R. H.; Pasquali, M.; Smalley, R. E.; Billups, W. E. *Chem. Mater.* **2006**, *18*, 1520-1524.

[20] Peng, H.; Alemany, L. B.; Margrave, J. L.; Khabashesku, V. N. *J. Am. Chem. Soc.* **2003**, *125*, 15174-15182.

[21] Liu, M.; Yang, Y.; Zhu, T.; Liu, Z. Carbon, **2005**, *43*, 1470-1478.

[22] Liu, M.; Yang, Y.; Zhu, T.; Liu, Z. *J. Phys. Chem. C* **2007**, *111*, 2379-2385.

[23] Zhang, M.; Yudasaka, M.; Miyauchi, Y.; Maruyama, S.; Ijima, S. *J. Phys. Chem. B* **2006**, *110*, 8935-8940.

[24] Nayak, R. R.; Shanmugharaj, A. M.; Ryu, S.H. *Macromol. Chem. Phys.* **2008**, *209*, 1137-1144.

[25] Shi, X.; Hudson, J. L.; Spicer, P. P.; Tour, J. M.; Krishnamoorti, R. ; Mikos, A. G. *Biomacromolecules*, **2006**, *7*, 2237-2242.

[26] Sitharaman, B.; Shi, X.; Tran, L. A.; Spicer, P. P.; Rusakova, I.; Wilson, L. J.; Mikos, A. G. *J. Biomater. Sci. Polymer Edn.*, **2007**, *18*, 655-671.

[27] Shi, X.; Sitharaman, B.; Pham, Q. P.; Liang, F.; Wu, K.; Billups, W. E.; Wilson, L. J.; Mikos, A.G. *Biomaterials*, **2007**, *28*, 4078-4090.

[28] Personal communication

[29] Martin, J. C.; Hargis, J. H. *J Am. Chem. Soc.* **1969**, *91*, 5399-5400.

[30] Swain, C. G.; Stockmayer, W. H.; Clarke, J. T. *J. Am. Chem. Soc.* **1950**, *72*, 5426-5434.

[31] Nozaki, K., Bartlett, P., *J. Am. Chem. Soc.*, **1946**, *68*, 1686-1692.

[32] Engel, P. S.; Billups, W.E.; Abmayr, D. W.; Tsvaygboym, K.; Wang, R. *J. Phys. Chem. C*, **2008**, *112*, 695-700..

[33] Hayakawa, Y.; Terasawa, N.; Sawada, H. *Polymer* **2001**, *42*, 4081-4086.

[34] Zhou, Z. B.; He, H. Y.; Weng, Z. Y.; Zhao, C.-X. *J. Fluorine Chem.* **2000**, *104*, 285-290.

[35] Sawada, H.; Nakayama, M. *J. Fluorine Chem.* **1990**, *46*, 423-431.

[36] Greene, F. D. *J Am. Chem. Soc.* **1956**, *78*, 2246-2250.

[37] Russell, K. E. *J. Am. Chem. Soc.* **1955**, *77*, 4814-4815.

[38] Zupanic, J. J.; Horn, K. A.; Schuster, G. B. *J. Am. Chem. Soc.* **1980**, *102*, 5279-5285.

[39] Nozaki, K. *Ind. Eng. Chem. Anal. Ed.* **1946**, *18*, 583.

[40] Holzinger, M.; Abraham, J.; Whelan, P.; Graupner, R.; Ley, L.; Hennrich, F.; Kappes, M.; Hirsch, A. *J. Am. Chem. Soc.* **2003**, *125*, 8566-8580.

[41] Coleman, K. S.; Bailey, S. R.; Fogden, S.; Green, M. L. H. *J. Am. Chem. Soc.* **2003**, *125*, 8722-8723.

[42] O'Connell, M. J.; Sivaram, S.; Doorn, S. K. *Phys. Rev. B* **2004**, *69*, 235415

[43] Krasutsky, P. A.; Kolomitsyn, I. V.; Carlson, R. M. *Org. Lett.* **2001**, *3*, 2997-2999.

[44] Xu, Y. Q.; Peng, H.; Hauge, R. H.; Smalley, R. E. *Nano Letters* **2005**, *5*, 163-168.

[45] Nozaki, K. *Ind. Eng. Chem. Anal. Ed.* **1946**, *18*, 583.

[46] Nikolaev, P.; Bronikowski, M. J.; Bradley, R. K.; Rohmund, F.; Colbert, D.; Smith, K. A.; Smalley, R. E. *Chem. Phys. Lett.* **1999**, *313*, 91-97.

[47] Chattopadhyay, J.; Sadana, A. K.; Liang, F.; Beach; J. M.; Xiao, Y.; Hauge; R. H; Billups, W.E. *Org Lett* **2005**, *7*, 4067–4069.

[48] Wang, F.; Dukovic, G.; Brus, L. E.; Heinz, T. F. *Phys. Rev. Lett.* **2004**, *92*, 177401-1 – 177401-4.

[49] Hudson J. L.; Casavant M. J.; Tour J. M. *J. Am. Chem. Soc.* **2004**, *126*, 11158–11159.

[50] Yoshida, M.; Morinaga, Y.; Iyoda, M.; Kikuchi, K.; Ikemoto, I.; Achiba, Y. *Tetrahedron Lett.* **1993**, *34*, 7629-7632.

[51] Kam, N. W. S.; Jessop, T. C.; Wender, P. A.; Dai, H. *J Am. Chem. Soc.* **2004**, *126*, 6850–6851.

[52] Pantarotto, D.; Briand, J-P.; Prato, M.; Bianco, A. *Chem. Commun.* **2004**, 16–17.

[53] Kam, N. W. S.; O'Connell, M. O.; Wisdom, J. A.; Dai, H. *Proc. Natl. Acad. Sci. USA* **2005**, *102*, 11600–11605.

[54] Pantarotto, D.; Singh, R.; McCarthy, D. Erhardt, M.; Briand, J-P.; Prato, M.; Kostarelos, K.; Bianco, A. *Angew. Chem. Int. Ed. Engl.* **2004**, *43*, 5242–5246.

[55] Singh, R.; Pantarotto, D.; Lacerda, L.; Pastorin, G.; Klumpp, C.; Prato, M.; Bianco, A.; Kostarelos, K. *Proc. Natl. Acad. Sci USA* **2006**, *103*, 3357–3362.

[56] Kozak, J. A.; Matsushita, M.; Nairn, A. C.; Calahan, M. D. *J. Gen. Physiology* **2005**, *126*, 499-514

[57] Weisman, R. B.; Bachilo, S. M.; Tsyboulski, D. *Appl. Phys. A* **2004**, *78*, 1111–1116.

[58] Lee, J. U.; Huh, J.; Kim, K. H.; Park. C.; Jo, W. H. *Carbon* **2007**, *45*, 1051–1057.

[59] Moghimi, S. M.; Szebeni, J. *Prog. Lipid Res.* **2003**, *42*, 463–478.

[60] Molineux G. *Cancer Treat. Rev.* **2002**, *28 (Suppl. A)*, 13–16.

[61] Roberts, M. J.; Bentley, M. D.; Harris, J. M. *Adv. Drug Deliver. Rev.* **2002**, *54*, 459–476.

[62] Cherukuri, P.; Gannon, C. J; Leeuw, T. K; Schmidt, H. K.; Smalley, R. E.; Curley, S. A.;Weisman, R. B. *Proc. Natl. Acad. Sci. USA* **2006**, *103*, 18882–18886.

[63] Parrish, B.; Breitenkamp, R. B.; Emrick, T. *J. Am. Chem. Soc.* **2005**, *127*, 7404–7410.

[64] Dumortier, H.; Lacotte, S.; Pastorin, G.; Marega, R.; Wu, W.; Bonifazi, D.; Briand, J-P.; Prato, M.; Muller, S.; Bianco, A. *Nano Letters* **2006**, *6*, 1522–1528.

[65] Huang, H.; Kowalewski, T.; Remsen, E. E.; Gertzmann, R.; Wooley, K. L. *J. Am. Chem. Soc.* **1997**, *119*, 11653–111659.

[66] Kang, Y.; Taton, T. A. *J. Am. Chem. Soc.* **2003**, *125*, 5650–5651.

[67] O'Reilly, R. K.; Hawker, C. J.; Wooley, K. L. *Chem Soc Rev* **2006**, *35*, 1068–1083.

[68] Tang, Y.; Liu, S. Y.; Armes, S. P.; Billingham, N. C. *Biomacromolecules* **2003**, *4*, 1636–1645.

[69] Niu, H.; Zhang, L.; Gao, M.; Chen, Y. *Langmuir* **2005**, *21*, 4205–4210.

[70] Matyjaszewski, K.; Xia, J. *Chem. Rev.* **2001**, *101*, 2921–2990.

[71] Matyjaszewski, K.; Spanswick, J.; Sumerlin, B. S. *Preparation, characterization,and applications of polymers synthesized by atom transfer radical polymerization.* In: Jagur-

Grodzinski, J., editor. *Living and Controlled Polymerization* New York: Nova Science

Publishers; **2006**. p. 1–38.

[72] Du. J.; Chen, Y. *Macromolecules* **2004**, *37*, 6322–6328.

[73] Dukovic, G.; White. B. E.; Zhou, Z.; Wang, F.; Jockusch, S.; Steigerwald, M. L.;

Heinz, T. F.; Friesner, R. A.; Turro, N. J.; Brus, L. E. *J. Am. Chem. Soc.* **2004**, *126*,

15269–15276.

[74] Weisman, R.B. *Fluorescence spectroscopy of single-walled carbon nanotubes*. In:

Rotkin, S. V.; Subramoney, S.; editors. *Applied Physics of Nanotubes: Fundamentals of

Theory, Optics, and Transport Devices*. Berlin: Springer; **2005**. p. 183–202.

[75] Davis, K.; Charleux, B.; Matyjaszewski, K. *J. Polymer Sci. A* **2000**, *38*, 2274-2283.

[76] Ma, Q.; Wooley, K. *J. Polymer Sci. A*, **2000**, *38*, 4805-4820.

[77] Burguiere, C.; Pascual, S.; Coutin, B.; Polton, A.; Tardi, M.; Charleux, B.;

Matyjaszewski, K.; Vairon, J.-P. *Macromol. Symp.* **2000**, *150*, 39–44.

[78] Davis, K.; Matyjaszewski, K. *Macromolecules*, **2000**, *33*, 4039-4047.

[79] Coessens, V.; Matyjaszewski, K. *J. Macromol. Sci., Pure Appl. Chem.* **1999**, *36*, 811.

[80] Personal communication